Inorganic Chemistry

Article

pubs.acs.org/IC

Screening Hofmann Compounds as CO_2 Sorbents: Nontraditional Synthetic Route to Over 40 Different Pore-Functionalized and Flexible Pillared Cyanonickelates

Jeffrey T. Culp,*[,†,‡] Catherine Madden,[†] Kristi Kauffman,[†] Fan Shi,[†,‡] and Christopher Matranga[†]

[†]National Energy Technology Laboratory, Pittsburgh, Pennsylvania 15236, United States

[‡]URS Corporation, South Park, Pennsylvania 15129, United States

Supporting Information

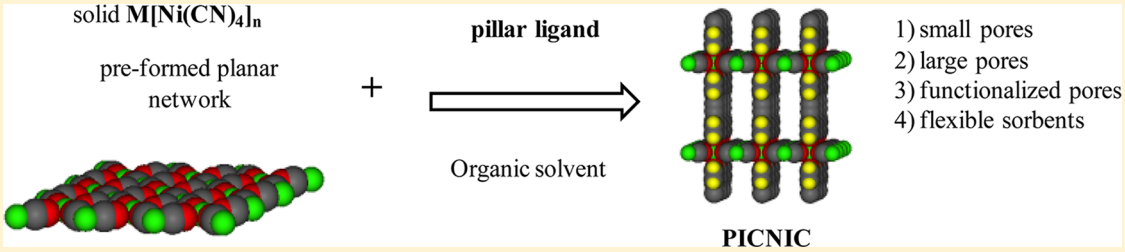

ABSTRACT: A simple reaction scheme based on the heterogeneous intercalation of pillaring ligands (HIPLs) provides a convenient method for systematically tuning pore size, pore functionality, and network flexibility in an extended series of pillared cyanonickelates (PICNICs), commonly referred to as Hofmann compounds. The versatility of the approach is demonstrated through the preparation of over 40 different PICNICs containing pillar ligands ranging from ∼4 to ∼15 Å in length and modified with a wide range of functional groups, including fluoro, aldehyde, alkylamine, alkyl, aryl, trifluoromethyl, ester, nitro, ether, and nonmetalated 4,4′-bipyrimidine. The HIPL method involves reaction of a suspension of preformed polymeric sheets of powdered anhydrous nickel cyanide with an appropriate pillar ligand in refluxing organic solvent, resulting in the conversion of the planar $[Ni_2(CN)_4]_n$ networks into polycrystalline three-dimensional porous frameworks containing the organic pillar ligand. Preliminary investigations indicate that the HIPL reaction is also amenable to forming $Co(L)Ni(CN)_4$, $Fe(L)Ni(CN)_4$, and $Fe(L)Pd(CN)_4$ networks. The materials show variable adsorption behavior for CO_2 depending on the pillar length and pillar functionalization. Several compounds show structurally flexible behavior during the adsorption and desorption of CO_2. Interestingly, the newly discovered flexible compounds include two flexible $Fe(L)Ni(CN)_4$ derivatives that are structurally related to previously reported porous spin-crossover compounds. The preparations of 20 pillar ligands based on ring-functionalized 4,4′-dipyridyls, 1,4-bis(4-pyridyl)benzenes, and *N*-(4-pyridyl)isonicotinamides are also described.

INTRODUCTION

Carbon dioxide separations using solid sorbents will require the development of porous materials with high affinities and high selectivities for CO_2 adsorption. Driven in part by this goal, research on porous coordination polymers (PCPs), commonly referred to as metal organic frameworks,[1,2] has become exceedingly popular over the past 15 years.[3−8] The building block approach to the design and synthesis of these materials provides a significant level of control over the pore chemistries, pore sizes, and surface areas of these materials. The development of synthetic routes toward materials with functional groups within the pore structure to enhance both the adsorption potential and selectivity of a particular guest has become an active area of research, especially in the field of CO_2 capture and separation. The approach typically involves either the use of ligands containing the desired functionality during the assembly of the PCP[9−12] or postsynthetic modification after the PCP has formed.[13−18]

The exceptional design flexibility of these materials is exemplified in a few well-documented cases such as the metal organic frameworks (MOFs),[7] zeolite imidazolate frameworks (ZIFs),[19] and Matériaux de l'Institut Lavoisier (MIL) series,[10] where a particular synthetic strategy or network topology has been found that allows multiple substitutions of bridging ligands and/or metal ions to form a structurally homologous series of materials from one general synthetic procedure. These modular approaches to material design offer great benefits for systematically designing a series of materials where the effects of pore modifications, including pore size and chemical functionalization, can be correlated with sorbent performance.

Another commonly employed modular design strategy for the preparation of PCPs involves the pillared-layer motif wherein an extended two-dimensional network is built into a three-dimensional solid through the incorporation of pillar

Received: August 29, 2012
Published: March 29, 2013

   dx.doi.org/10.1021/ic301893p | *Inorg. Chem.* 2013, 52, 4205−4216

ligands which link one layer to the next.[12,20−23] Polymeric cyano-bridged networks containing d^8 tetracyano complexes (commonly referred to as Hofmann[24] compounds) with their inherent planar $M[M'(CN)_4]_n$ networks are well-suited for this pillared-layer design strategy.[25−34] Because of their linear bridging abilities, dipyridyl derivatives such as 4,4′-bipyridine, 1,4-bis(4-pyridyl)benzenes, and *N*-(4-pyridyl)isonicotinamides are excellent candidates as potential pillar ligands in these systems. As cyano-bridged networks, these pillared Hofmann materials are also closely related to the widely studied family of Prussian blue based porous sorbents.[35−45]

Because of its commercial availability and ability to adopt a convenient rigid linear bridging arrangement, 4,4′-bipyridine (4,4′-Bpy) has steadily gained popularity as a versatile ligand in the field of coordination polymers.[46] It is somewhat surprising, considering the growing interest in pore-functionalized coordination polymers, that more materials containing functionalized versions of this common ligand are not reported. In addition, the 4,4′-bipyridine molecule is well-suited to perform as a functionalized ligand since substitution can occur at the 3-position and not interfere with coordination of the ring nitrogen. These 3-functionalized derivatives of 4,4′-bipyridine, however, are not readily available through commercial sources, and few direct literature preparations are available. Recent advances in Suzuki coupling reactions and the commercial availability of many of the necessary starting reagents and palladium catalysts have made these compounds much more accessible.[47] Since these linear dipyridyl compounds are very attractive as potential pillar ligands, we developed a synthetic route to several 3-R-4,4′-bipyridines along with a number of structurally related and ring-functionalized 1,4-bis(4-pyridyl)-benzenes and *N*-(4-pyridyl)isonicotinamides.

These ligands were found to work well as pillars in the synthesis of three-dimensional Hofmann compounds which we refer to in the following discussion as pillared cyanonickelates, or PICNICs. These materials are conveniently synthesized in bulk with near-quantitative yields through a heterogeneous intercalation of pillaring ligand (HIPL) reaction, resulting in the expansion of a polymeric quasi-two-dimensional nickel−cyanide network into covalently linked pillared porous three-dimensional structures. The method is found to be highly versatile with nearly three dozen pillar ligands successfully incorporated into the PICNIC structure, including several newly reported ring-functionalized bipyridyl, dipyridylamide, and dipyridylbenzene ligands. The ligands can be varied in both length and functionalization to give a wide range of porous materials all derived from the same structural motif. In this sense, PICNICs can be viewed as a novel family of porous materials with readily tunable pore properties akin to other well-known tailorable systems such as MOFs, ZIFs, and MILs.

A previous report revealed that the PICNIC compound Ni(1,2-bis(4-pyridyl)ethylene)$Ni(CN)_4$ shows structurally dynamic behavior during the adsorption and desorption of gases, including CO_2 and N_2.[28] This flexibility appears to be a common trait in many other PICNIC materials as several new flexible members in the family, including flexible $Co(L)Ni(CN)_4$ and $Fe(L)Ni(CN)_4$ derivatives, have been discovered and are reported herein. The CO_2-induced structural flexibility in the $Fe(L)Ni(CN)_4$ compounds is especially interesting considering the spin-crossover behavior reported for several analogous $Fe(L)M(CN)_4$ compounds.[25,26,30,31,48] Flexible PCPs (or flexible MOFs) are an interesting class of materials from both a fundamental and a practical standpoint.[28,49−54] The structure change and guest adsorption in these materials is driven by a complicated interplay of energetics describing the phase transition, stabilizing effects of guest adsorption, relief of mechanical strain in the crystal, and nucleation effects. Understanding this interplay and being able to selectively tune dynamic behavior in a sorbent is a key step in the rational design of new separation materials for both liquid and gas applications. The ability to systematically tune this dynamic behavior in the PICNIC structure makes them an exceptional platform for advancing our understanding of these materials.

EXPERIMENTAL SECTION

All starting materials were purchased from commercial sources in at least reagent grade purity and used as received. Tricyclohexylphosphine and tris(dibenzylideneacetone)dipalladium(0) are abbreviated as $P(Cy)_3$ and $Pd_2(DBA)_3$, respectively. Anhydrous 1,4-dioxane, acetonitrile, ethanol, and toluene were purchased from commercial sources and transferred under N_2 using a gastight syringe. Water was purified using a Barnstead EASYpure LF water purification system and degassed by refluxing under N_2 3−4 h prior to use. All reactions were performed under N_2 using standard Schlenk line techniques. The pillar ligand 4,4′-azopyridine (azopyr) is commercially available from Sigma-Aldrich. The pillar ligand 2,6-naphthyridine was purchased from the Florida Center for Heterocyclic Compounds and used as received. The pillar ligand 4,4′-bipyrimidine (4,4′-Bpm) was purchased from Oakwood Products, Inc. and used as received. The pillar ligands 1,2-bis(4-pyridyl)acetylene (dpac),[55] 1,4-bis(4-pyridyl)buta-1,3-diyne (DPBD),[56,57] 1,4-bis(4′-pyridylethynyl)benzene (DPAC-Bz),[58] and *N*-(4-pyridyl)isonicotinamide[59] were prepared by literature methods. The CHN analyses were provided by Robertson Microlit Laboratories, Inc., Ledgewood, NJ. The NMR measurements were done using a Bruker 300 MHz proton NMR spectrometer. Melting points were determined using a Mettler STARe TGA/DSC thermogravimetric analyzer on samples of 4−6 mg loaded in 100 μL aluminum pans with a temperature ramp of 5 °C/min under N_2.

Synthesis of Pillar Ligands. *Functionalized 4,4′-Bipyridines (Bpy-R).* The preparation of 3-R-4,4′-bipyridines was carried out using a Suzuki coupling reaction between an excess of 1 equiv of pyridine-4-boronic acid and a 3-R-4-halopyridine where the halo group can be chloro or bromo or by reaction of 4-bromopyridine with a 3-R-pyridine-4-boronic acid. The reaction procedure was borrowed extensively from a method reported by Kudo et al. for the coupling of pyridineboronic acids.[47] All compounds were prepared by the same general method and purified by recrystallization from either hexanes or ethyl acetate. The detailed preparation of 3-amino-4,4′-bipyridine is used as an example. Synthetic details for the remaining Bpy-R compounds are included in the Supporting Information.

3-Amino-4,4′-bipyridine (Bpy-NH_2). A three-necked flask was charged with 1.9 g (15 mmol) of 3-amino-4-chloropyridine, 2.7 g (22 mmol) of pyridine-4-boronic acid, 225 mg (0.28 mmol) of tris(dibenzylideneacetone)dipalladium(0) ($Pd_2(DBA)_3$), and 180 mg (0.64 mmol) of tricyclohexylphosphine ($P(Cy)_3$) and purged with N_2. The mixture was suspended in 40 mL of deoxygenated 1,4-dioxane (commercial anhydrous grade packaged under Ar). A solution of 8 g (38 mmol) of K_3PO_4 in 25 mL of deoxygenated water was added by syringe through a septum. The flask was added to an oil bath at 60 °C and slowly heated to reflux (100 °C). The mixture was held at reflux with rapid stirring overnight (∼18 h). Upon being cooled to room temperature, the mixture was poured into a separatory funnel and the lower aqueous phase removed and discarded. The dioxane layer was collected and filtered and the dioxane removed under reduced pressure. The residue was triturated in 75 mL of ethyl acetate, treated with activated carbon and anhydrous magnesium sulfate, and then heated to reflux for 10 min with stirring. The mixture was filtered hot through a fine glass frit. The filtrate was concentrated and cooled to yield 2.1 g (12.3 mmol) of the tan crystalline product. Mp: 170 °C (lit.[60] 166−168 °C). ^{1}H NMR (300 MHz, $CDCl_3$): δ 8.75, m, 2H; 8.21 s, 1H; 8.11, d, 1H; 7.43, m, 2H; 7.03, d, 1H; 3.85, s, 2H. Anal.

dx.doi.org/10.1021/ic301893p | *Inorg. Chem.* 2013, 52, 4205−4216

Chart 1. Structures and Abbreviations for Pillar Ligands (L) Used To Assemble PICNIC Coordination Polymers as $(Ni(L)[Ni(CN)_4])_n$

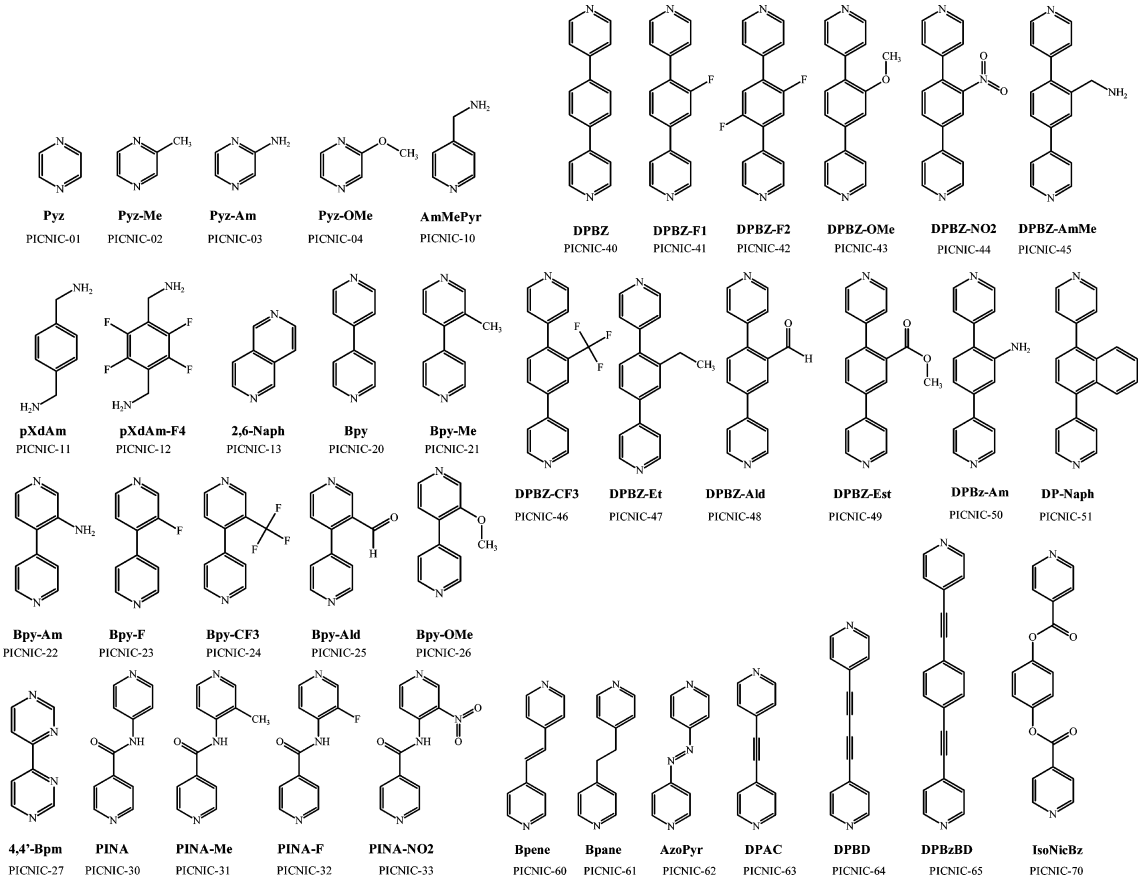

Calcd for $C_{10}H_9N_3$ (171.2): C, 70.16; H, 5.30; N, 24.54. Found: C, 69.87; H, 4.99; N, 24.07.

Functionalized 1,4-Bis(4-pyridyl)-3-R-benzenes (DPBz-R). The preparation of 1,4-bis(4-pyridyl)-3-R-benzenes was carried out using a Suzuki coupling reaction similar to the method described above for the preparation of 3-R-4,4′-bipyridines by reaction of an excess of ~2.5−3.0 equiv of 4-pyridineboronic acid with 1 equiv of a 3-R-1,4-dihalobenzene, where halo is chloro, bromo, or iodo. The detailed preparation of 1,4-bis(4-pyridyl)aniline ($DPBz\text{-}NH_2$) is given as an example. Synthetic procedures for the remaining DPBz-R compounds are included in the Supporting Information.

1,4-Bis(4-pyridyl)aniline ($DPBz\text{-}NH_2$). A three-necked flask was charged with 1.3 g (5.2 mmol) of 1,4-dibromoaniline, 2.5 g (18 mmol) of pyridine-4-boronic acid, 300 mg (0.33 mmol) of $Pd_2(DBA)_3$, and 225 mg (0.8 mmol) of $P(Cy)_3$ and purged with N_2. The mixture was suspended in 40 mL of deoxygenated 1,4-dioxane (commercial anhydrous grade packaged under Ar). A solution of 4 g (19 mmol) of K_3PO_4 in 20 mL of degassed water was added by syringe through a septum. The reaction was heated at reflux (100 °C) under N_2 with rapid stirring overnight (~18 h). Upon being cooled to room temperature, the mixture was poured into a separatory funnel and the lower aqueous phase removed and discarded. The dioxane layer was collected and filtered and the dioxane removed under reduced pressure. The residue was dissolved in chloroform and washed twice with 5 g of Na_2CO_3 in 25 mL of water. The chloroform solution was dried with anhydrous magnesium sulfate and the solvent removed under reduced pressure. The solid was taken up in 80 mL of hot ethyl acetate, treated with activated carbon, and filtered hot through a fine glass frit. The solid was crystallized by concentration and cooling of the filtrate to yield 0.75 g (3.0 mmol) of beige product. Mp: 197 °C. ^{1}H NMR (300 MHz, $CDCl_3$): δ 8.70, m, 4H; 7.49, m, 4H; 7.27, m, 1H; 7.12, m, 1H; 7.04, d, 1H. Anal. Calcd for $C_{16}H_{13}N_3$ (247.3): C, 77.71; H, 5.30; N, 16.99. Found: C, 76.92; H, 5.34; N, 16.32.

Functionalized N-(4-Pyridyl)isonicotinamides (PINA-R). The synthesis of the PINA-R compounds was accomplished by using a modification of a previously reported method for the preparation of *N*-(4-pyridyl)isonicotinamide[59] wherein isonicotinoyl chloride hydrochloride was reacted with 1 equiv of the appropriate 3-R-4-aminopyridine at 80 °C in dry pyridine overnight. The products were recrystallized from acetone/water. The synthesis of PINA-F is given as an example. Synthetic procedures for the remaining DPBz-R compounds are included in the Supporting Information.

N-(3-Fluoro-4-pyridyl)isonicotinamide (PINA-F). A solution of 1.03 g (0.0092 mol) of 4-amino-3-fluoropyridine in 25 mL of dry pyridine was added to a mixture of 1.60 g (0.009 mol) of isonicotinoyl chloride hydrochloride in 25 mL of dry pyridine. The flasks were then transferred into a hot oil bath and reacted at 80 °C under N_2 for 18 h. The mixture was then concentrated to a few milliliters under reduced pressure, and 50 mL of a 5% aqueous solution of sodium bicarbonate was added. The precipitate was collected by filtration, recrystallized from acetone/water, and dried to yield 1.61g (0.0074 mol) of a light beige solid. Mp: 180 °C. ^{1}H NMR (300 MHz, $CDCl_3$): δ 8.86, d, 2H; 8.47, m, 3H; 8.37, s, 1H; 7.73, d, 2H. Anal. Calcd for $C_{11}H_8FN_3O$ (217.2): C, 60.83; H, 3.71; N, 19.35. Found: C, 60.66; H, 3.38; N, 19.25.

Synthesis of PICNICs. *Nickel Compounds.* The pillared cyanonickelate compounds $Ni(L)[Ni(CN)_4]$, where L is a pillar ligand, were prepared by adaptation of a previously reported method[28,61] by reaction of 1.05:1 molar ratios of pillar ligands to anhydrous $Ni_2(CN)_4$ (prepared by drying the hydrate under vacuum at 130 °C for 2−3 h) in dry toluene or dry acetonitrile/dry toluene mixtures at reflux under N_2. For pillar ligands in the PINA-R series, reactions were done in dry acetonitrile due to low solubility of the ligands in toluene (note that addition of the dry acetonitrile to anhydrous $Ni_2(CN)_4$ is mildly exothermic and results in an immediate color change of the $Ni_2(CN)_4$ due to coordination of the acetonitrile

dx.doi.org/10.1021/ic301893p | Inorg. Chem. 2013, 52, 4205−4216

Scheme 1. Formation of PICNICs via the HIPL Reaction

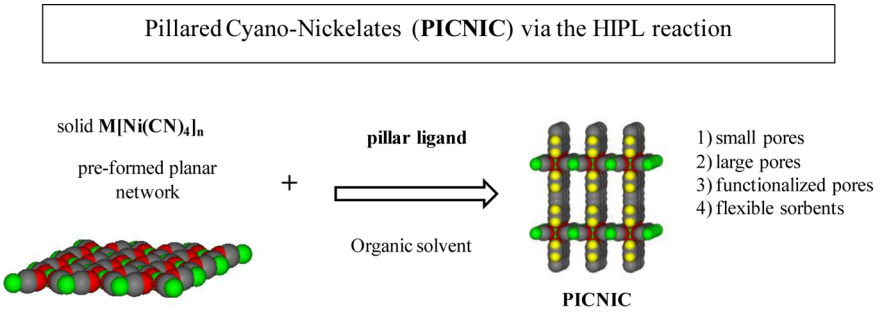

solvent). The anhydrous $Ni_2(CN)_4$ starting materials and $Ni(L)[Ni(CN)_4]$ products are insoluble in the reaction solvent and as such are present throughout the reaction as a suspension. The typical reactant loading is ~1 mmol/30 mL of solvent with a reaction time of 24 h sufficient for most pillar ligands, with some sterically hindered pillars requiring up to 72 h for completion. Reaction progress can be monitored qualitatively by observing the color change of the initially orange anhydrous $Ni_2(CN)_4$ coordination polymer to what is often a light violet or dull green color of the $Ni(L)[Ni(CN)_4]$ products or qualitatively by taking small aliquots of the suspended solid and filtering out the product for subsequent thermogravimetric analyses in air where the formula weights of the products can be determined by the residual weight percent of NiO above 500 °C. It is noted that reaction times can be reduced for more sterically demanding insertion reactions when performed solvothermally in sealed Teflon-lined high-pressure Parr reactors at temperatures of 150 °C using dry toluene. Each of the pillar ligands listed in Chart 1 could be intercalated into a $Ni(L)[Ni(CN)_4]$ product using this basic reaction scheme; however, PICNIC-61 and PICNIC-65 irreversibly collapse to nonporous phases after removal of guest solvents. The PICNICs containing Pyz, Bpy, Bpane, Bpene, and DPAC pillar ligands have previously been described.[28,33] Characterization of PICNIC compounds by TGA and X-ray powder diffraction is included in the Supporting Information. Prior to CO_2 adsorption measurements, the PICNIC compounds were activated by extraction in boiling chloroform or acetone until TGA showed solvent exchange was complete (typically 2−4 h) and then dried under vacuum at 115 °C for a minimum of 6 h.

PICNICs Containing Other Transition Metals. Preliminary reactions were performed to test whether PICNIC derivatives could be formed with additional transition metals. Reactions to form $Co(L)[Ni(CN)_4]_n$, where L = AmMe-Pyr and pXdAm, $Fe(L)[Ni(CN)_4]_n$, where L = Pyz, Bpy, Bpene, and pXdAm, and $Fe(L)Pd(CN)_4$, where L = Bpy, were accomplished using a method similar to that of the Ni-containing PICNICs with minor modification. For the Co- and Fe-based PICNICs, the hydrated polymeric $Co[Ni(CN)_4]_n$, $Fe[Ni(CN)_4]_n$, and $Fe(L)[Pd(CN)_4]_n$ were more effective when used directly without the need to remove coordinated waters prior to the intercalation reaction when dry ethanol or dry acetonitrile was used as the reaction solvent. Sample characterizations are included in the Supporting Information.

Instrumentation. Isotherms were collected on a pressure−composition isotherm measurement system (Advanced Materials Corp.) for pressures up to ~18 atm for CO_2 over a temperature range of −25 to +30 °C. The instrument is designed on the basis of a conventional Sievert apparatus. Prior to the measurements, samples (~500−750 mg) were degassed under vacuum at 115 °C for >6 h. Low-pressure N_2 isotherms and five-point BET surface areas were measured on a Quantachrome Autosorb 1C volumetric instrument on samples (~100 mg) degassed under dynamic vacuum for >6 h at 115 °C. Powder X-ray diffraction measurements were performed on a PANalytical X'Pert Pro MPD powder diffractometer having a $\theta-\theta$ configuration, a Cu X-ray source operated at 45 kV and 40 mA, and an X'Celerator detector with a monochromator. Thermogravimetric analyses were performed using a Mettler STARe TGA/DSC thermogravimetric analyzer. For PICNIC decomposition measurements, samples (5−10 mg) were run in Pt pans at 15 °C/min under a dry air purge of 100 mL/min to temperatures >550 °C. To determine the sample purity, the following calculations are performed using the TGA data. The expected formula weight of the desired PICNIC compound was calculated on the basis of the $Ni(L)Ni(CN)_4$ structural unit. The complete oxidation in air will lead to two NiO groups per formula unit, which have a formula weight of 149.38. The ratio of the formula weight of nickel oxide to the formula weight of the PICNIC is 149.39/(expected formular weight of PICNIC). Dividing the mass of NiO obtained in the TGA run in air by the mass of the corresponding guest-free PICNIC should result in the same ratio. On the TGA curve, the material was determined to be guest free at the plateau after guest solvents were lost (see the Supporting Information, Figures S16−S66). For the FeNi and CoNi PICNICs, oxide formulas of $FeNiO_{1.5}$ and $CoNi_{1.5}$ were used to determine formula weights on the basis of common oxidation states and powder diffraction analysis (see the Supporting Information, Figures S67 and S68).

RESULTS AND DISCUSSION

Synthesis of Pillar Ligands. Due to their commercial availability and ability to adopt a convenient linear bridging arrangement, pyrazine and 4,4′-bipyridine are commonly used ligands in the preparation of coordination polymers. Several functionalized versions of pyrazine are available from commercial suppliers; however, the symmetry of the molecule requires functional groups at the position α to the ring nitrogen, which could cause complications in coordination chemistry due to the possibility of the functional group to sterically hinder access to the ring nitrogen, resulting in a single coordination of the ligand at the unhindered nitrogen and the failure to act as a bridging ligand. For the PICNIC compounds, the amino- and methylpyrazines successfully resulted in porous structures, whereas the methoxy derivative gave a very low porosity solid, and the attempt at the chloro derivative was unsuccessful as determined from TGA (see the Supporting Information).

The situation is improved with functionalized 4,4′-bipyridine derivatives since functionalization can occur at the 3-position and not interfere with coordination of the ring nitrogen. These 3-functionalized derivatives of 4,4′-bipyridine, however, are not readily available through commercial sources. We were able to prepare both the 3-functionalized 4,4-bipyridine derivatives and related 1,4-bis(4-pyridyl)benzenes by slight modification of a convenient method reported by Kudo[47] in which pyridine-4-boronic acid is coupled with a 3-functionalized 4-halopyridine or a 3-functionalized 1,4-dihalobenzene, the palladium catalyst $Pd_2(DBZ)_3$, K_3PO_4, and tricyclohexylphosphine in a mixture of dioxane and water. Products were obtained in fair yields of sufficient purity by recrystallization. Furthermore, the reaction conditions were amenable to a wide range of functional groups and were even found to be effective for aryl chlorides. Using

dx.doi.org/10.1021/ic301893p | Inorg. Chem. 2013, 52, 4205−4216

this general synthetic procedure, a large number of 3-functionalized bipyridines (Bpy-R) and dipyridylbenzenes (DPBz-R) were prepared. The ligand abbreviations and associated structures are shown in Chart 1.

Another route to functionalized pillar ligands was found by simply using the well-known amide coupling reaction between an amine and an acid chloride as used to form *N*-(4-pyridyl)isonicotinamide.[59] Modifications of this reaction using commercially available 3-substituted 4-aminopyridine derivatives yielded three functionalized versions of the pillar ligand as shown in Scheme 1 (PINA-R). Additional pillar ligands used in the preparation of PICNICs obtained through commercial sources or by literature preparations are also included in Chart 1.

Synthesis of PICNICs. The preparation of the PICNIC materials was accomplished in essentially quantitative yield using a generalized synthetic method we call HIPL and is outlined in Scheme 1. The synthetic technique is a modification to a similar method first reported by Mathey et al. over two decades ago.[61] The brief report by Mathey suggested that pillared cyanonickelates could be formed by the reaction of pillaring ligands such as pyrazine or 4,4′-bipyridine with a suspension of anhydrous polymeric $Ni_2(CN)_4$ for a few minutes in boiling chloroform; however, no detailed investigations of the materials or further refinement or discussion of the method appeared in the literature.

We investigated the method previously and found it convenient for the preparation of polycrystalline PICNICs with common pillar ligands such as pyrazine, 4,4′-bipyridine, 1,2-dipyridylacetylene, and 1,2-bis(4-pyridyl)ethylene.[28,33] While the products of the reaction scheme may lack the high degree of crystallinity typically obtained through more conventional solution-based or solvothermal synthetic methods, the quantitative yields and exceptional convenience of the method make it very well-suited for preparing a highly diverse array of structurally analogous samples of sufficient structural integrity to allow for a rapid screening of material structure/property relationships, such as CO_2 adsorption affinity, for example. Thus, we decided to take full advantage of the HIPL method and greatly expanded it in scope. The method was found to be effective using pillar ligands that coordinate through pyrazine, pyridine, or amine nitrogen and is amenable to a wide variety of functional groups.

While the exact mechanism of the HIPL reaction is not known, it most likely proceeds through a surface adsorption/intercalation process since the polymeric $Ni_2(CN)_4$ is highly insoluble in common organic solvents. What is somewhat remarkable is how efficiently relatively long and even functionalized linkers can insert into the structure. As such, the HIPL method takes advantage of the stable preformed polymeric 2-D $Ni_2(CN)_4$ networks which direct the final layered structure and helps to suppress potential complications that may arise when coordination polymers are assembled using functionalized ligands with multiple coordination sites and free metal ions from solution. This structure-directing ability is perhaps best exemplified in the preparation of PICNIC-27, with the 4,4′-Bpm pillar ligand producing a rare open pore structure containing a nonmetalated 2,2′-bipyridyl structural unit.[62−65]

The reaction is facilitated by the presence of reactive unsaturated Ni sites produced after dehydration of $Ni_2(CN)_4$ hydrate and by the small particle size of the $Ni_2(CN)_4$ starting material, which aids in the suspension of the particles and provides a high surface area for the intercalation reaction. The reaction also has the benefit of forming the product in essentially quantitative yields using only a few percent excess of molar equivalents of pillar ligand to $Ni_2(CN)_4$. Such high percentage yields can often be difficult to achieve using traditional synthetic approaches where the coordination polymer is precipitated from a coordinating solvent solution or prepared using solvothermal methods.

While attempts to use hydrated $Ni_2(CN)_4$ directly (without prior evacuation of coordinated water) were not as effective, exploratory reactions using $Fe(H_2O)_2[Ni(CN)_4]$ hydrate and $Co(H_2O)_2[Ni(CN)_4]$ hydrate were found to proceed well in dry ethanol or dry acetonitrile without first drying the starting polymeric cyanometalates. It is interesting to compare the method for reactions involving Fe since derivates of pillared $FeNi(CN)_4$ compounds have previously been reported using traditional precipitation reactions from solution. For the Fe(pyrazine)$Ni(CN)_4$ compound, formation of the product occurs in near-quantitative yield from the reaction of molar equivalents of a ferrous salt with pyrazine and $[Ni(CN)_4]^{2-}$ in methanol/water mixtures.[32] For solution reactions involving the more reactive 4,4′-azopyridine pillar ligand, however, the propensity of the Fe^{2+} and 4,4′-azopyridine linker to form a polymeric product complicates the reaction, and formation of the targeted Fe(4,4′-azopyridine)$Ni(CN)_4$ compound required a 100-fold excess of Fe^{2+}.[25] A report for the solution precipitation preparation of Fe(4,4′-dipyridylacetylene)$M(CN)_4$ showed the potential for the pillar ligand to be adsorbed into the pore network as a guest.[26] Investigations in our laboratory also indicated that forming Fe-based PICNICs with bpy or bpene pillar ligands using solution reactions was difficult. Tests using the HIPL method were more effective with reactions using molar equivalents of $FeNi(CN)_4$ or $FePd(CN)_4$ and pillar linkers, including pyz, bpy, bpene, and pXdAm, producing porous products. Considering the exceptional spin-crossover behavior[25,26,32,48,66−68] reported for many Fe(L)$M(CN)_4$ compounds, it appears promising that the HIPL reaction may provide a means of preparing many more magnetically interesting compounds in this series which may be otherwise difficult to obtain by precipitation from solution.

General Structure of PICNICs. While the polycrystalline nature of the materials is well-suited for the kinetic demands of the reaction scheme, their small particle sizes make structure determinations for these compounds challenging due to the broad nature of the diffraction peaks. Model compounds exist in the literature, however, that do provide a means to assign a qualitative description of how the PICNICs are assembled. The crystal structures of several related compounds, including Fe(bpene)$Pt(CN)_4$,[31] Fe(DPAC)$M(CN)_4$,[26] Fe(pyrazine)$M(CN)_4$,[32,48] Fe(4,4′-azopyridine)$M(CN)_4$,[25] Zn(*N*-(4-pyridyl)-isonicotinamide)$Ni(CN)_4$,[27] and Ni(α,ω-diaminoalkane)$Ni(CN)_4$,[29] all show the same general structural motif, which involves an inorganic 2-D $M^A[M^B(CN)_4]$ grid network where the M^A metal ion has octahedral coordination and the M^B complex is square planar. Pillaring of the 2-D networks is achieved through the coordination in the direction perpendicular to the square planar complex of an organic diaza bridging ligand (pillar ligands) to the octahedral M^{II} complex. This results in formation of an extended 3-D network. Moreover, the absence of pillar ligands on the four-coordinated square planar d^8 tetracyanometalate significantly enhances the porosity of these materials. As such, they are extended versions of the well-known Hofmann clathrates,[24,29,69−73] where coordinated NH_3

dx.doi.org/10.1021/ic301893p | *Inorg. Chem.* 2013, 52, 4205−4216

ligands on the octahedral metal sites have been replaced with pillar ligands.

The proposed general structure for the PICNIC materials involves the same structural motif as reported for other similar pillar Hofmann compounds. On the basis of this structural model, the interlayer spacing in each PICNIC can be determined by the *d*-spacing of the (001) diffraction peak in the X-ray powder diffraction pattern. The interlayer spacing for each compound prepared and the associated diffraction patterns are included in the Supporting Information. A representative sample of diffraction patterns for several PICNICs showing the span of interlayer spacing in the series is shown in Figure 1. The interlayer spacing for each material is close to that predicted from typical N−Ni bond lengths and the molecular dimensions of the respective pillar ligand.

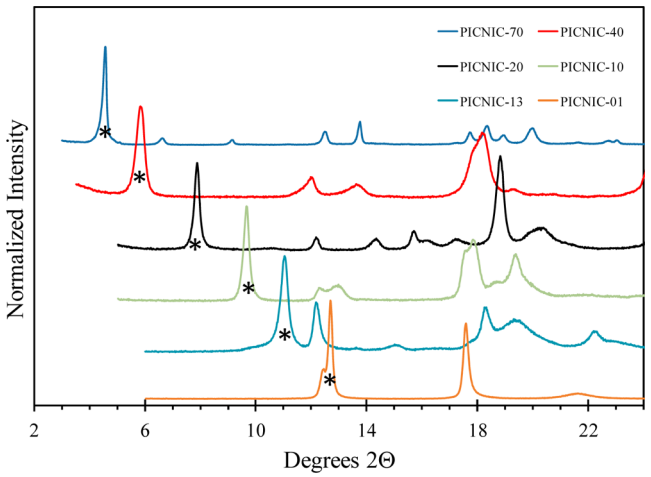

Figure 1. Representative series of powder X-ray diffraction patterns for several PICNICs. The range of interlayer spacings (ca. 7−19 Å) in the materials is indicated by the position of the (001) interlayer reflection marked by an asterisk in the figure. See Chart 1 for ligand and PICNIC abbreviations.

Evidence for the presence of a porous structure in the PICNIC compounds can be gained by thermal gravimetric analysis, which shows a clear step that accompanies the loss of guest solvents prior to the combustion of the compound to the metal oxide in air (see the Supporting Information). The original solvent guests can be exchanged by simple refluxing for several hours of the material in acetone or chloroform. This solvent extraction procedure also has the added benefit of helping to remove any excess ligand which may have adsorbed in the pore structure during the synthesis.[26,31,61] The solvent guests can be removed by heating under vacuum to produce a family of porous materials with interesting CO_2 adsorption behaviors.

CO_2 Adsorption. *Pore-Functionalized PICNICs.* Included in the current Article is one of the most extensive groups of pore-functionalized derivatives within a structurally related family of porous coordination polymers reported to date. Some of the best known families of structurally homologous porous coordination polymers containing organic functional groups within their pore structures include ZIFs,[19] isorecticular metal organic frameworks (IRMOFs),[7] and the MIL series.[10] Similar to the widely studied ZIF, IRMOF, and MIL materials, the PICNIC family of materials have a broad distribution in pore dimensions and pore functionalization while maintaining an open pore structure available for CO_2 adsorption.

The shortest pillar ligands include those based on the pyrazine ligand. Powder X-ray diffraction patterns for Ni(L)-$Ni(CN)_4$, where L = Pyz, Pyz-Am, and Pyz-Me, are indicative of a structurally homologous series with a pillared motif similar to that reported for $Fe(Pyz)M(CN)_4$ (see the Supporting Information, Figure S3). The CO_2 adsorption isotherms measured at 0 °C for four Pyz-PICNICs are shown in Figure 2A. As expected within an isostructural series, the adsorption capacity decreases in an inverse relationship with the size of the functional group. The adsorption capacity for PICNIC-01 approaches 1.5 CO_2 per pore and decreases to slightly less than 1 CO_2 per pore for PICNIC-03, where Pyz-Me is the pillar ligand, whereas the CO_2 uptake for PICNIC-04 with the −OMe substituent is negligible. The incorporation of the amine functional group in PICNIC-02 has little effect on the CO_2 affinity of the pore, likely as a result of the insufficient basicity of the aromatic amine to significantly affect the CO_2 adsorption potential. It is interesting to note that the CO_2 capacity of PICNIC-03 with Pyz-Me as the pillar ligand is slightly below 1 CO_2 per pore, suggesting that the pore dimensions are on the order of the molecular dimensions of CO_2. As shown in Figure 2B, the pore constriction has a significant effect on the adsorption of N_2, which is decreased to a negligible amount in

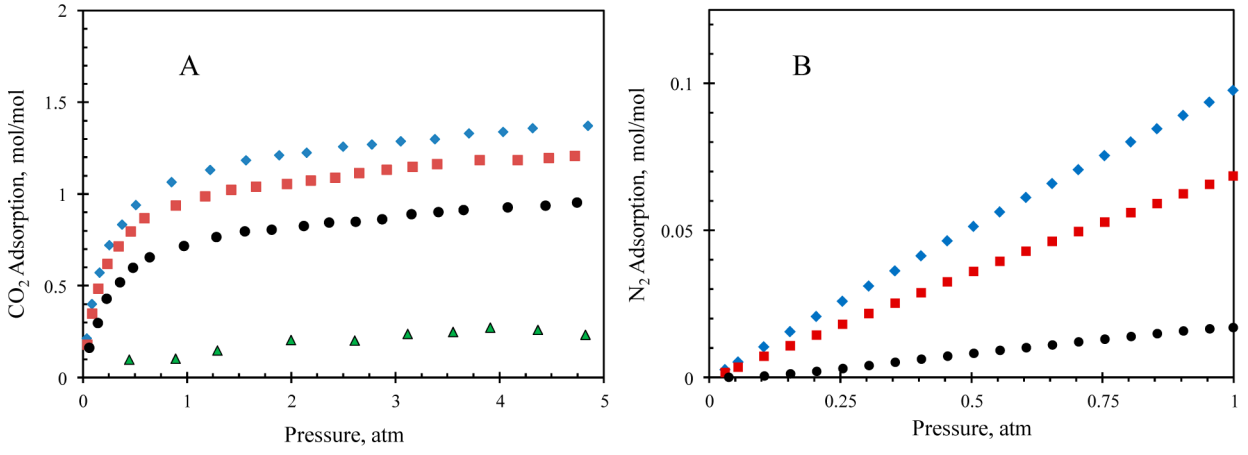

Figure 2. Adsorption isotherms for the $Ni(Pyz\text{-}R)Ni(CN)_4$ series: (A) CO_2 at 0 °C, (B) N_2 at 0 °C. Key: PICNIC-01, R = H (blue tilted squares); PICNIC-02, R = NH_2 (red squares); PICNIC-03, R = CH_3 (black circles); PICNIC-04, R = OCH_3 (green triangles).

dx.doi.org/10.1021/ic301893p | *Inorg. Chem.* 2013, 52, 4205−4216

the PICNIC-03 material. The pure isotherm data suggest that the pore constriction provided by the methyl functional group may provide an effective means for increasing CO_2 adsorption selectivity versus other larger gases such as CH_4 and N_2.

Inclusion of substituted PINA-R pillars offers the potential for incorporating two functional groups into the pore structure, with one being the functional group on the 3-position of one of the pyridines in the molecule and the other being the amide linker between the pyridine rings. The affinity of the PINA molecule to generate hydrogen-bonding interactions is clearly observed in the reported crystal structure of the material.[74] Powder X-ray diffraction patterns for the HIPL-prepared PINA-R derivatives of $Ni(L)Ni(CN)_4$, where L = PINA, PINA-F, PINA-Me, and PINA-NO_2, are indicative of a structurally homologous series with a pillared motif similar to that reported for $Zn(PINA)Ni(CN)_4$ (see the Supporting Information, Figure S2). The CO_2 adsorption isotherms for the four PICNIC compounds are shown in Figure 3. All four

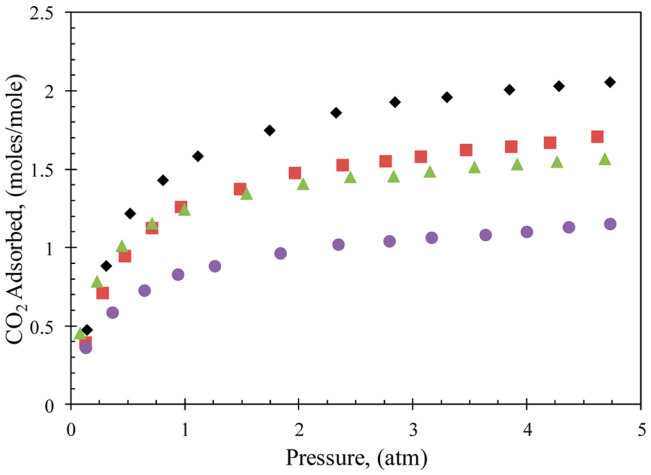

Figure 3. CO_2 adsorption isotherms at 0 °C on the Ni(PINA-R)$Ni(CN)_4$ series: R = H, PICNIC-30 (black tilted squares); R = CH_3, PICNIC-31 (green triangles); R = F, PICNIC-32 (red squares); R = NO_2, PICNIC-33 (purple circles). See Chart 1 for ligand and PICNIC abbreviations.

compounds are porous structures, with the nonfunctionalized PINA pillar in PICNIC-30 providing the material with the highest adsorption capacity for CO_2 in the series. As observed with the pyrazine series, none of the functional groups on the pillar ligand show any significant enhancement to the CO_2 adsorption potential. The total adsorption capacity for CO_2 decreases with increasing functional group size from ~2 CO_2/mol for PICNIC-30 to ~1.5 CO_2 for PICNIC-31 to ~1 CO_2 for PICNIC-33. The CO_2 capacity for PICNIC-32 with a fluoro functional group is slightly lower than expected on the basis of this trend due to a slightly smaller interlayer spacing in the material (see the Supporting Information, Figure S2). All of the samples show a relatively low saturation pressure of ~2 atm of CO_2.

A third structurally analogous series of PICNICs was successfully prepared via substitution of BPY pillars for BPY-R pillars as verified by the similar diffraction patterns (see the Supporting Information, Figure S1) observed for the materials. Normalized CO_2 adsorption isotherms measured at 0 °C for the seven PICNIC samples containing the Bpy-R pillar ligands are shown in Figure 4. The isotherm for the related 4,4′-Bpm

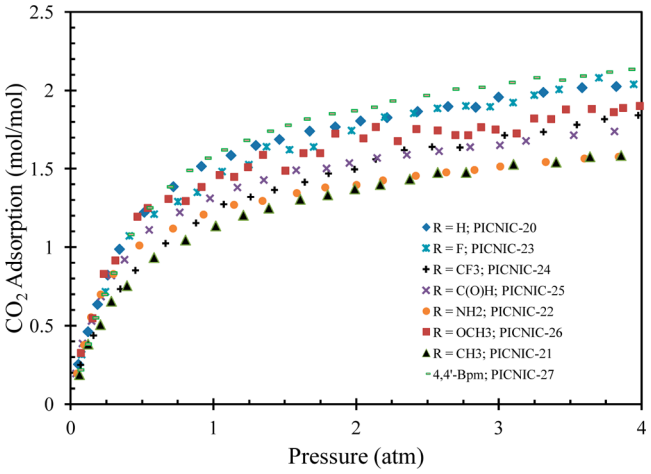

Figure 4. Adsorption isotherms for CO_2 at 0 °C on the Ni(Bpy-R)$Ni(CN)_4$ series. See Chart 1 for ligand and PICNIC abbreviations.

pillared PICNIC is included as well. Again, the CO_2 adsorption capacity shows trends similar to those observed for the PICNIC compounds with the Pyz-R and PINA-R pillar ligands, where the functional group in the pore is detrimental to the adsorption capacity due to the steric influence of the functional group. The two PICNICs out of order with regard to the trend are the two compounds with OMe and C(O)H functional groups which show slightly higher CO_2 uptakes than the CH_3 and NH_2 functionalized materials. The five-point N_2 BET surface areas for the series of materials are listed in Table 1. The

Table 1. N_2 Five-Point BET Surface Areas (SAs) of the Bpy-R Series of PICNICs

sample	pillar ligand	fw	five-point BET SA (m^2/g)	SA (m^2/mmol)
PICNIC-20	Bpy	377.6	622	235
PICNIC-21	Bpy-CH3	391.7	466	183
PICNIC-22	Bpy-NH2	392.7	453	178
PICNIC-23	Bpy-F	395.6	600	237
PICNIC-24	Bpy-CF3	445.6	448	200
PICNIC-25	Bpy-Ald	405.7	443	180
PICNIC-26	Bpy-OMe	407.7	441	180
PICNIC-27	4,4′-Bpm	379.6	542	206

surface areas follow trends similar to those of the CO_2 absorption behaviors in the materials, with the Bpy, Bpy-F, and 4,4′-Bpm pillared PICNICs having the highest surface areas and the remaining Bpy-R pillared compounds having lower and very similar surface areas.

The similarity in isotherm behavior for the PICNIC-20 through PICNIC-26 samples is further evidence that the materials are isostructural and amenable to inclusion of the wide range of functional groups included on the BPY-R ligands. Nevertheless, as observed in the PYZ-R and PINA-R pillared PICNICs, the functional groups on the BPY-R ligands appear to have no significant enhancement to the CO_2 adsorption affinity of the pore systems. The presence of the functional group is in fact even detrimental in terms of gravimetric uptake, where the less massive nonfunctionalized BPY sample PICNIC-20 performs best in both the low- and high-pressure regions.

The CO_2 adsorption capacities for the Pyz-R, PINA-R, and Bpy-R series are consistent with a structurally homologous family of materials where the pore functional groups occupy a

dx.doi.org/10.1021/ic301893p | Inorg. Chem. 2013, 52, 4205−4216

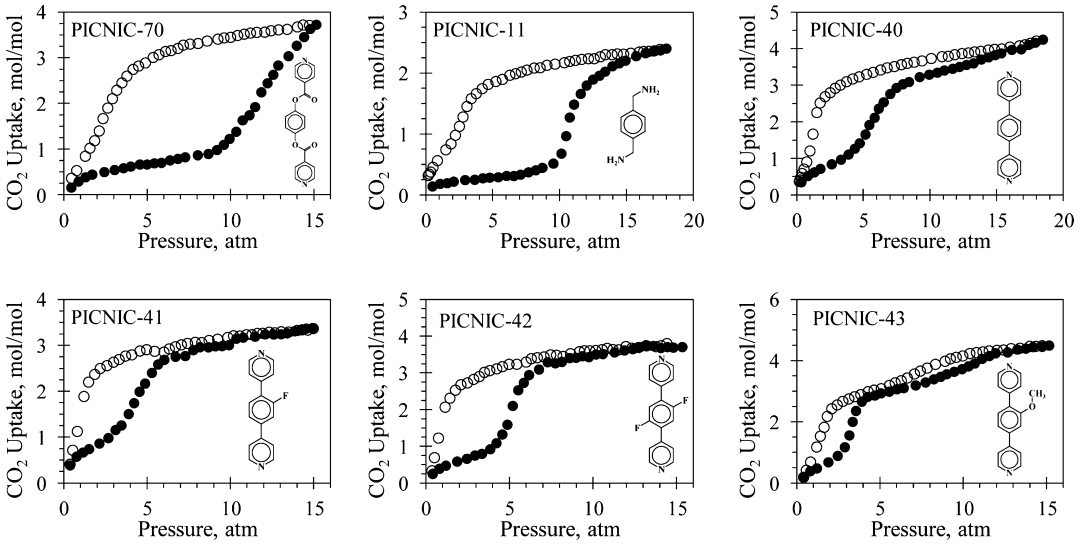

Figure 5. Adsorption (solid symbols) and desorption (open symbols) isotherms for CO_2 at −15 °C on several newly discovered structurally dynamic PICNICs (the structure of the pillar ligand is shown).

portion of the void space and thereby limit the total CO_2 uptake. The reduction in void volume due to the functional group correlates well with the decrease in CO_2 adsorption capacity within each series of materials. What is perhaps unexpected is how the functional groups appear to have little or no effect on the CO_2 affinity in the low-pressure regions of the isotherms, the region most important in postcombustion capture of CO_2 from power plant flue gas. In each series of materials, the PICNIC containing the nonfunctionalized pillar ligand functions as well or better than most of the pore-functionalized materials.

This result may be due to several factors affecting the CO_2 adsorption in these materials. One influence may be due to the electronic properties of the pyridine ring acting to diminish the effectiveness of the functional group. This is highly likely, for example, in the case of the $-NH_2$ functional group, where the basicity of the amine nitrogen is decreased several orders of magnitude relative to that of the alkylamine analogue. A second factor to be considered is the relatively narrow pore space which exists between the pillar ligands. This inter pillar distance is on the order of the length of a CO_2 molecule. Computation modeling of the CO_2 packing arrangement in the structurally similar $Fe(Pyz)Ni(CN)_4$ material showed a favored orientation where the CO_2 was bridged between two pyrazine pillars via hydrogen bonds between the ring hydrogens and CO_2 oxygens, with significant CO_2−CO_2 interactions in the adsorbed state.[75] This preferred packing arrangement for CO_2 may explain why the nonfunctionalized pillars provide a highly competitive CO_2 adsorption potential compared to the functionalized materials since the steric influence of the functional group would be a strong driving force for an alternative, and perhaps less energetically favorable, CO_2 packing arrangement. In addition, the presence of a functional group in a confined space may limit the ability of the adsorbed CO_2 molecule and functional group to orient in the proper positions in which to take advantage of the attractive forces that would be present between the two in a nonhindered environment.[76] Efforts are under way to obtain single crystals for several samples so that detailed structural models of the materials can be obtained and the effects of the functional groups on the packing arrangement of CO_2 can be calculated to better understand this intriguing result.

Structurally Dynamic PICNICs. A recent report highlighted the ability of PICNIC-60 to act as a structurally dynamic sorbent with the Bpene pillar ligand.[28] The behavior was unusual in the fact that shorter pillar ligands such as Pyz and Bpy did not show structural flexibly. Perhaps even more unusual was the lack of structural flexibility with other pillar ligands of similar molecular geometry such as DPAC and Bpane.[28] As discussed above, none of the PINA-R derivatives (PICNIC-30, -31, -32, and -33) show structurally dynamic behavior even though the length and geometry of the PINA-R pillar ligands are very similar to those of Bpene.

These results indicate that the structurally dynamic behavior of PICNIC-60 is not a simple function of interlayer spacing or molecular geometry. This conclusion is further demonstrated by several newly discovered flexible PICNICs whose isotherms are shown in Figure 5. The isotherms are all plotted at the same temperature of −15 °C. The pillar ligands vary in both functionality and molecular dimensions and include the nonlinear linker pXdAm, along with several linear DPBz-R analogues. The interlayer spacing is shortest for PICNIC-11 (∼10 Å) with the pXdAm pillar ligand and longest in PICNIC-70 (∼19 Å) with the IsoNicBz pillar ligand.

Several interesting results are noted in the isotherm data shown in Figure 5. First, the widths of the hysteresis loops and adsorption threshold pressures (P_{th}) vary over a relatively wide pressure range of 3−10 atm. Additionally, each of the flexible PICNICs with the exception of pXdAm shows an uptake of approximately 1 equiv of CO_2 prior to the P_{th}. For the pXdAm PICNIC, the uptake of CO_2 prior to P_{th} is essentially half that of the others. It is also interesting to note the similarity in P_{th} for PICNIC-11 and -70 even though the pXdAm and IsoNicBz pillar ligands are structurally quite different and the CO_2 adsorption capacities of the two materials differ by at least a factor of 2.

This result is somewhat surprising since one might expect the PICNIC-70 material with the much longer IsoNicBz ligand to have a larger energy requirement for structural reorganization. In contrast, the isotherm results for PICNIC-40, -41, -42, and -43, which all contain similar DPBz-R analogues, all show similar P_{th} values, as might be expected due to the similarity in pillar ligands. In fact, the P_{th} values for the DPBz-R PICNICs

dx.doi.org/10.1021/ic301893p | Inorg. Chem. 2013, 52, 4205−4216

are only slightly higher than that of PICNIC-60 and show similar CO_2 adsorption capacities as well.[28] This is in line with what one might expect on the basis of the molecular dimensions of the pillar ligands.

The interpretation, however, gets more complicated when additional DPBz-R PICNICs are studied. The isotherms plotted in Figure 6 for three additional DPBz-R-based

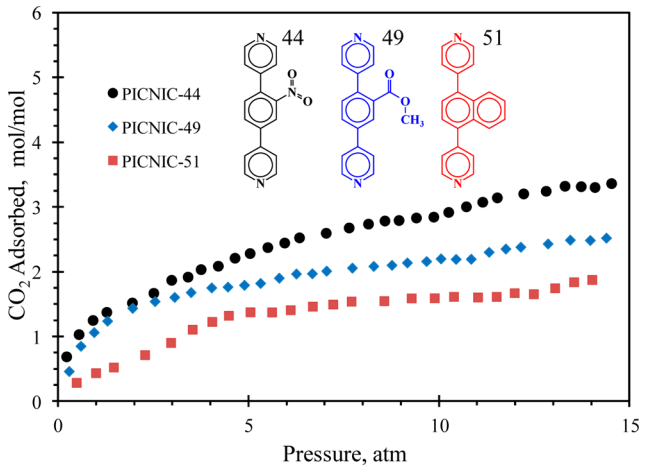

Figure 6. Adsorption isotherms measured at 0 °C for CO_2 on three nonflexible Ni(DPBz-R)Ni(CN)$_4$-based PICNICs (structures of pillar ligands are shown). The adsorption behavior is in contrast to that of PICNIC-40, -41, -42, and -43 with similar DPBz-R ligands as shown in Figure 5.

PICNICs do not show the same dynamic isotherms. The isotherms for PICNIC-44, -49, and -51 show more type I behavior, albeit there does exist a slightly distorted low-pressure region for PICNIC-51. A significant contrast in behaviors is also observed when comparing the similar DPBz-Est and DPBz-OMe PICNICs. The DPBz-Est pillared PICNIC-49 CO_2 isotherm in Figure 6 shows nonflexible behavior, while the DPBz-OMe pillared PICNIC-43 CO_2 isotherm shown in Figure 5 is more complex with two separate transitions. The two materials also show a large difference in their level of structural stability between their guest-loaded and guest-free states as evidenced by their respective powder X-ray diffractions patterns (see Figures S9 and S10 in the Supporting Information).

Another example of a large contrast in sorbent behavior resulting from a relatively small change in pillar chemistry is obtained when the pXdAm pillar in PICNIC-11 is replaced with a fluorinated ring derivative, pXdAm-F$_4$, to give PICNIC-12. While PICNIC-11 is structurally dynamic during CO_2 adsorption, PICNIC-12 does not reopen to adsorb CO_2. As indicated by the powder diffraction patterns for PICNIC-12 shown in Figure 7, a significant loss of structural order occurs in PICNIC-12 when the guest toluene molecules are removed from the pore system after the initial synthesis. However, readsorption of toluene by the material regenerates the original structure. Thus, the structural transition between collapsed and open pore structures is reversible in PICNIC-12, but the energy required to drive the structural transition cannot be supplied by CO_2 adsorption alone.

A final and equally impressive demonstration of this fine balance between pillar ligand and sorbent property in the PICNIC compounds is shown by comparison of the CO_2 adsorption isotherms for PICNIC-60 and PICNIC-62 in Figure

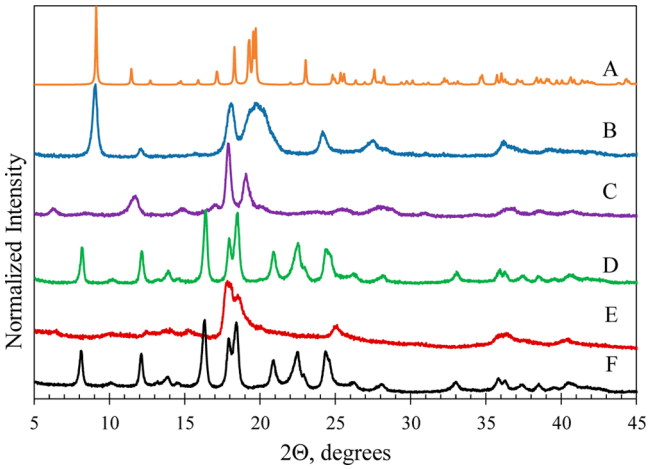

Figure 7. Powder X-ray diffraction patterns for PICNIC-11 (B) toluene loaded and (C) guest free and PICNIC-12 (D) toluene loaded, (E) guest free, and (F) after readsorption of toluene. The pillar ligands are pXdAm and pXdAm-F4, respectively. The structure transition of PICNIC-11 is reversible for CO_2 adsorption as shown in Figure 5, but the structure transition of PICNIC-12 is not reversible for CO_2 adsorption. PICNIC-12 will, however, reversibly desorb and adsorb toluene as shown by the three lower diffraction patterns. The calculated XRD pattern of the structurally related Cd(pXdAm)Ni(CN)$_4$-*o*-toluidine (A) as reported by Yuge et al. is included as a reference.[34].

8. Both materials were prepared by the HIPL method, and the two pillar ligands involved, Bpene and AzoPyr, respectively,

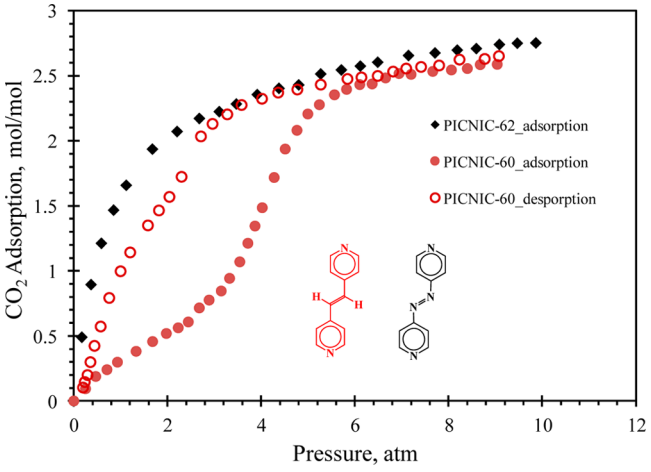

Figure 8. Contrasting CO_2 adsorption behaviors at 0 °C for PICNIC-60 and PICNIC-62 even though the pillar ligands involved, Bpene and AzoPyr, respectively, are nearly identical in molecular dimensions.

differ only in the substitution of a C═C bond for a N═N bond between the two pyridine rings. While the normalized adsorption capacities are nearly identical, PICNIC-60 is structurally dynamic and PICNIC-62 is not.

The mechanism for the behavior of these materials is still under investigation in our laboratory. It is clear in some cases, e.g., PICNIC-60 and PICNIC-11, from X-ray powder diffraction analysis that the isotherm behavior in the flexible PICNICs is due to a structural transition that affects the interlayer spacing in the materials. This structural transition appears to result from a change in the in-plane bonding geometry of the Ni−CN−Ni network, which effectively

dx.doi.org/10.1021/ic301893p | Inorg. Chem. 2013, 52, 4205−4216

changes the tilt angle of the pillar ligand. This variation in tilt angle affects the interpillar distance and the available free volume for guest adsorption. However, for some of the flexible PICNICs the shifts in interlayer spacings are much more subtle, suggesting that a mechanism involving ring orientation of the pillar ligands may be at play. The phase transition has been shown to be an interplay of energetic terms which ultimately lower the thermodynamic potential of the system and drive both the structure change and incorporation of gas guest. As such, one expects that even subtle changes in the ligand structure, hydrogen bonding within the material, ligand–ligand interactions, and the ability of a gas guest to adsorb and stabilize the open pore network would collectively play a role in dictating the conditions for this phase change to occur. In this regard, the PICNIC architecture affords an opportunity to systematically interrogate these energetics by varying the pillar ligands.

PICNICs Containing Other Metals. With the success of the HIPL technique in the preparation of nickel-based PICNICs, preliminary investigations were conducted to test the wider applicability of the method in the synthesis of Fe- and Co-containing PICNICs. Porous materials were formed for Co(AmMe-Pyr)Ni(CN)$_4$, Co(pXdAm)Ni(CN)$_4$, Fe(Pyz)Ni(CN)$_4$, Fe(Bpy)Ni(CN)$_4$, Fe(Bpene)Pd(CN)$_4$, and Fe(pXdAm)Ni(CN)$_4$ by a method similar to that used in the preparation of the nickel-based PICNICs. The CO_2 adsorption isotherms for several of these compounds are shown in Figures 9 and 10. The CO_2 adsorption behavior follows trends similar

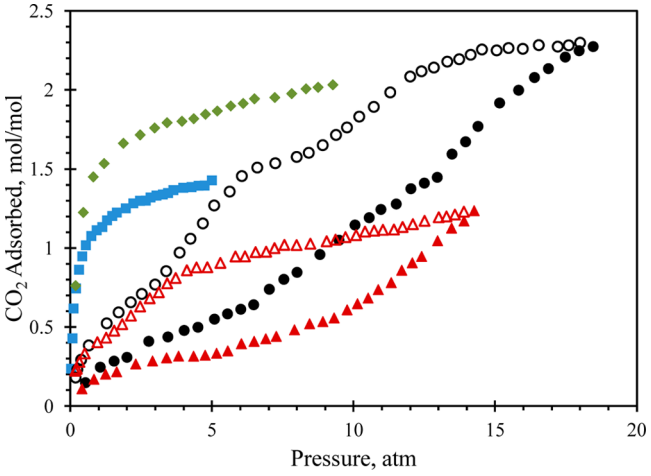

Figure 9. Adsorption (solid symbols)/desorption (open symbols) cycles for CO_2 on Fe(L)M(CN)$_4$ PICNIC derivatives, where M = Ni, L = Bpy (green tilted squares, T = 0 °C), M = Ni, L = Pyz (blue squares, T = 0 °C), M = Ni, L = Bpene (black circles, T = 0 °C), and M = Ni, L = pXdAm (red triangles, T = −25 °C). See Chart 1 for ligand abbreviations.

to those observed with the nickel-based PICNICs, with the Bpene and pXdAm pillar ligands giving structurally dynamic materials and the Pyz and Bpy pillars giving nonflexible samples. The Fe(Pyz)Ni(CN)$_4$ prepared by the HIPL method reported herein shows the expected color change related to the spin-crossover transition[32] and CO_2 adsorption behavior similar to the results reported by Southon et al. for the Fe(Pyz)Ni(CN)$_4$ material prepared by the conventional precipitation method.[48] The results are encouraging since, to date, only a few pillar ligands have been reported for iron-based PICNICs in the literature and each of these reported structures shows

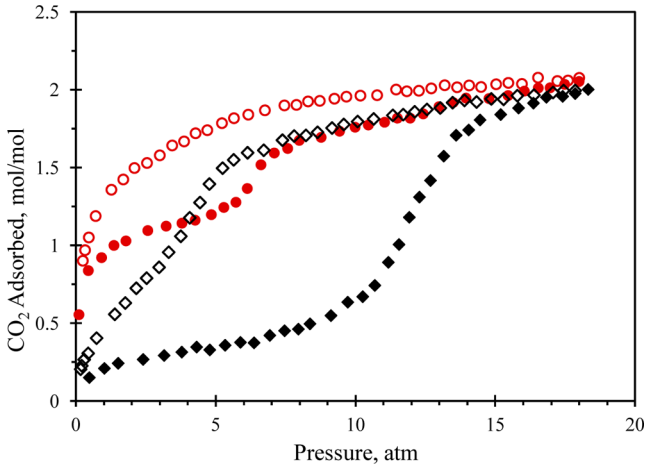

Figure 10. Adsorption (solid symbols)/desorption (open symbols) cycles for CO_2 measured at −15 °C for two Co(L)Ni(CN)$_4$ PICNICs, where L = AmMe-Pyr (red circles) and pXdAm (black tilted squares). See Chart 1 for ligand abbreviations.

interesting spin-crossover behavior. On the basis of the preliminary results reported herein, the HIPL method may provide a convenient avenue to the preparation of other magnetically interesting Fe-based PICNICs that are challenging to produce by traditional precipitation methods, some of which, e.g., the Bpene and pXdAm materials, may show unusual CO_2 adsorption influences on their structural and magnetic properties.

CONCLUSION

A number of ring-functionalized dipyridyl-based bridging ligands were synthesized using Suzuki coupling reactions and traditional amide coupling reactions. The functionalized ligands were used in the formation of a structurally homologous series of porous materials built on the pillared cyanonickelate structure motif. The porous coordination polymers were prepared in essentially quantitative yield by a convenient heterogeneous intercalation of pillaring ligand reaction using insoluble polymeric nickel cyanide as a structural building block. The use of a preformed 2-D network as a building block helped to direct the final structure of the material into a 3-D porous framework with little interference from the functional groups. The structure-directing property of the prefabricated 2-D Ni$_2$(CN)$_4$ networks is particularly well-demonstrated by the formation of PICNIC-27, a rarely observed porous coordination polymer containing a nonmetalated 4,4′-bipyrimidine pillar ligand.[63] The CO_2 adsorption isotherms and powder X-ray diffraction analyses were consistent with the formation of an isostructural series of PICNICs when pillar ligands of similar molecular geometries were used. The CO_2 adsorption behaviors within an isostructural series showed a decrease in capacity for the functionalized materials due to occupation of the void volume by the functional groups. In spite of the large number of functional groups incorporated into the materials, none were found which showed any significant enhancement of CO_2 affinity in the materials.

Several of the PICNICs showed structurally dynamic behavior during the adsorption and desorption of guests. The structural flexibility is likely the result of corrugated Ni$_2$(CN)$_4$ sheets that have the ability to adjust the bond angles within the cyanide-bridged network, which ultimately affects the tilt angle

dx.doi.org/10.1021/ic301893p | Inorg. Chem. 2013, 52, 4205−4216

of the pillar ligands; however, the adsorption/desorption mechanisms in these materials are still under investigation in our laboratory. The structurally dynamic materials showed a range of threshold pressures for CO_2 adsorption. As such, PICNICs are an unusual class of compounds where the structural flexibility of the material can be tuned by small adjustments in the properties of the pillaring ligand. With the interest in structurally dynamic materials as gas-selective sorbents, PICNICs may prove to be a valuable class of sorbent for understanding the subtle interplay between thermodynamics and host−guest behavior. The ability to potentially tune the P_{th} and ΔP_{hys} in these materials may also provide benefits in applications involving high-pressure capture of CO_2.

The assembly technique used for the synthesis of nickel-based PICNICs was also found to be suitable for preparing other derivatives containing iron and cobalt in place of the six-coordinate nickel site. The iron and cobalt analogues also showed the ability to form structurally dynamic materials similar to the nickel-based compounds. The iron-based materials are particularly attractive in light of the recent literature reports of similar compounds having spin-crossover behavior at room temperature. Thus, the HIPL method may prove to be an alternative synthetic route or a convenient method for rapidly screening a large number of $Fe(L)M(CN)_4$ compounds for spin-crossover behavior. The structurally dynamic behavior that appears to be a common trait for these pillared cyanonickelates could also lead to several new $Fe(L)M(CN)_4$ compounds with interesting associations between host−guest interactions or CO_2 adsorption/desorption and magnetic properties.

■ ASSOCIATED CONTENT

Supporting Information

CHN analysis for pillar ligands, NMR analysis of pillar ligands, calculated formula weights of PICNICs from TGA, powder X-ray diffraction patterns for PICNICs, TGA of PICNICs, and powder XRD of residual iron−nickel oxides and cobalt−nickel oxides after TGA.. This material is available free of charge via the Internet at http://pubs.acs.org.

■ AUTHOR INFORMATION

Corresponding Author

*Fax: (412)-386-4542. E-mail: jeffrey.culp@contr.netl.doe.gov.

Notes

This Article was prepared as an account of work sponsored by an agency of the U.S. Government. Neither the U.S. Government nor any agency thereof, nor any of their employees, makes any warranty, express or implied, or assumes any legal liability or responsibility for the accuracy, completeness, or usefulness of any information, apparatus, product, or process disclosed, or represents that its use would not infringe privately owned rights. Reference herein to any specific commercial product, process, or service by trade name, trademark, manufacturer, or otherwise does not necessarily constitute or imply its endorsement, recommendation, or favoring by the U.S. Government or any agency thereof. The views and opinions of authors expressed herein do not necessarily state or reflect those of the U.S. Government or any agency thereof.

The authors declare no competing financial interest.

■ ACKNOWLEDGMENTS

This technical effort was performed in support of National Energy Technology's ongoing research in CO_2 capture under RES Contract DE-FE0004000. Catherine Madden was supported by the U.S. Department of Energy (DOE) Office of Fossil Energy Mickey Leland Energy Fellowship (MLEF) Program. We thank Dr. Bret Howard at the National Energy Technology Laboratory for assistance with the X-ray powder diffraction measurements.

■ REFERENCES

(1) Batten, S. R.; Champness, N. R.; Chen, X. M.; Garcia-Martinez, J.; Kitagawa, S.; Ohrstrom, L.; O'Keeffe, M.; Suh, M. P.; Reedijk, J. *CrystEngComm* **2012**, *14*, 3001.
(2) Biradha, K.; Ramana, A.; Vittal, J. J. *Cryst. Growth Des.* **2009**, *9*, 2969.
(3) Li, J. R.; Ma, Y. G.; McCarthy, M. C.; Sculley, J.; Yu, J. M.; Jeong, H. K.; Balbuena, P. B.; Zhou, H. C. *Coord. Chem. Rev.* **2011**, *255*, 1791.
(4) Li, J. R.; Sculley, J.; Zhou, H. C. *Chem. Rev.* **2012**, *112*, 869.
(5) Liu, J.; Thallapally, P. K.; McGrail, B. P.; Brown, D. R. *Chem. Soc. Rev.* **2012**, *41*, 2308.
(6) Meek, S. T.; Greathouse, J. A.; Allendorf, M. D. *Adv. Mater.* **2011**, *23*, 249.
(7) Yaghi, O. M.; O'Keeffe, M.; Ockwig, N. W.; Chae, H. K.; Eddaoudi, M.; Kim, J. *Nature* **2003**, *423*, 705.
(8) Zhou, H. C.; Long, J. R.; Yaghi, O. M. *Chem. Rev.* **2012**, *112*, 673.
(9) Banerjee, R.; Furukawa, H.; Britt, D.; Knobler, C.; O'Keeffe, M.; Yaghi, O. M. *J. Am. Chem. Soc.* **2009**, *131*, 3875.
(10) Devic, T.; Horcajada, P.; Serre, C.; Salles, F.; Maurin, G.; Moulin, B.; Heurtaux, D.; Clet, G.; Vimont, A.; Greneche, J. M.; Le Ouay, B.; Moreau, F.; Magnier, E.; Filinchuk, Y.; Marrot, J.; Lavalley, J. C.; Daturi, M.; Ferey, G. *J. Am. Chem. Soc.* **2010**, *132*, 1127.
(11) Eddaoudi, M.; Kim, J.; Rosi, N.; Vodak, D.; Wachter, J.; O'Keeffe, M.; Yaghi, O. M. *Science* **2002**, *295*, 469.
(12) Kitaura, R.; Fujimoto, K.; Noro, S.; Kondo, M.; Kitagawa, S. *Angew. Chem., Int. Ed.* **2002**, *41*, 133.
(13) Cohen, S. M. *Chem. Rev.* **2012**, *112*, 970.
(14) Costa, J. S.; Gamez, P.; Black, C. A.; Roubeau, O.; Teat, S. J.; Reedijk, J. *Eur. J. Inorg. Chem.* **2008**, 1551.
(15) Demessence, A.; D'Alessandro, D. M.; Foo, M. L.; Long, J. R. *J. Am. Chem. Soc.* **2009**, *131*, 8784.
(16) Hong, D. Y.; Hwang, Y. K.; Serre, C.; Ferey, G.; Chang, J. S. *Adv. Funct. Mater.* **2009**, *19*, 1537.
(17) Hwang, Y. K.; Hong, D. Y.; Chang, J. S.; Jhung, S. H.; Seo, Y. K.; Kim, J.; Vimont, A.; Daturi, M.; Serre, C.; Ferey, G. *Angew. Chem., Int. Ed.* **2008**, *47*, 4144.
(18) Morris, W.; Doonan, C. J.; Furukawa, H.; Banerjee, R.; Yaghi, O. M. *J. Am. Chem. Soc.* **2008**, *130*, 12626.
(19) Phan, A.; Doonan, C. J.; Uribe-Romo, F. J.; Knobler, C. B.; O'Keeffe, M.; Yaghi, O. M. *Acc. Chem. Res.* **2010**, *43*, 58.
(20) Gao, C. Y.; Liu, S. X.; Xie, L. H.; Ren, Y. H.; Cao, J. F.; Sun, C. Y. *CrystEngComm* **2007**, *9*, 545.
(21) Maji, T. K.; Uemura, K.; Chang, H. C.; Matsuda, R.; Kitagawa, S. *Angew. Chem., Int. Ed.* **2004**, *43*, 3269.
(22) Song, P.; Liu, B.; Li, Y. Q.; Yang, J. Z.; Wang, Z. M.; Li, X. G. *CrystEngComm* **2012**, *14*, 2296.
(23) Wang, X. F.; Wang, Y.; Zhang, Y. B.; Xue, W.; Zhang, J. P.; Chen, X. M. *Chem. Commun.* **2012**, *48*, 133.
(24) Hofmann, K. A.; Höchtlen, F. *Ber. Dtsch. Chem. Ges.* **1903**, *36*, 1149.
(25) Agusti, G.; Cobo, S.; Gaspar, A. B.; Molnar, G.; Moussa, N. O.; Szilagyi, P. A.; Palfi, V.; Vieu, C.; Munoz, M. C.; Real, J. A.; Bousseksou, A. *Chem. Mater.* **2008**, *20*, 6721.
(26) Bartual-Murgui, C.; Salmon, L.; Akou, A.; Ortega-Villar, N. A.; Shepherd, H. J.; Munoz, M. C.; Molnar, G.; Real, J. A.; Bousseksou, A. *Chem.—Eur. J.* **2012**, *18*, 507.

(27) Chen, X.; Zhou, H.; Chen, Y. Y.; Yuan, A. H. *CrystEngComm* **2011**, *13*, 5666.
(28) Culp, J. T.; Smith, M. R.; Bittner, E.; Bockrath, B. *J. Am. Chem. Soc.* **2008**, *130*, 12427.
(29) Iwamoto, T. *J. Inclusion Phenom. Mol. Recognit. Chem.* **1996**, *24*, 61.
(30) Lemus-Santana, A. A.; Rodriguez-Hernandez, J.; Gonzalez, M.; Demeshko, S.; Avila, M.; Knobel, M.; Reguera, E. *J. Solid State Chem.* **2011**, *184*, 2124.
(31) Munoz-Lara, F. J.; Gaspar, A. B.; Munoz, M. C.; Arai, M.; Kitagawa, S.; Ohba, M.; Real, J. A. *Chem.—Eur. J.* **2012**, *18*, 8013.
(32) Niel, V.; Martinez-Agudo, J. M.; Munoz, M. C.; Gaspar, A. B.; Real, J. A. *Inorg. Chem.* **2001**, *40*, 3838.
(33) Culp, J. T.; Natesakhawat, S.; Smith, M. R.; Bittner, E.; Matranga, C.; Bockrath, B. *J. Phys. Chem. C* **2008**, *112*, 7079.
(34) Yuge, H.; Noda, Y.; Iwamoto, T. *Inorg. Chem.* **1996**, *35*, 1842.
(35) Chapman, K. W.; Southon, P. D.; Weeks, C. L.; Kepert, C. J. *Chem. Commun.* **2005**, 3322.
(36) Culp, J. T.; Matranga, C.; Smith, M.; Bittner, E. W.; Bockrath, B. *J. Phys. Chem. B* **2006**, *110*, 8325.
(37) Hu, L.; Zhang, P.; Chen, Q. W.; Yan, N.; Mei, J. Y. *Dalton Trans.* **2011**, *40*, 5557.
(38) Kaye, S. S.; Long, J. R. *J. Am. Chem. Soc.* **2005**, *127*, 6506.
(39) Kaye, S. S.; Long, J. R. *Chem. Commun.* **2007**, 4486.
(40) Motkuri, R. K.; Thallapally, P. K.; McGrail, B. P.; Ghorishi, S. B. *CrystEngComm* **2010**, *12*, 4003.
(41) Natesakhawat, S.; Culp, J. T.; Matranga, C.; Bockrath, B. *J. Phys. Chem. C* **2007**, *111*, 1055.
(42) Reguera, L.; Balmaseda, J.; Del Castillo, L. F.; Reguera, E. *J. Phys. Chem. C* **2008**, *112*, 5589.
(43) Thallapally, P. K.; Motkuri, R. K.; Fernandez, C. A.; McGrail, B. P.; Behrooz, G. S. *Inorg. Chem.* **2010**, *49*, 4909.
(44) Windisch, C. F.; Thallapally, P. K.; McGrail, B. P. *Spectrochim. Acta, Part A* **2009**, *74*, 629.
(45) Windisch, C. F.; Thallapally, P. K.; McGrail, B. P. *Spectrochim. Acta, Part A* **2010**, *77*, 287.
(46) Biradha, K.; Sarkar, M.; Rajput, L. *Chem. Commun.* **2006**, 4169.
(47) Kudo, N.; Perseghini, M.; Fu, G. C. *Angew. Chem., Int. Ed.* **2006**, *45*, 1282.
(48) Southon, P. D.; Liu, L.; Fellows, E. A.; Price, D. J.; Halder, G. J.; Chapman, K. W.; Moubaraki, B.; Murray, K. S.; Letard, J. F.; Kepert, C. J. *J. Am. Chem. Soc.* **2009**, *131*, 10998.
(49) Bureekaew, S.; Shimomura, S.; Kitagawa, S. *Sci. Technol. Adv. Mater.* **2008**, 9.
(50) Ferey, G.; Serre, C. *Chem. Soc. Rev.* **2009**, *38*, 1380.
(51) Hamon, L.; Llewellyn, P. L.; Devic, T.; Ghoufi, A.; Clet, G.; Guillerm, V.; Pirngruber, G. D.; Maurin, G.; Serre, C.; Driver, G.; van Beek, W.; Jolimaitre, E.; Vimont, A.; Daturi, M.; Ferey, G. *J. Am. Chem. Soc.* **2009**, *131*, 17490.
(52) Kauffman, K. L.; Culp, J. T.; Allen, A. J.; Espinal, L.; Wong-Ng, W.; Brown, T. D.; Goodman, A.; Bernardo, M. P.; Pancoast, R. J.; Chirdon, D.; Matranga, C. *Angew. Chem., Int. Ed.* **2011**, *50*, 10888.
(53) Mu, B.; Li, F.; Huang, Y. G.; Walton, K. S. *J. Mater. Chem.* **2012**, *22*, 10172.
(54) Serre, C.; Bourrelly, S.; Vimont, A.; Ramsahye, N. A.; Maurin, G.; Llewellyn, P. L.; Daturi, M.; Filinchuk, Y.; Leynaud, O.; Barnes, P.; Ferey, G. *Adv. Mater.* **2007**, *19*, 2246.
(55) Champness, N. R.; Khlobystov, A. N.; Majuga, A. G.; Schroder, M.; Zyk, N. V. *Tetrahedron Lett.* **1999**, *40*, 5413.
(56) Dellaciana, L.; Haim, A. *J. Heterocycl. Chem.* **1984**, *21*, 607.
(57) Rodriguez, J. G.; MartinVillamil, R.; Cano, F. H.; Fonseca, I. *J. Chem. Soc., Perkin Trans. 1* **1997**, 709.
(58) Fasina, T. M.; Collings, J. C.; Lydon, D. P.; Albesa-Jove, D.; Batsanov, A. S.; Howard, J. A. K.; Nguyen, P.; Bruce, M.; Scott, A. J.; Clegg, W.; Watt, S. W.; Viney, C.; Marder, T. B. *J. Mater. Chem.* **2004**, *14*, 2395.
(59) Gardner, T. S.; Wenis, E.; Lee, J. *J. Org. Chem.* **1954**, *19*, 753.
(60) Seki, K.; Ohkura, K.; Terashima, M.; Kanaoka, Y. *Heterocycles* **1986**, *24*, 799.
(61) Mathey, Y.; Mazieres, C.; Setton, R. *Inorg. Nucl. Chem. Lett.* **1977**, *13*, 1.
(62) Bodarhouillon, F.; Humbert, T.; Marsura, A.; Devains, J. B. R.; Dusausoy, O.; Bouhmaida, N.; Ghermani, N. E.; Dusausoy, Y. *Inorg. Chem.* **1995**, *34*, 5205.
(63) Jacobs, T.; Clowes, R.; Cooper, A. I.; Hardie, M. J. *Angew. Chem., Int. Ed.* **2012**, *51*, 5192.
(64) Janiak, C.; Uehlin, L.; Wu, H. P.; Klufers, P.; Piotrowski, H.; Scharmann, T. G. *J. Chem. Soc., Dalton Trans.* **1999**, 3121.
(65) Maekawa, M.; Tominaga, T.; Sugimoto, K.; Okubo, T.; Kuroda-Sowa, T.; Munakata, M.; Kitagawa, S. *CrystEngComm* **2012**, *14*, 1345.
(66) Bartual-Murgui, C.; Ortega-Villar, N. A.; Shepherd, H. J.; Munoz, M. C.; Salmon, L.; Molnar, G.; Bousseksou, A.; Real, J. A. *J. Mater. Chem.* **2011**, *21*, 7217.
(67) Bonhommeau, S.; Molnar, G.; Galet, A.; Zwick, A.; Real, J. A.; McGarvey, J. J.; Bousseksou, A. *Angew. Chem., Int. Ed.* **2005**, *44*, 4069.
(68) Halder, G. J.; Kepert, C. J.; Moubaraki, B.; Murray, K. S.; Cashion, J. D. *Science* **2002**, *298*, 1762.
(69) Buttner, H. G.; Kearley, G. J.; Howard, C. J.; Fillaux, F. *Acta Crystallogr.* **1994**, *B50*, 431.
(70) Dunbar, K. R.; Heintz, R. A. In *Progress in Inorganic Chemistry*; Karlin, K. D., Ed.; Wiley: New York, 1997; Vol. *45*, p 283.
(71) Iwamoto, T. *J. Mol. Struct.* **1981**, *75*, 51.
(72) Iwamoto, T.; Miyoshi, T.; Sasaki, Y. *Acta Crystallogr.* **1974**, *B30*, 292.
(73) Rayner, J. H.; Powell, H. M. *J. Chem. Soc.* **1952**, 319.
(74) Kumar, D. K.; Jose, D. A.; Das, A. *Langmuir* **2004**, *20*, 10413.
(75) Culp, J. T.; Chen, D.-L.; Liu, J.; Chirdon, D.; Goodman, A.; Johnson, J. K. *Eur. J. Inorg. Chem.* **2013**, *2013*, 511.
(76) Vogiatzis, K. D.; Mavrandonakis, A.; Klopper, W.; Froudakis, G. E. *ChemPhysChem* **2009**, *10*, 374.

Supporting information for:

"Screening Hofmann Compounds as CO_2 Sorbents: Nontraditional Synthetic Route to Over 40 Different Pore-Functionalized and Flexible Pillared Cyanonickelates "

Jeffrey T. Culp;[1,2] Catherine Madden;[1] Kristi Kauffman;[1] Fan Shi;[1,2] and Christopher Matranga[1]

[1]National Energy Technology Laboratory, Pittsburgh, PA 15236, USA
[2]URS Corporation, South Park, PA 15129

Contents

Chart S1. Pillar ligand (L) abbreviations and associated PICNIC compounds $Ni(L)Ni(CN)_4$.

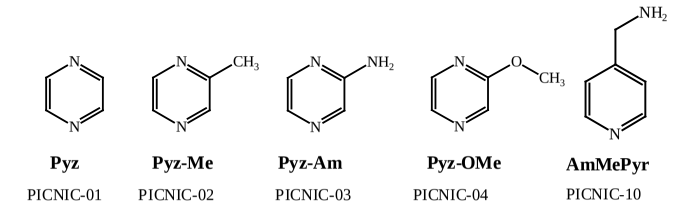

Pyz PICNIC-01 | **Pyz-Me** PICNIC-02 | **Pyz-Am** PICNIC-03 | **Pyz-OMe** PICNIC-04 | **AmMePyr** PICNIC-10

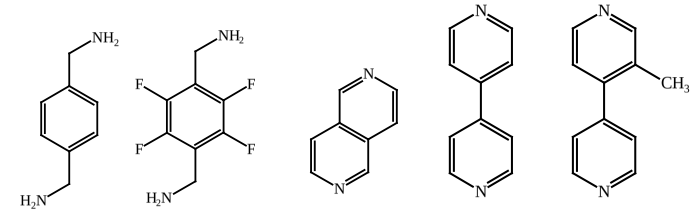

pXdAm PICNIC-11 | **pXdAm-F4** PICNIC-12 | **2,6-Naph** PICNIC-13 | **Bpy** PICNIC-20 | **Bpy-Me** PICNIC-21

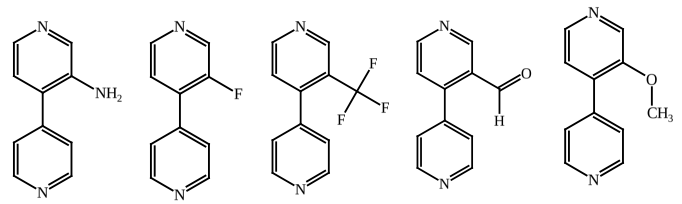

Bpy-Am PICNIC-22 | **Bpy-F** PICNIC-23 | **Bpy-CF3** PICNIC-24 | **Bpy-Ald** PICNIC-25 | **Bpy-OMe** PICNIC-26

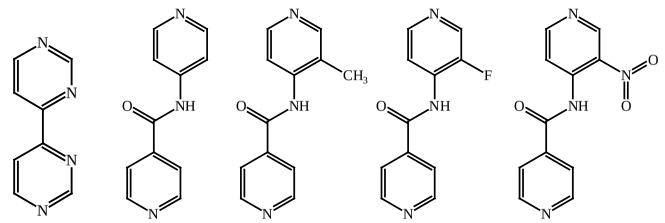

4,4'-Bpm PICNIC-27 | **PINA** PICNIC-30 | **PINA-Me** PICNIC-31 | **PINA-F** PICNIC-32 | **PINA-NO2** PICNIC-33

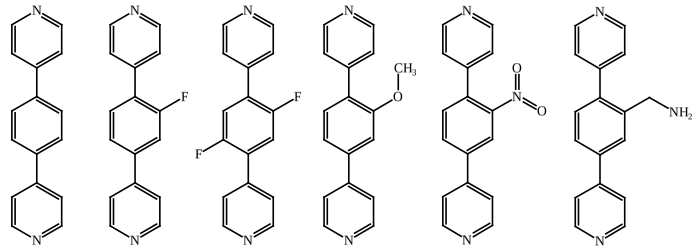

DPBZ PICNIC-40 | **DPBZ-F1** PICNIC-41 | **DPBZ-F2** PICNIC-42 | **DPBZ-OMe** PICNIC-43 | **DPBZ-NO2** PICNIC-44 | **DPBZ-AmMe** PICNIC-45

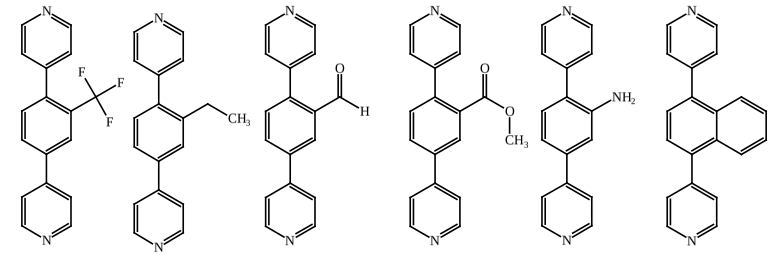

DPBZ-CF3 PICNIC-46 | **DPBZ-Et** PICNIC-47 | **DPBZ-Ald** PICNIC-48 | **DPBZ-Est** PICNIC-49 | **DPBz-Am** PICNIC-50 | **DP-Naph** PICNIC-51

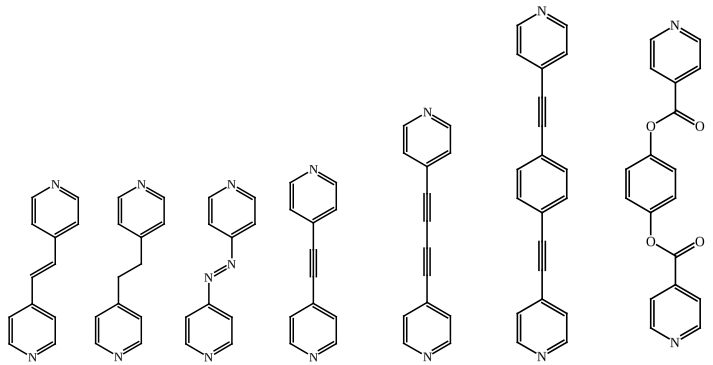

Bpene PICNIC-60 | **Bpane** PICNIC-61 | **AzoPyr** PICNIC-62 | **DPAC** PICNIC-63 | **DPBD** PICNIC-64 | **DPBzBD** PICNIC-65 | **IsoNicBz** PICNIC-70

Synthetic details

Functionalized 4,4'-bipyridines (Bpy-R)

3-fluoro-4,4'-bipyridine (Bpy-F). The ligand was prepared from the Suzuki coupling of pyridine-4-boronic acid (22 mmol) and 3-fluoro-4-chloropyridine (15 mmol) using the same catalyst and solvent ratios as used to prepare Bpy-Am. The product was recrystallized from hexanes to yield 5.8 mmol of white product. MP 139 C (lit 139-141 C)[1] ; ^{1}H NMR (300 MHz; $CDCl_3$) 8.73,d,2H; 8.58,d,1H; 8.52,d,1H; 7.50,m,2H; 7.40,m,1H. Anal. Calcd for: $C_{10}H_7FN_2$ (174.2) C 68.96, H4.05, N16.08; Found: C 69.07, H 3.76, N 15.99.

3-methyl-4,4'-bipyridine (Bpy-Me). The ligand was prepared from the Suzuki coupling of pyridine-4-boronic acid (22 mmol) and 3-methyl-4-chloropyridine hydrogen chloride (15 mmol) using the same catalyst and solvent ratios as used to prepare Bpy-Am with the exception that twice the amount of K_3PO_4 was used to neutralize the HCl salt. The product was recrystallized from hexanes to yield 12.6 mmol of pale yellow product. MP 89 C; ^{1}H NMR (300 MHz; acetone, D6) 8.73,m,2H; 8.57,m,1H; 8.52,m,1H; 7.44,m,2H; 7.25,m,1H; 2.31,s,3H. Anal. Calcd for: $C_{11}H_{10}N_2$ (170.2) C 77.62, H 5.92, N 16.46; Found: C 77.45, H 5.86, N 16.39.

[1] Martens, R. J.; Denhertog, H. J.; Vanammers, M. *Tet. Lett.* 1964, **43-44**, 3207.

3-trifluoromethyl-4,4'-bipyridine (Bpy-CF3). The ligand was prepared from the Suzuki coupling of pyridine-4-boronic acid (15 mmol) and 3-trifluoromethyl-4-chloropyridine hydrogen chloride (10 mmol) using the same catalyst and solvent ratios as used to prepare Bpy-Am with the exception that twice the amount of K_3PO_4 was used to neutralize the HCl salt. The product was recrystallized from hexanes to yield 6.5 mmol of white product. MP 66 C; ^{1}H NMR (300 MHz; $CDCl_3$) 9.89,d,1H; 9.05,s,1H; 8.75,m,2H; 7.30,m,3H. Anal. Calcd for: $C_{11}H_7F_3N_2$ (224.2) C 58.93, H 3.15, N 12.50; Found: C 59.13, H 2.71, N 12.21.

3-carboxaldehyde-4,4'-bipyridine (Bpy-Ald). The ligand was prepared from the Suzuki coupling of pyridine-4-boronic acid (26 mmol) and 3-carboxaldehyde-4-chloropyridine (18 mmol) using the same catalyst and solvent ratios as used to prepare Bpy-Am. The product was recrystallized from hexanes to yield 6.1 mmol of white product. MP 144 C; ^{1}H NMR (300 MHz; $CDCl_3$). 10.08,s,1H; 9.21,s,1H; 8.90,d,1H; 8.80,d,2H; 7.34,m,3H. Anal. Calcd for: $C_{11}H_8N_2O$ (184.2) C 71.73, H 4.38, N 15.21; Found: C 70.83, H 4.09, N 14.83.

3-methoxy-4,4'-bipyridine (Bpy-OMe). The ligand was prepared from the Suzuki coupling of 3-methoxypyridine-4-boronic acid (1.0 g, 5.8 mmol) with 4-bromopyridine hydrogen chloride (1.0 g, 5.0 mmol) using a procedure similar to that used to prepare Bpy-Am with some modification. The reaction was done under N_2 in 10 mL dioxane/6 mL deoxygenated H_2O and catalyzed with 55 mg Pd_2DBA_3, 45 mg $P(Cy)_3$ and 3.0 g K_3PO_4. The product was extracted from the cooled aqueous dioxane reaction mixture with ethyl acetate due to the formation of a suspension in the reaction mixture that made filtration difficult. The extracts were treated with activated carbon and anhydrous $Mg(SO_4)$, filtered through a fine glass frit. The filtrate was evacuated under reduced pressure and the residue was recrystallized in hexanes to yield 1.2 mmol of white product. MP 86 C; ^{1}H NMR (300 MHz; $CDCl_3$) 8.68,m,2H; 8.42,s,1H; 8.36,d,1H; 7.48,m,2H; 7.26,d,1H; 3.94,s,3H. Anal. Calcd for: $C_{11}H_{10}N_2O$ (186.2) C 70.95, H 5.41, N 15.04; Found: C 69.97, H 5.43, N 14.79.

Functionalized 1,4-bis(4-pyridyl)-3-(R)-benzenes (DPBz-R)

1,4-bis(4-pyridyl)benzene (DPBz). The ligand was prepared from the Suzuki coupling of 18 mmol pyridine-4-boronic acid and 5 mmol 1,4-dibromobenzene using a method similar to that used to prepare DPBz-Am. Recrystallization from acetonitrile yielded 2.8 mmol of white product. MP 193 C; ^{1}H NMR (300 MHz; $CDCl_3$) 8.68,dd,4H; 7.75,s,4H; 7.53,dd,4H. Anal. Calcd for: $C_{16}H_{12}N_2$(232.3) C 82.73, H 5.21, N 12.06; Found: C 82.64, H 4.89, N 11.98.

1,4-bis(4-pyridyl)-fluorobenzene (DPBz-F1). The ligand was prepared from the Suzuki coupling of 8 mmol pyridine-4-boronic acid and 4 mmol 1,4-dibromo-fluorobenzene using a method similar to that used to prepare DPBz-Am. Recrystallization from dichloromethane/petroleum ether yielded 1.3 mmol of white product. MP 184 C; ^{1}H NMR (300 MHz; $CDCl_3$). Anal. Calcd for: $C_{16}H_{11}FN_2$(250.3) C 76.79, H 4.43, N 11.19; Found: C 76.02, H 4.05, N 10.82.

1,4-bis(4-pyridyl)-3,5-difluorobenzene (DPBz-F2). The ligand was prepared from the Suzuki coupling of 8 mmol pyridine-4-boronic acid and 4 mmol 1,4-dibromo-2,5-difluorobenzene using a method similar to that used to prepare DPBz-Am. Recrystallization from dichloromethane/petroleum ether yielded 1.5 mmol of white product. ^{1}H NMR (300 MHz; $CDCl_3$) 8.72,m,4H; 7.49,d,4H; 7.33,t,2H. Anal. Calcd for: $C_{16}H_{10}F_2N_2$(268.3) C 71.64, H 3.76, N 10.44; Found: C 71.24, H 3.36, N 10.48.

1,4-bis(4-pyridyl)-methoxybenzene (DPBz-OMe). The ligand was prepared from the Suzuki coupling of 18 mmol pyridine-4-boronic acid and 5 mmol 1,4-dichloro-2-methoxybenzene using a method similar to that used to prepare DPBz-Am. Recrystallization from dichloromethane/petroleum ether yielded 2.6 mmol of beige product. MP 158 C; ^{1}H NMR (300 MHz; $CDCl_3$) 8.62,m,4H; 7.47,m,5H; 7.30,m,1H; 7.20,m,1H; 3.90,s,3H. Anal. Calcd for: $C_{17}H_{14}N_2O$(262.3) C 77.84, H 5.38, N 10.68; Found: C 77.62, H 5.14, N 10.51.;

1,4-bis(4-pyridyl)-methylbenzoate (DPBz-Est). The ligand was prepared from the Suzuki coupling of 18 mmol pyridine-4-boronic acid and 5 mmol methyl 2,5-dibromobenzoate using a method similar to that used to prepare DPBz-Am. Recrystallization from ethyl acetate yielded 2.6 mmol of beige product. MP 145 C; ^{1}H NMR (300 MHz; $CDCl_3$) 8.66,m,4H; 8.23,d,1H; 8.07,m,1H; 7.76,m,2H; 7.61,m,1H; 7.35,m,2H. Anal. Calcd for: $C_{18}H_{14}N_2O_2$(290.3) C 74.47, H 4.86, N 9.65; Found: C 73.87, H 4.79, N 9.16.

1,4-bis(4-pyridyl)-nitrobenzene (DPBz-NO2). The ligand was prepared from the Suzuki coupling of 18 mmol pyridine-4-boronic acid and 5 mmol 1,4-dibromo-2-nitrobenzene using a method similar to that used to prepare DPBz-Am. Recrystallization from dichloromethane / petroleum ether yielded 3.1 mmol of beige product. MP 183 C; ^{1}H NMR (300 MHz; $CDCl_3$) 8.70,m,4H;8.43,m,1H; 8.24,m,1H ; 7.83,m,2H; 7.75,m,1H; 7.42,m,2H. Anal. Calcd for: $C_{16}H_{11}N_3O_2$(277.3) C 69.31, H 4.00, N 15.15; Found: C 69.68, H 3.88, N 14.57.

1,4-bis(4-pyridyl)-ethylbenzene (DPBz-Et). The ligand was prepared from the Suzuki coupling of 18 mmol pyridine-4-boronic acid and 5 mmol 1,4-dibromo-2-ethylbenzene using a method similar to that used to prepare DPBz-Am. Recrystallization from dichloromethane/petroleum ether yielded 3.3 mmol of white product. MP 103 C; ^{1}H NMR (300 MHz; $CDCl_3$) 8.66,m,4H; 7.80,d,1H; 7.70,dd,2H; 7.68,d,1H; 7.36,dd,2H; 7.33,s,1H; 2.68,q,2H; 1.14,t,3H. Anal. Calcd for: $C_{18}H_{16}N_2$(260.3) C 83.04, H 6.19, N 10.76; Found: C 82.64, H 5.92, N 10.78.

1,4-bis(4-pyridyl)-trifluoromethylbenzene (DPBz-CF3). The ligand was prepared from the Suzuki coupling of 8 mmol pyridine-4-boronic acid and 2.3 mmol 1,4-dibromo-2-trifluoromethylbenzene using a method similar to that used to prepare DPBz-Am. Recrystallization by concentration of dichloromethane/petroleum ether followed by addition of hexanes yielded 1.0 mmol of pale yellow product. MP 109 C; ^{1}H NMR (300 MHz; $CDCl_3$) 8.70,m,4H; 8.0,d,1H; 7.85,dd,1H; 7.54,dd,2H; 7.43,d,1H; 7.28, d, 2H. Anal. Calcd for: $C_{17}H_{11}F_3N_2$(300.3) C 68.00, H 3.69, N 9.33; Found: C 67.20, H 3.32, N 9.13.

1,4-bis(4-pyridyl)-naphthalene (DPNaph). The ligand was prepared from the Suzuki coupling of 18 mmol pyridine-4-boronic acid and 5 mmol 1,4-dibromonaphthalene using a method similar to that used to prepare DPBz-Am. Recrystallization from ethyl acetate yielded 3.7 mmol of beige product. MP 205 C; ^{1}H NMR (300 MHz; $CDCl_3$) 8.74,m,4H; 7.89,m,2H; 7.51-7.44,m,8H. Anal. Calcd for: $C_{20}H_{14}N_2$(282.3) C 85.08, H 5.00, N 9.92; Found: C 84.02, H 4.54, N 9.59.

N-(2,5-dichlorobenzyl)acetamide. The synthesis of N-(2,5-dichlorobenzyl)acetamide was adapted from a similar procedure reported for the preparation of N-(benzyl)acetamide. (Smiszek-Lindert, W.; Kusz, J. *Acta Cryst.* **2007**, E63, o3713-U2161.). 1,4-dichlorobenzylamine (5.0 g, 28 mmol) was slowly added to 45 mL glacial acetic acid at room temperature. After the addition was complete, the solution was heated to reflux for 3.5 hours after which the acetic acid was removed under reduced pressure to give a viscous oil which solidified upon standing. The solid was dissolved into 35 mL of ethanol and treated with ~200 mg activated carbon and filtered. Addition of 65 mL of water to the filtrate gave a precipitate that was dissolved with heating. Subsequent cooling of the solution gave 4.3 g of white crystalline product. (70%) MP 128 C; ^{1}H NMR (300 MHz; $CDCl_3$) 7.25, m, 3H; 5.90, s, 1H; 4.46, d, 2H; 2.04, s, 3H.

N-(2,5-di(pyridin-4-yl)benzyl)acetamide. The N-(2,5-di(pyridin-4-yl)benzyl)acetamide ligand was prepared from the Suzuki coupling of 18 mmol pyridine-4-boronic acid and 5 mmol N-(2,5-dichlorobenzyl)acetamide using a method similar to that used to prepare DPBz-Am. Recrystallization from ethyl acetate yielded 4.2 mmol of beige product which was taken to the next step without further purification. Anal. Calcd for: $C_{19}H_{17}N_3O$(303.4) C 75.23, H 5.65, N 13.85; Found: C 73.76, H 5.72, N 12.81; MP 196 C

1,4-bis(4-pyridyl)-3-(aminomethyl)benzene (DPBz-MeAm). The free amine was prepared by the acid hydrolysis of N-(2,5-di(pyridin-4-yl)benzyl)acetamide in 6 M HCl by the following procedure. A 1.2 g sample of N-(2,5-di(pyridin-4-yl)benzyl)acetamide was dissolved in 50 mL of 6 M HCl. The solution was heated to reflux for 2 hours and then concentrated to a volume of ca. 10 mL. Addition of ethanol precipitated the 1,4-bis(4-pyridyl)-3-(aminomethyl)-benzene as the 3HCl salt which was isolated by filtration and air dried to give 1.85 g of product. The HCl salt was neutralized by dissolving in 25 mL of water followed by the addition of a solution of 2.5 g KOH in 25 mL H_2O. Addition of the base resulted in the precipitation of a white solid which was isolated by filtration and washed with water. The product was dried under vacuum at room temperature over night to yield 750 mg (2.9 mmol) of 1,4-bis(4-pyridyl)-3-(aminomethyl)benzene. MP 156 C; ^{1}H NMR (300 MHz; $CDCl_3$) 8.66,dd,4H; 7.80,d,1H; 7.56,m,3H; 7.32,m,3H; 3.87, s, 2H; 1.28,s,2H. Anal. Calcd for: $C_{17}H_{15}N_3$(261.3) C 78.13, H 5.79, N 16.08; Found: C 76.96, H 5.72, N 15.99.

Functionalized 4-(pyridyl)isonicotinamides (PINA-R).

4-(3-nitropyridyl)isonicotinamide (PINA-NO2): A solution of 2.12 g (0.0152 mol) of 4-amino-3-nitropyridine in 25 mL of dry pyridine was added to a mixture of 2.71 g (0.015 mol) of isonicotinoyl chloride hydrochloride in 25 mL of dry pyridine. The flasks were then transferred into a hot oil bath and reacted at 80 C under N_2 for 18hrs. The mixture was then concentrated to a few mL under reduced pressure and 50 mL of a 5% aqueous solution of sodium bicarbonate was added. The precipitate was collected by filtration and recrystallized from acetone/water and dried to yield 3.23g (0.0132 mol) of a light beige solid: MP 137 C; ^{1}H NMR (300 MHz; $CDCl_3$) 11.58,s,1H; 9.48,s,1H; 8.91,m,3H 8.81,d,1H; 7.82,m,2H. Anal. Calcd for: $C_{11}H_8N_4O_3$(244.2) C 54.10, H 3.30, N 22.94; Found: C 54.18, H 2.71, N 22.83.

4-(3-methylpyridyl)isonicotinamide (PINA-Me): A solution of 1.22 g (0.0113 mol) of 4-amino-3-methylpyridine in 25 mL of dry pyridine was added to a mixture of 1.96 g (0.011 mol) of isonicotinoyl chloride hydrochloride in 25 mL of dry pyridine. The flasks were then transferred into a hot oil bath and reacted at 80 C under N_2 for 18hrs. The mixture was then concentrated to a few mL under reduced pressure and 50 mL of a 5% aqueous solution of sodium bicarbonate was added. The precipitate was collected by filtration and recrystallized from acetone/water and dried to yield 2.2g (0.0102 mol) of a light beige solid yield %; MP 163 C;^{1}H NMR (300 MHz; $CDCl_3$) 8.87,m,2H; 8.50,d,1H; 8.46,s,1H; 8.23,d,1H; 8.00,s,1H; 7.74,m,2H; 2.38,s,3H. Anal. Calcd for: $C_{12}H_{11}N_3O$(213.2) C 67.59, H 5.20, N 19.71; Found: C 66.75, H 4.97, N 18.98.

Table S1. CHN analyses for pillar ligands

Sample	Chem Form	Form Wt		C	H	N
PINA	C11H9N3O	199.21	expected	66.32	4.55	21.09
			actual	65.67	3.96	20.38
PINA-Me	C12H11N3O	213.24	expected	67.59	5.2	19.71
			actual	65.75	4.97	18.98
PINA-F	C11H8FN3O	217.2	expected	60.83	3.71	19.35
			actual	60.66	3.38	19.25
PINA-NO2	C11H8N4O3	244.21	expected	54.1	3.3	22.94
			actual	54.18	2.71	22.83
Bpy-Me	C11H10N2	170.21	expected	77.62	5.92	16.46
			actual	77.45	5.86	16.39
Bpy-NH2	C10H9N3	171.2	expected	70.16	5.3	24.54
			actual	69.87	4.99	24.07
Bpy-F	C10H7FN2	174.17	expected	68.96	4.05	16.08
			actual	69.07	3.76	15.99
Bpy-CF3	C11H7F3N2	224.18	expected	58.93	3.15	12.5
			actual	59.13	2.71	12.21
Bpy-Ald	C11H8N2O	184.19	expected	71.73	4.38	15.21
			actual	70.83	4.09	14.83
Bpy-OMe	C11H10N2O	186.21	expected	70.95	5.41	15.04
			actual	69.97	5.43	14.79
Azo-Bpy	C10H8N4	184.2	expected	65.21	4.38	30.42
			actual	64.33	4.32	30.29
DPAC	C12H8N2	180.21	expected	79.98	4.47	15.55
			actual	79.78	4.45	15.67
DPBD	C14H8N2	204.23	expected	82.33	3.95	13.72
			actual	81.95	4.02	13.77
DPAC-Bz	C20H12N2	280.32	expected	85.69	4.31	9.99
			actual	85.19	4.02	9.93
DPNaph	C24H14N6Ni2	503.79	expected	57.22	2.8	16.68
			actual	55.6	2.47	16.44
IsoNic-Bz	C22H12N6Ni2O4	541.76	expected	48.77	2.23	15.51
			actual	47.83	1.81	15.71
DPBz	C20H12N6Ni2	453.74	expected	52.94	2.67	18.52
			actual	52.75	2.75	17.89
DPBz-NH2	C20H13N7Ni2	468.75	expected	51.25	2.8	20.92
			actual	52.78	2.84	20.09
DPBz-Est	C22H14N6Ni2O2	511.77	expected	51.63	2.76	16.42
			actual	51.86	2.94	16.02
DPBz-MeAm	C17H15N3	261.32	expected	78.13	5.79	16.08
			actual	76.96	5.72	15.99
DPBz-Ald	C17H12N2O	260.29	expected	78.44	4.65	10.76
			actual	75.95	4.67	10.06
DPBz-NO2	C20H11N7Ni2O2	498.73	expected	48.16	2.22	19.66
			actual	49.6	2.4	19.21
DPBz-pF2	C20H10F2N6Ni2	489.72	expected	49.05	2.06	17.16
			actual	48.58	2.42	17.05
DPBz-OMe	C21N14N6Ni2O	483.76	expected	52.14	2.92	17.37
			actual	51.31	3.1	17.43
DPBz-F	C20H11FN6Ni2	471.73	expected	50.92	2.35	17.82
			actual	50.91	2.61	17.58
DPBz-Et	C18H16N2	260.33	expected	83.04	6.19	10.76
			actual	82.64	5.92	10.78
DPBz-CF3	C17H11F3N2	300.28	expected	68	3.69	9.33
			actual	67.2	3.32	9.13

Table S2. Melting points and NMR analyses of pillar ligands

ligand	mp	lit MP	NMR peaks (300 MHz)
PINA	192	196 (1)	(CDCl3) 8.81,m,2H; 8.60,s,1H; 8.56,m,2H;
			7.72,m,2H; 7.64,m,2H
PINA-Me	163		(CDCl3) 8.87,m,2H; 8.50,d,1H; 8.46,s,1H; 8.23,d,1H;
			8.00,s,1H; 7.74,m,2H; 2.38,s,3H
PINA-F	180		(CDCl3) 8.86,d,2H; 8.47,m,3H; 8.37,s,1H; 7.73,d,2H
PINA-NO2	137		(CDCl3) 11.58,s,1H; 9.48,s,1H; 8.91,m,3H
			8.81,d,1H; 7.82,m,2H
Bpy-Me	89		(acetone,D6) 8.73,m,2H; 8.57,m,1H; 8.52,m,1H;
			7.44,m,2H; 7.25,m,1H; 2.31,s,3H
Bpy-NH2	170	166-168 (2)	(CDCL3) 8.75,m,2H; 8.21s,1H;8.11,d,1H;
			7.43,m,2H; 7.03,d,1H; 3.85,s,2H
Bpy-F	139	139-141 (3)	(CDCL3) 8.73,d,2H; 8.58,d,1H; 8.52,d,1H;
			7.50,m,2H; 7.40,m,1H
Bpy-CF3	66		(CDCl3) 9.89,d,1H; 9.05,s,1H; 8.75,m,2H;7.30,m,3H
Bpy-Ald	144		(CDCL3) 10.08,s,1H; 9.21,s,1H; 8.90,d,1H;
			8.80,d,2H; 7.34,m,3H
Bpy-OMe	86		(CDCl3) 8.68,m,2H; 8.42,s,1H; 8.36,d,1H;
			7.48,m,2H; 7.26,d,1H; 3.94,s,3H
DPAC	117	118 (4)	(CDCl3) 8.69, d, 4H; 7.45, dd, 4H
DPBD	205	206 (5)	(CDCl3) 8.61,m,4H; 7.36,m,4H
DPBz	193		(CDCl3) 8.61,m,4H; 7.36,m,4H
DPBz-F1	184		(CDCl3) 8.70,m,4H; 7.62-7.43,m,7H
DPBz-F2	no melt		(CDCl3) 8.72,m,4H; 7.49,d,4H; 7.33,t,2H
DPBz-NO2	183		(CDCl3) 8.70,m,4H;8.43,m,1H; 8.24,m,1H ; 7.83,m,2H;
			7.75,m,1H; 7.42,m,2H
DPBz-NH2	197		(CDCl3) 8.70,m,4H; 7.49,m,4H; 7.27,m,1H
			7.12,m,1H; 7.04,d,1H
DPBz-OMe	158		(CDCl3) 8.62,m,4H; 7.47,m,5H; 7.30,m,1H;
			7.20,m,1H; 3.90,s,3H
DPBz-Est	145		(CDCl3) 8.66,m,4H; 8.23,d,1H; 8.07,m,1H; 7.76,m,2H;
			7.61,m,1H; 7.35,m,2H
DPBz-MeAm	156		(CDCl3) 8.66,dd,4H; 7.80,d,1H; 7.56,m,3H; 7.32,m,3H;
			3.87, s, 2H; 1.28,s,2H
DP-Napth	205		(CDCl3) 8.74,m,4H; 7.89,m,2H; 7.51-7.44,m,8H
DPAC-Bz	198	192-193 (6)	(CDCl3) 8.67,d,4H; 7.60, s, 4H; 7.44,dd, 4H
IsoNicBz	230	222 (7)	(CDCl3) 8.86,m,4H; 7.99,m,4H; 7.30,s,4H
DpBz-CF3	109		(CD2Cl2) 8.70,m,4H; 8.0,d,1H; 7.85,dd,1H; 7.54,dd,2H;
			7.43,d,1H; 7.28, d, 2H)
DPBz-Et	103		(CDCl3) 8.66,m,4H; 7.80,d,1H; 7.70,dd,2H; 7.68,d,1H;
			7.36,dd,2H; 7.33,s,1H; 2.68,q,2H; 1.14,t,3H
DPBz-Ald	142		(CDCL3) 10.07,s,1H; 8.78,dd,4H; 8.37,s,1H;8.00,d,1H;
			7.61,m,3H; 7.39,d,2H
N-(2,5-dichlorobenzyl)acetamide	128		(CDCl3) 7.25, m, 3H; 5.90, s, 1H; 4.46, d, 2H; 2.04, s, 3H
N-(2,5-di(pyridin-4-yl)benzyl)acetamide	196		

(1) Kumar, K.D. *et al*., *Langmuir* 2004, **20**, 10413.
(2) Seki, K. *et al*., *Heterocycles*, 1986, **24**, 799
(3) Martens, R. J. *et al*., *Tet. Lett.*, 1964, **5**, 3207.
(4) Schmidt, B. *et al*., *Chem. Eur. J*., 2011, **17**, 7032.
(5) Merkul, E. *et al*., *Eur. J. Org. Chem.*, 2011, 238.
(6) Fasina, T. M. *et al*., *J. Mater. Chem.*, 2004, **14**, 2395.
(7) Shao, X.-B., *et al*., *J. Org. Chem*., 2004, **69**, 899.

Table S3. TGA results for PICNICs. All samples ran in air at 15 C/min to a temperature > 550 C.

Pillared CyanoNickelate	Pillar Ligand	ligand mol wt	Form. Wt.	calc wt% NiO	meas. wt% NiO	calc fw	% of expected fw
PiCNic-1	Pyz	80.1	301.6	49.5	50.2	297.6	99
PiCNic-2	Pyz-Am	95.1	316.6	47.2	48.3	309.3	98
PiCNic-3	Pyz-Me	94.1	315.6	47.3	47.7	313.2	99
PiCNic-4	Pyz-OMe	110.1	331.6	45.1	42.5	351.5	106
PiCNic-10	AmMe-Pyr	108.1	329.6	45.3	45.0	332.0	101
PiCNic-11	pXdAm	136.2	357.7	41.8	40.9	365.3	102
PiCNic-12	pXdAm-F4	208.2	429.7	34.8	35.0	426.9	99
PiCNic-13	2,6-Naph	130.1	351.6	42.5	42.7	349.9	100
PiCNic-20	Bpy	156.2	377.7	39.6	39.3	380.2	101
PiCNic-21	Bpy-Me	170.2	391.7	38.1	37.3	400.5	102
PiCNic-22	Bpy-NH2	171.2	392.7	38.0	38.9	384.1	98
PiCNic-23	Bpy-F	174.2	395.7	37.8	37.3	400.5	101
PiCNic-24	Bpy-CF3	224.2	445.7	33.5	33.7	443.3	99
PiCNic-25	Bpy-Ald	184.2	405.7	36.8	37.1	402.7	99
PiCNic-26	Bpy-OMe	186.2	407.7	36.6	37.9	394.2	97
PICNic-27	4,4'-Bpm	158.2	379.7	39.3	40.2	371.6	98
PiCNic-30	PINA	199.2	420.7	35.5	36.0	415.0	99
PiCNic-31	PINA-Me	213.2	434.7	34.4	34.9	428.1	98
PiCNic-32	PINA-F	217.2	438.7	34.1	33.6	444.6	101
PiCNic-33	PINA-NO2	244.2	465.7	32.1	30.6	488.2	105
PiCNic-40	DPBZ	232.3	453.8	32.9	32.3	462.5	102
PiCNic-41	DPBZ-F1	250.3	471.8	31.7	32.0	466.9	99
PiCNic-42	DPBZ-F2	268.3	489.8	30.5	30.9	483.5	99
PiCNic-43	DPBZ-OMe	262.3	483.8	30.9	31.6	472.8	98
PiCNic-44	DPBz-NO2	277.3	498.8	30.0	29.9	499.7	100
PiCNic-45	DPBz-AmMe	261.3	482.8	30.9	31.9	468.3	97
PiCNic-46	DPBz-CF3	300.3	521.8	28.6	29.9	499.7	96
PiCNic-47	DPBz-Et	260.3	481.8	31.0	33.3	448.6	93
PiCNic-48	DPBZ-Ald	260.3	481.8	31.0	32.9	454.1	94
PiCNic-49	DPBZ-Est	290.3	511.8	29.2	28.8	518.8	101
PiCNic-50	DPBz-NH2	247.3	468.8	31.9	31.8	469.8	100
PiCNic-51	DP-Naph	282.3	503.8	29.7	30.7	486.6	97
PiCNic-60	Bpene	182.2	403.7	37.0	37.5	398.4	99
PiCNic-62	AzoPyr	184.2	405.7	36.8	36.5	409.3	101
PiCNic-63	DPAC	180.2	401.7	37.2	37.8	395.2	98
PiCNic-64	DPBD	204.2	425.7	35.1	35.0	426.9	100
PicNic-65	DPAC-Bz	280.3	501.8	29.8	29.4	508.2	101
PiCNic-70	IsoNicBz	320.3	541.8	27.6	28.3	527.9	97
Fe(Pyz)Ni(CN)4	Pyz	80.1	298.7	51.7	53.3	289.9	97
Fe(Bpy)Ni(CN)4	Bpy	156.2	374.8	41.2	41.8	369.6	99
Fe(Bpene)Pd(CN)4	Bpene	182.2	448.5	45.1	45.0	449.6	100
Fe(pXdAm)Ni(CN)4	pXdAm	136.2	354.8	43.5	44.4	348.0	98
Co(pXdAm)Ni(CN)4	pXdAm	136.2	357.9	44.0	44.2	356.6	100
Co(AmMePyr)Ni(CN)4	AmMePyr	108.1	329.8	47.8	47.3	333.2	101
Pillared CyanoNickelate	Pillar Ligand	ligand mol wt	Form. Wt.	calc wt% NiO	meas. wt% NiO	calc fw	% of expected fw

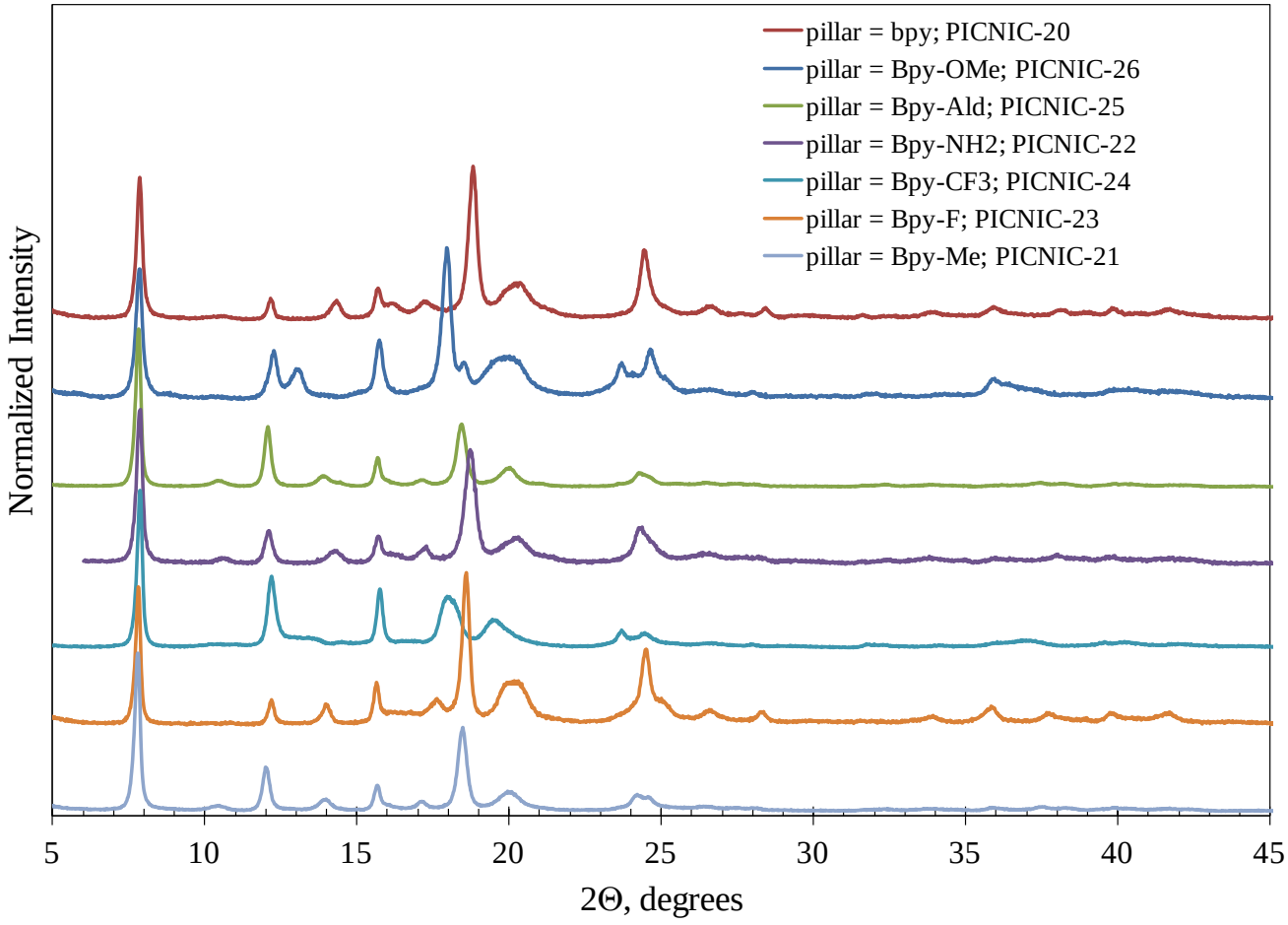

Figure S1. Powder x-ray diffraction patterns for the guest free Ni(Bpy-R)Ni$(CN)_4$ series of PICNICs.

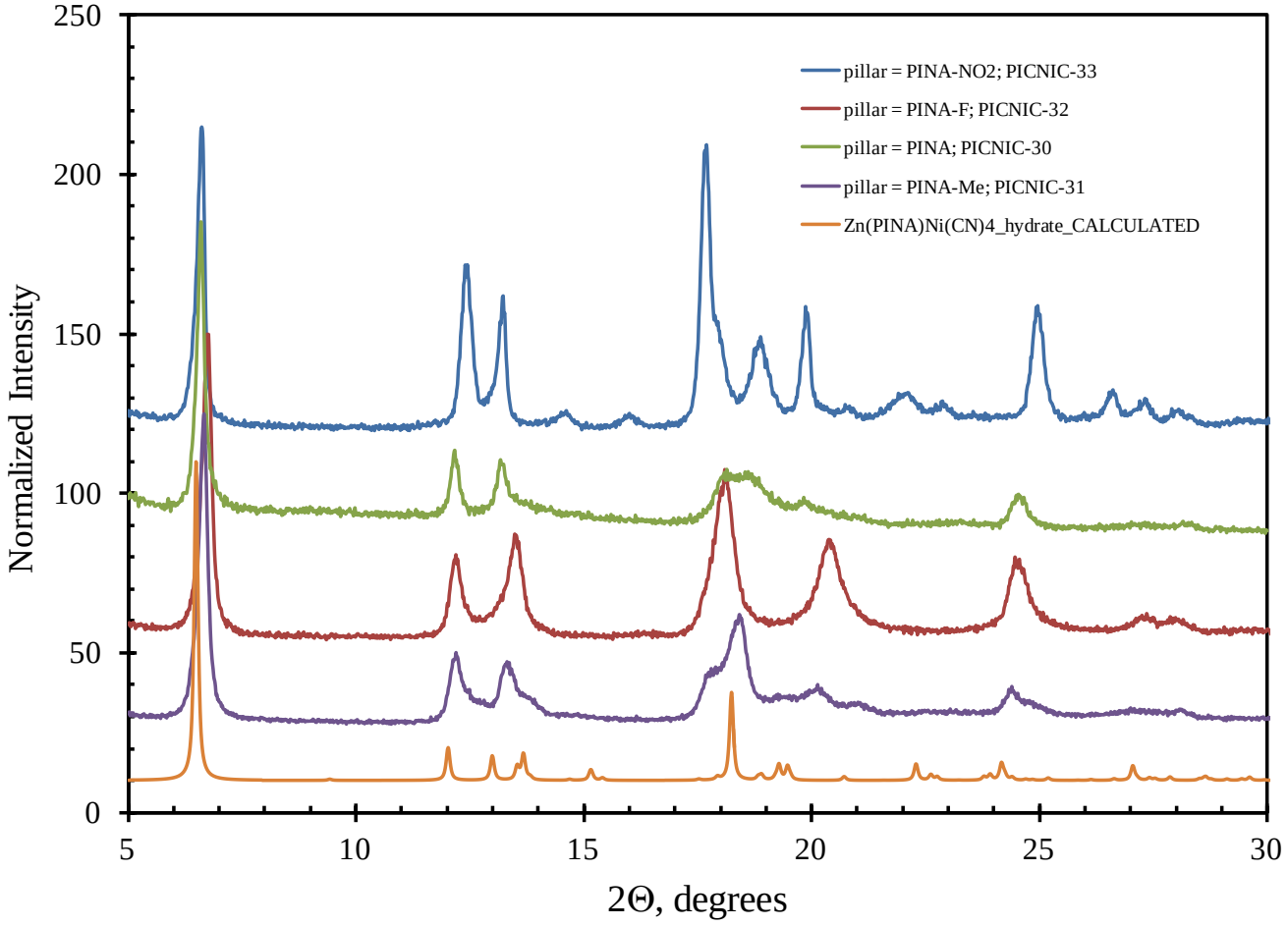

Figure S2. Powder x-ray diffraction patterns for the acetonitrile guest loaded Ni(PINA-R)Ni(CN)$_4$ series of PICNICs. The calculated pattern for the reported structure of Zn(PINA)Ni(CN)$_4$ is included for reference (Chen, X.; Zhou, H.; Chen, Y. Y.; Yuan, A. H. *Crystengcomm* **2011**, *13*, 5666).

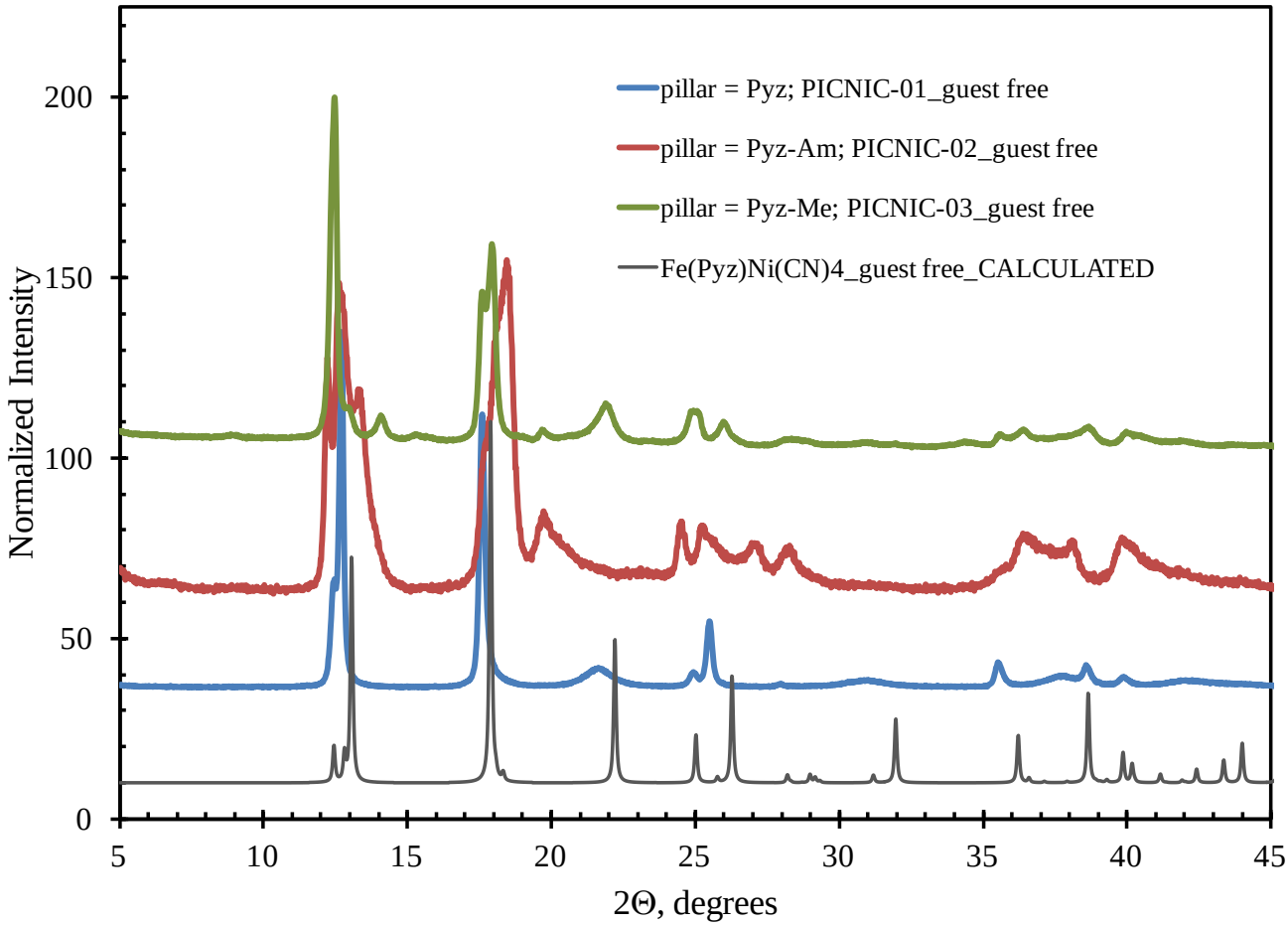

Figure S3. Powder x-ray diffraction patterns for the Ni(PINA-R)Ni(CN)$_4$ series of PICNICs. The calculated pattern for the reported stucture of Fe(Pyz)Ni(CN)$_4$ is included for reference (Southon, P. D.; Liu, L.; Fellows, E. A.; Price, D. J.; Halder, G. J.; Chapman, K. W.; Moubaraki, B.; Murray, K. S.; Letard, J. F.; Kepert, C. J. *J. Am. Chem. Soc.* **2009**, *131*, 10998).

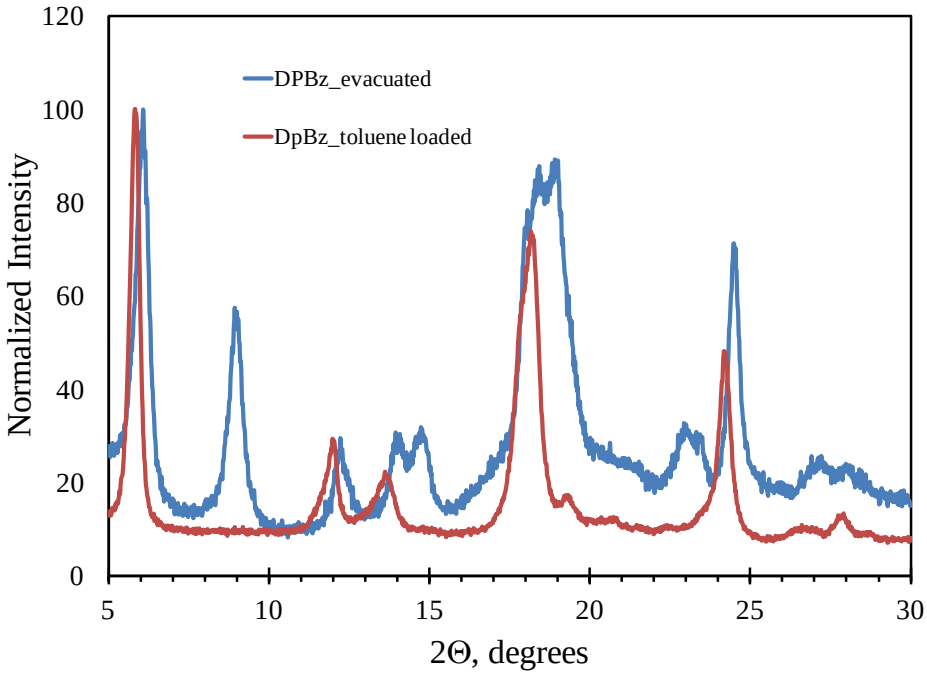

Figure S4. Powder xrd data for Ni(DPBz)Ni(CN)$_4$ "PICNIC-40" guest loaded and guest free.

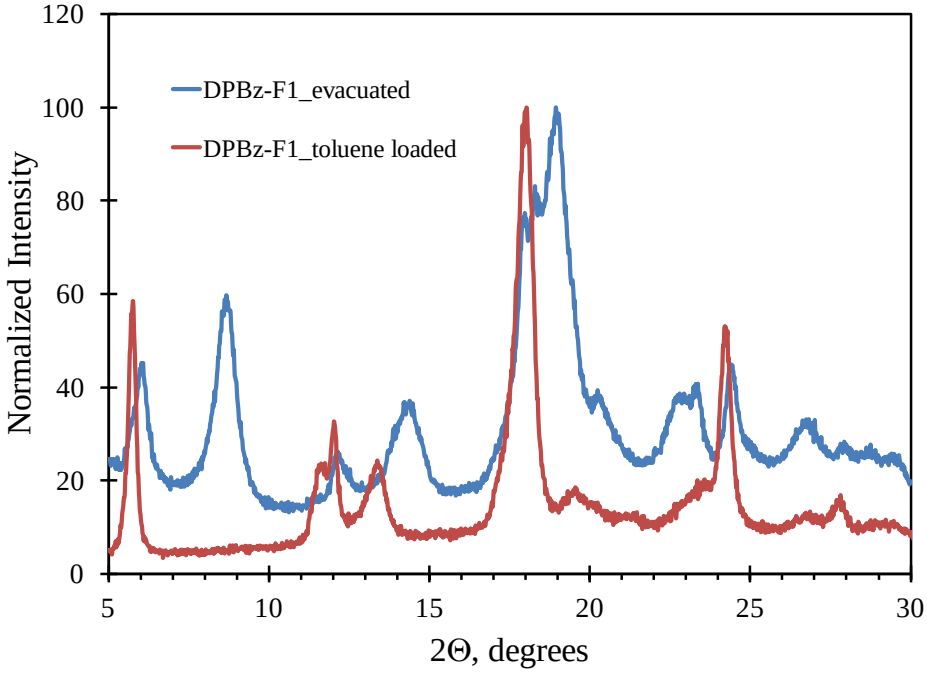

Figure S5. Powder xrd data for Ni(DPBz-F1)Ni(CN)$_4$ "PICNIC-41" guest loaded and guest free.

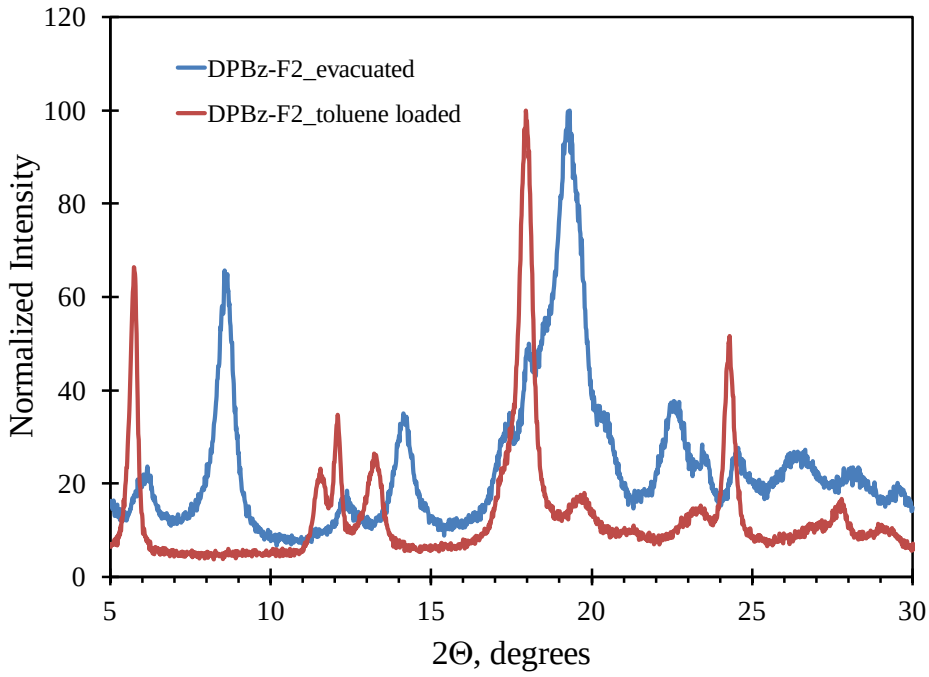

Figure S6. Powder xrd data for Ni(DPBz-F2)Ni(CN)$_4$ "PICNIC-42" guest loaded and guest free.

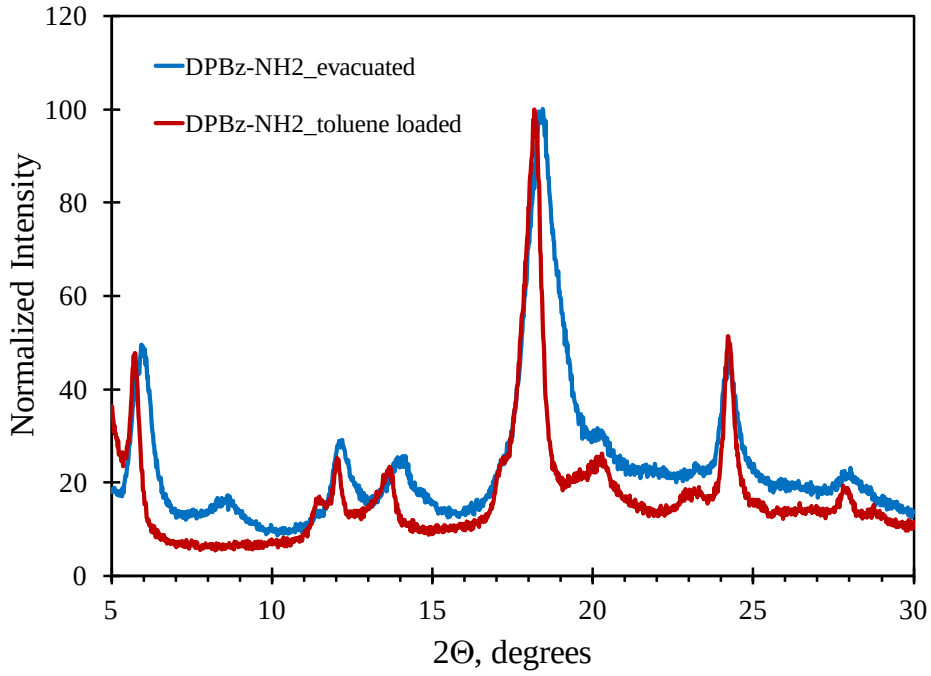

Figure S7. Powder xrd data for Ni(DPBz-NH2)Ni(CN)$_4$ "PICNIC-50" guest loaded and guest free.

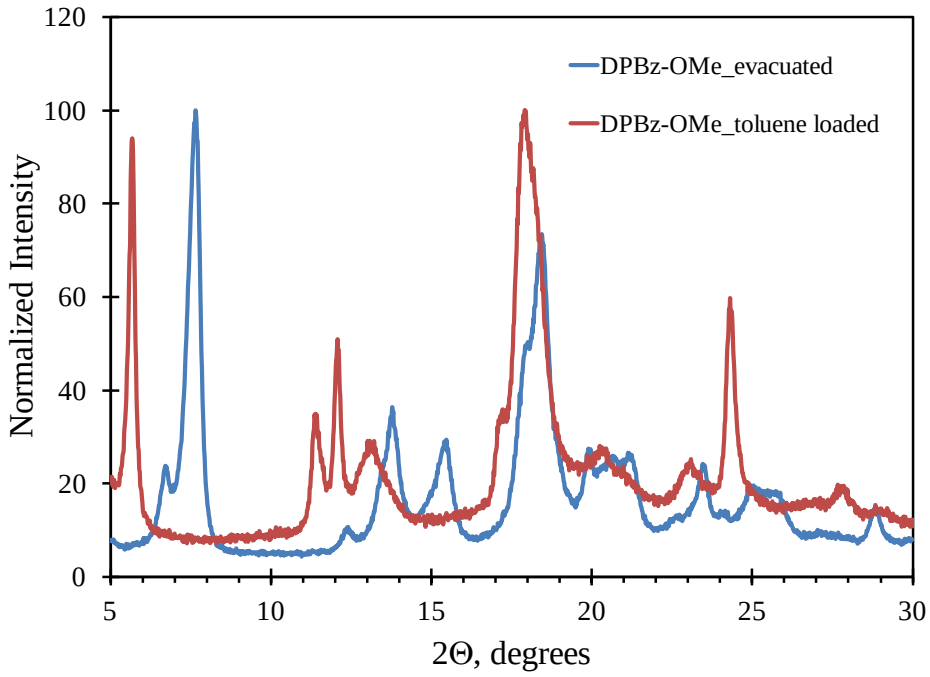

Figure S8. Powder xrd data for Ni(DPBz-OMe)Ni(CN)$_4$ "PICNIC-43" guest loaded and guest free.

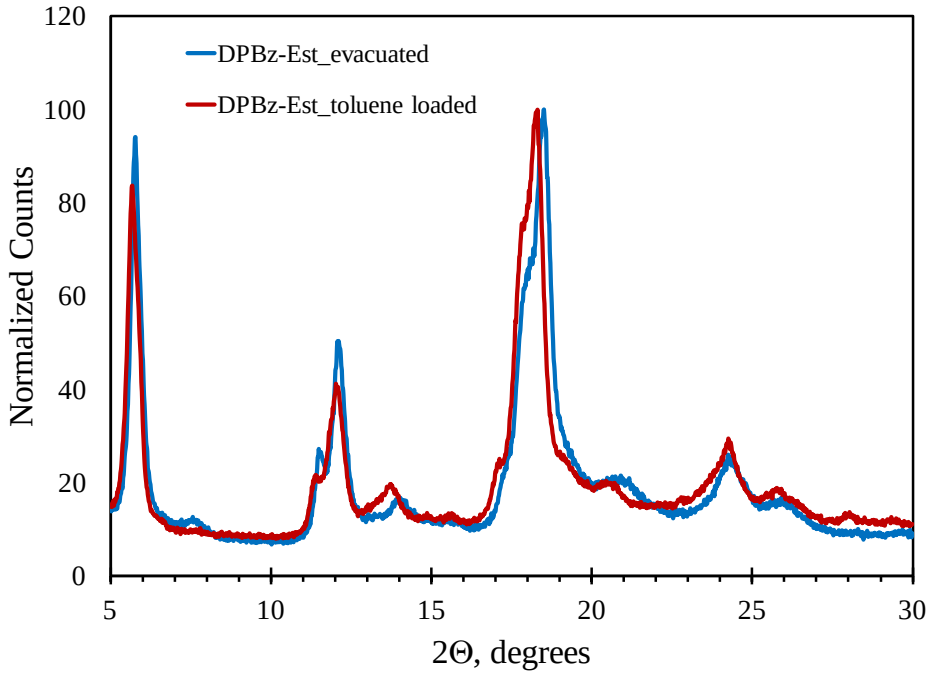

Figure S9. Powder xrd data for Ni(DPBz-Est)Ni(CN)$_4$ "PICNIC-49" guest loaded and guest free.

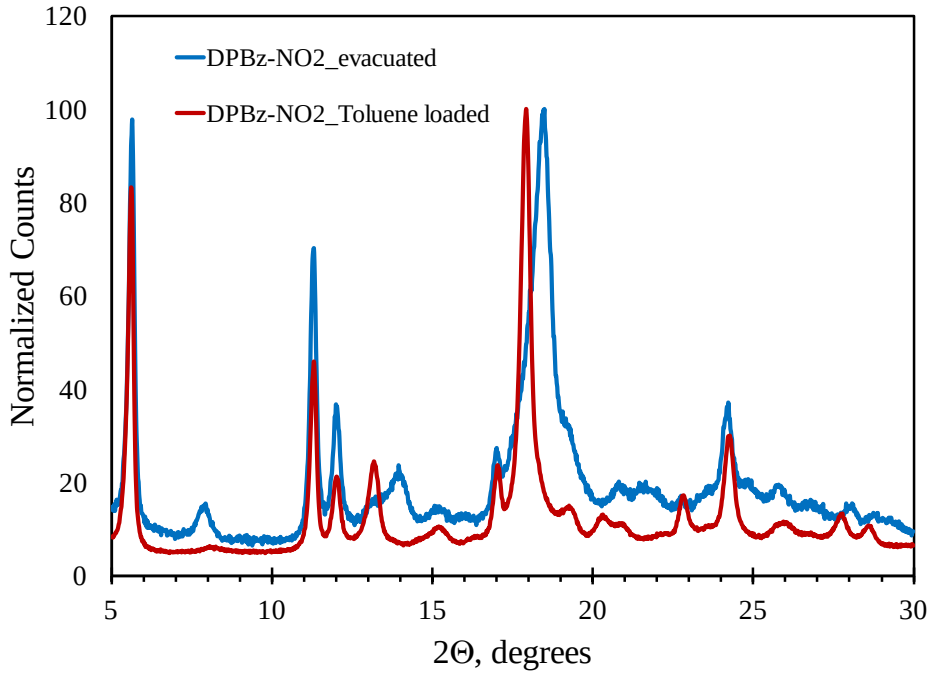

Figure S10. Powder xrd data for Ni(DPBz-NO2)Ni(CN)$_4$ "PICNIC-44" guest loaded and guest free.

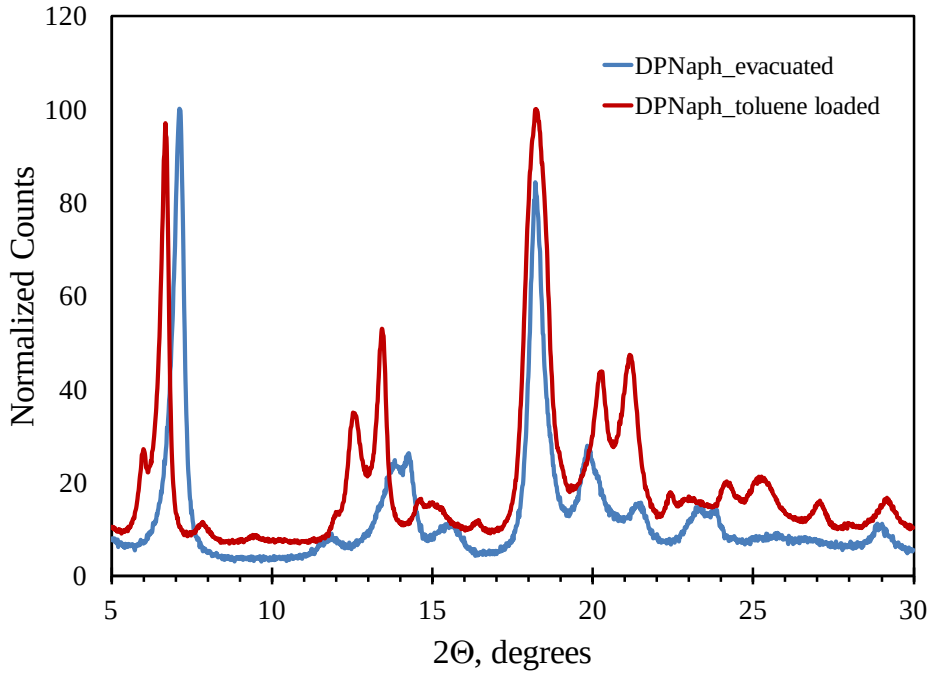

Figure S11. Powder xrd data for Ni(DPNaph)Ni(CN)$_4$ "PICNIC-51" guest loaded and guest free.

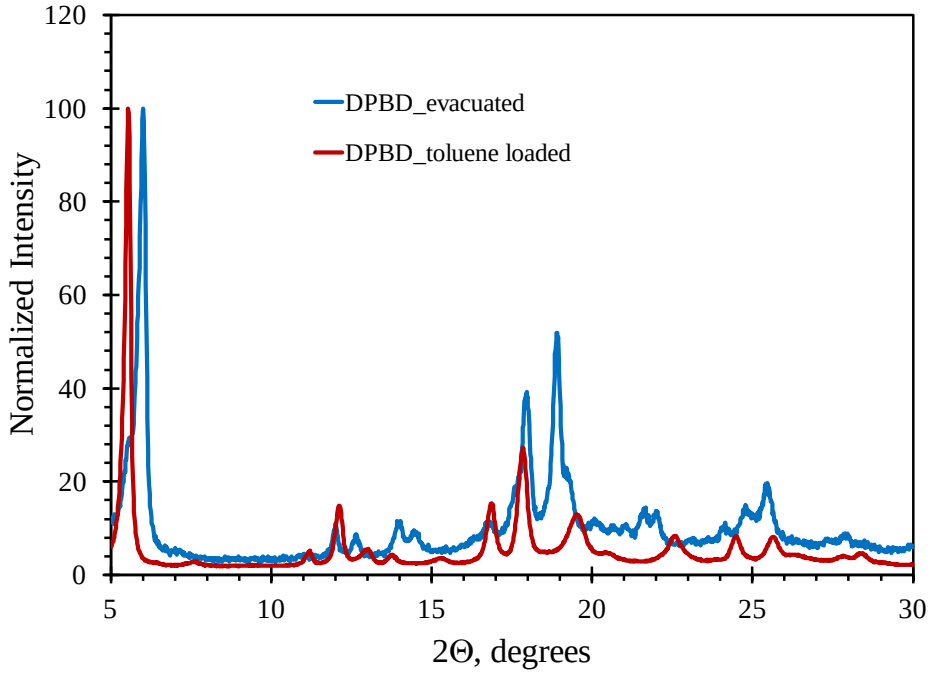

Figure S12. Powder xrd data for Ni(DPBD)Ni(CN)$_4$ "PICNIC-64" guest loaded and guest free.

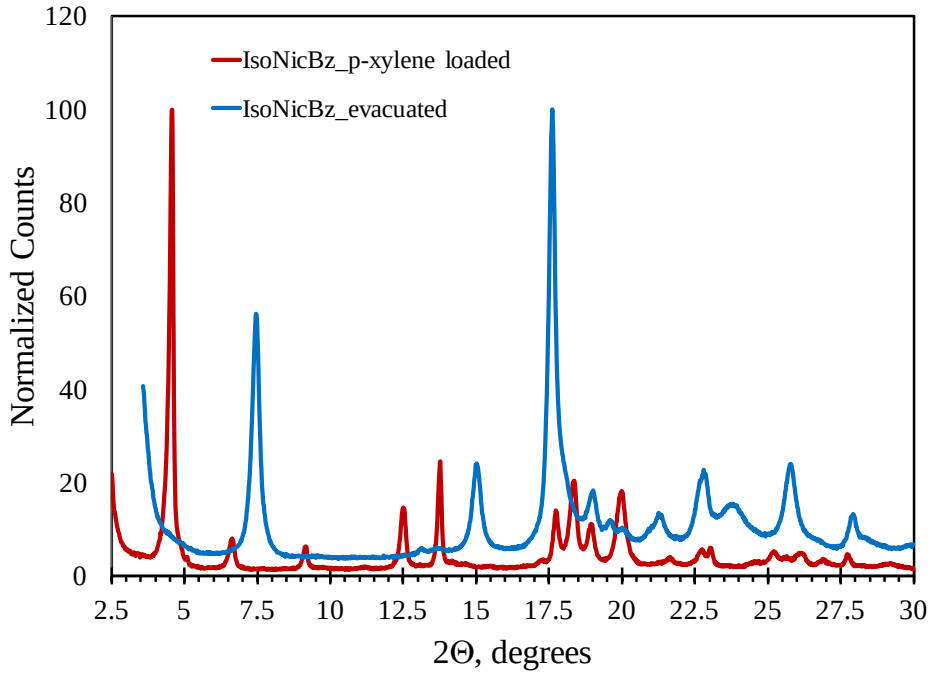

Figure S13. Powder xrd data for Ni(IsoNicBz)Ni(CN)$_4$ "PICNIC-70" guest loaded and guest free.

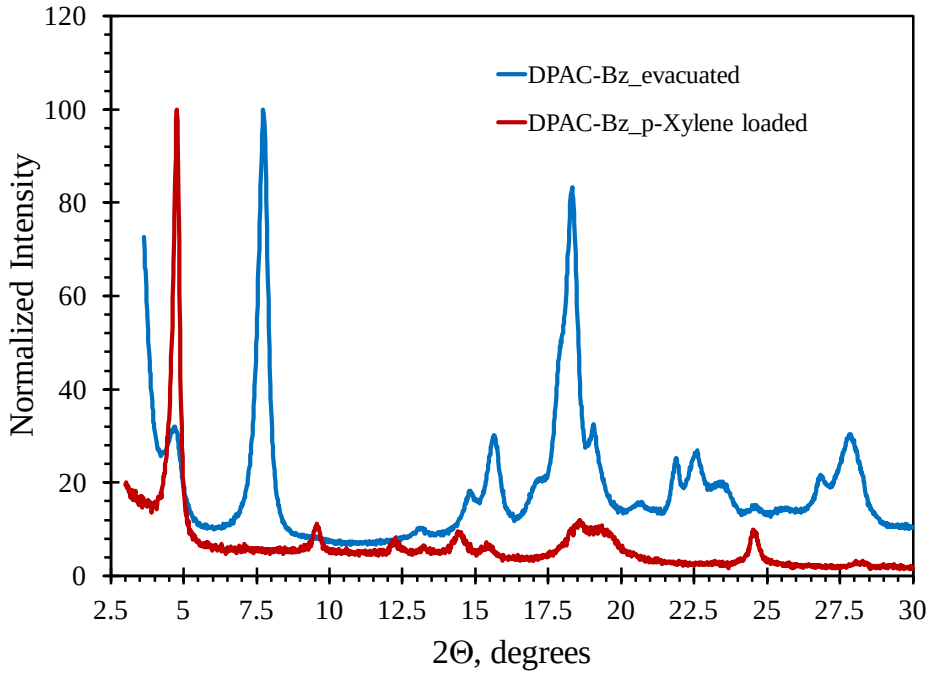

Figure S14. Powder xrd data for Ni(DPAC-Bz)Ni(CN)$_4$ "PICNIC-65" guest loaded and guest free.

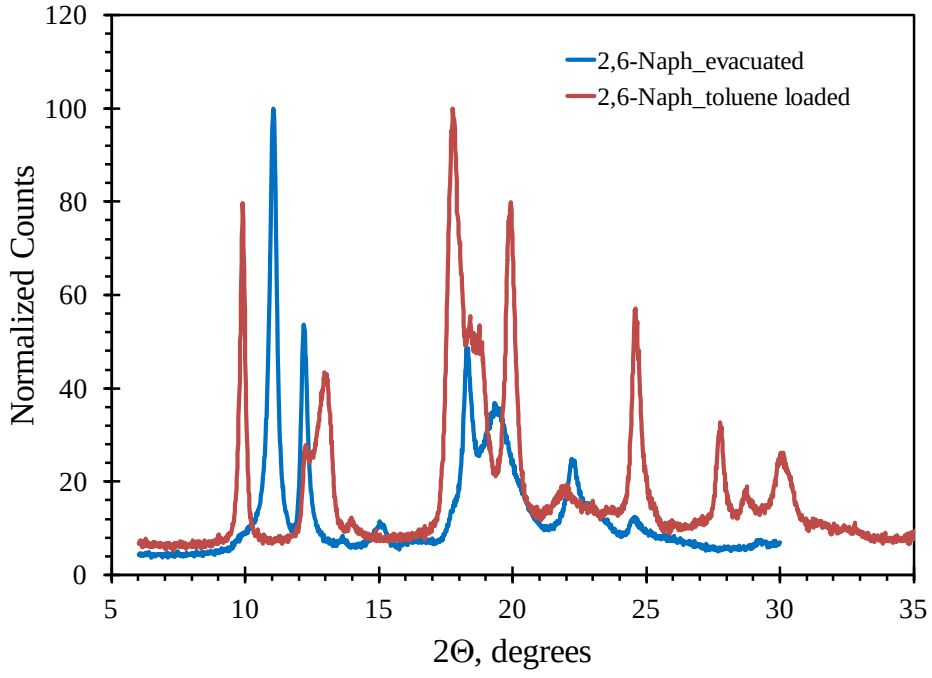

Figure S15. Powder xrd data for Ni(2,6-Naph)Ni(CN)$_4$ "PICNIC-13" guest free.

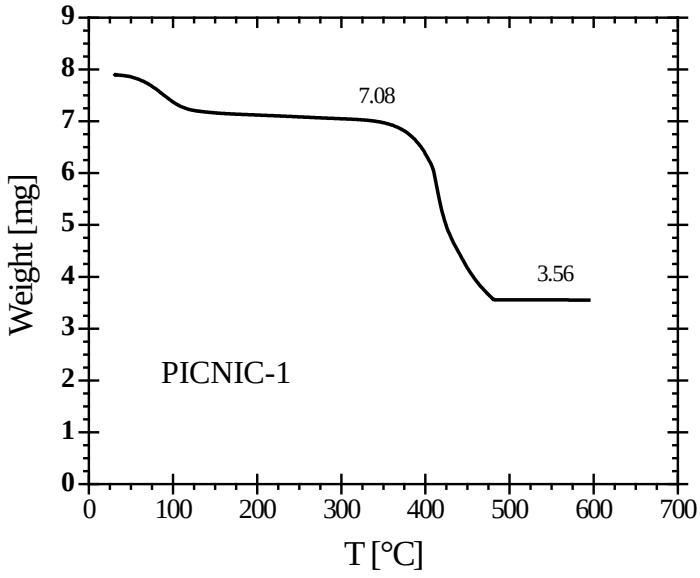

Figure S16. Ni(Pyz)Ni(CN)$_4$-toluene washed with CH_3Cl, ran in air 15 C/min.

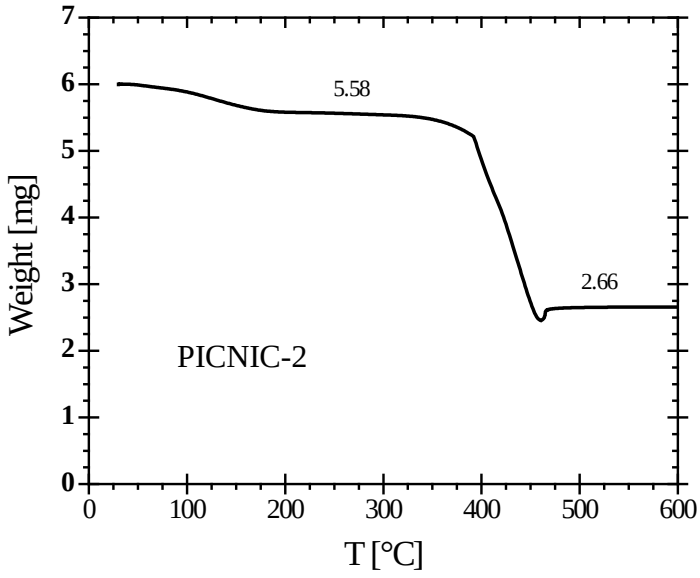

Figure S17. Ni(Pyz-Am)Ni(CN)$_4$-acetonitrile/toluene, ran in air 15 C/min.

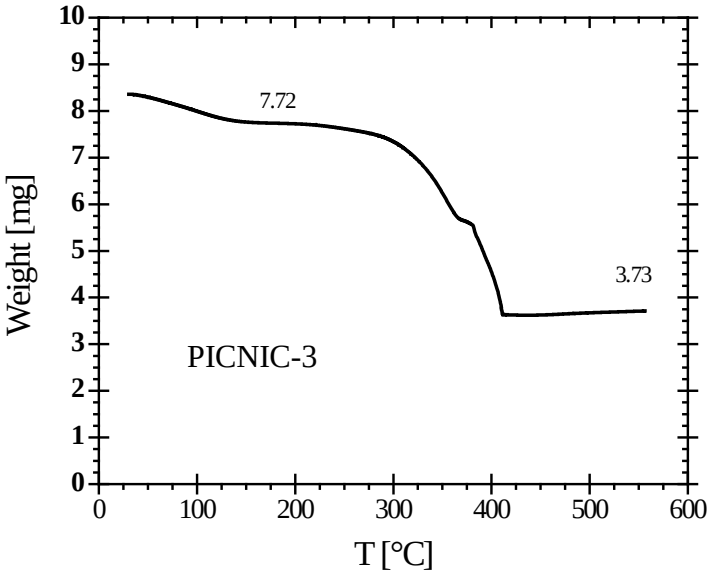

Figure S18. Ni(Pyz-Me)Ni(CN)$_4$-acetonitrile/toluene, ran in air 15 C/min.

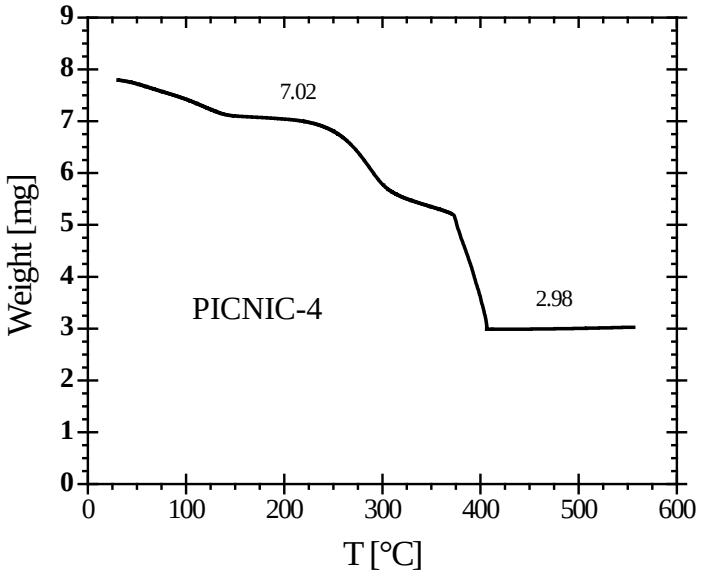

Figure S19. Ni(Pyz-OMe)Ni(CN)4-acetonitrile/toluene, ran in air 15 C/min.

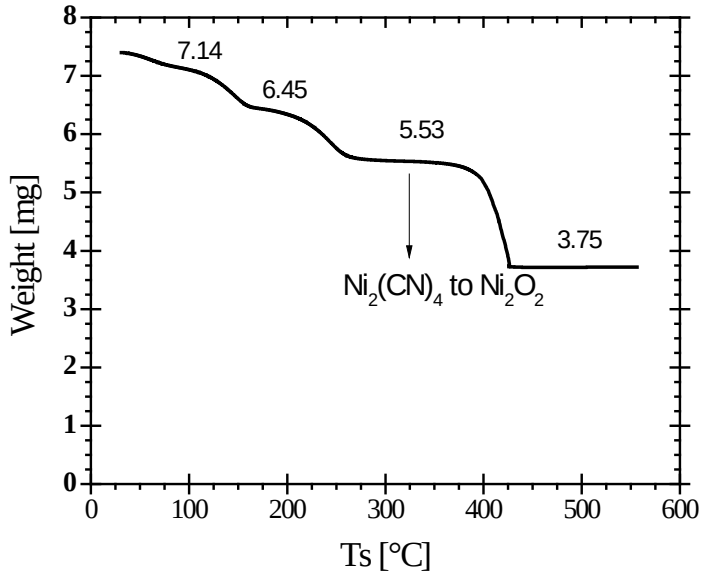

Figure S20. Product of HIPL reaction with $Ni_2(CN)_4$ and Pyz-Cl in toluene/acetonitrile ran in air 15 C/min. Expected formula weight of Ni(Pyz-Cl)$Ni(CN)_4$ is 336.0 which would give a ratio of Ni_2O_2 to Ni(Pyz-Cl)$Ni(CN)_4$ of 0.445. This ratio is not observed indicating the failure to form the targeted product.

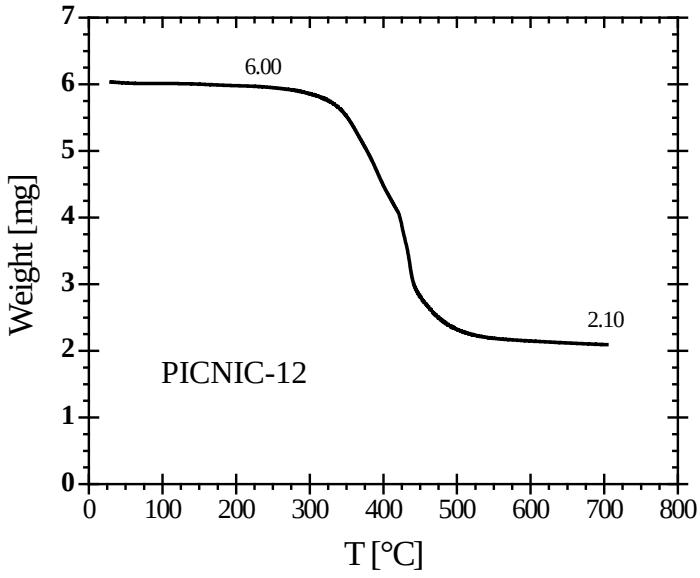

Figure S21. Ni(pXdAm-F4)Ni(CN)$_4$ evacuated, ran in air 15 C/min.

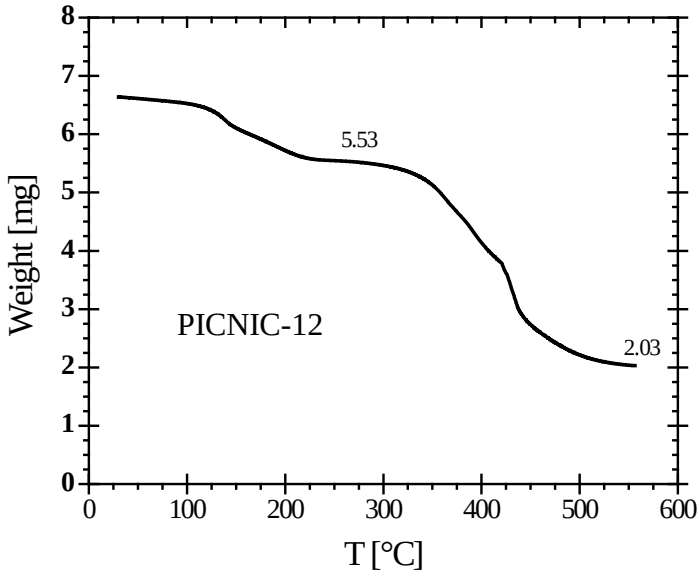

Figure S22. Ni(pXdAm-F4)Ni(CN)$_4$ evacuated then soaked in toluene, ran in air 15 C/min.

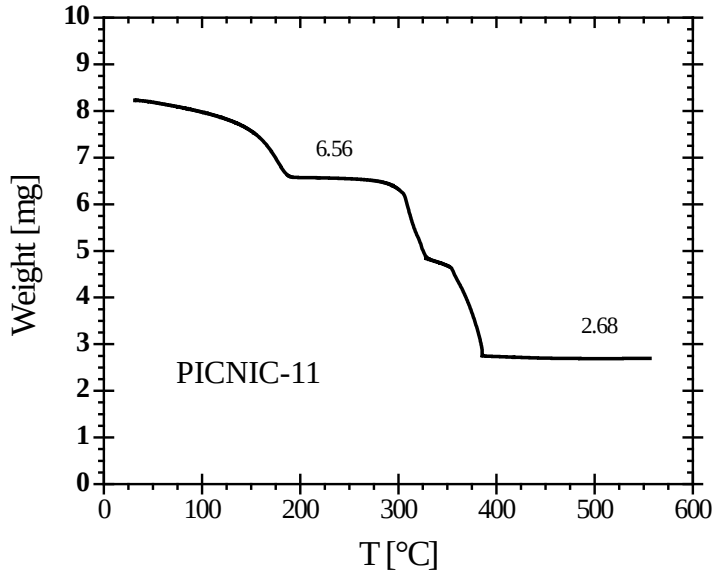

Figure S23. Ni(pXdAm)Ni(CN)$_4$-acetonitrile/toluene, ran in air 15 C/min.

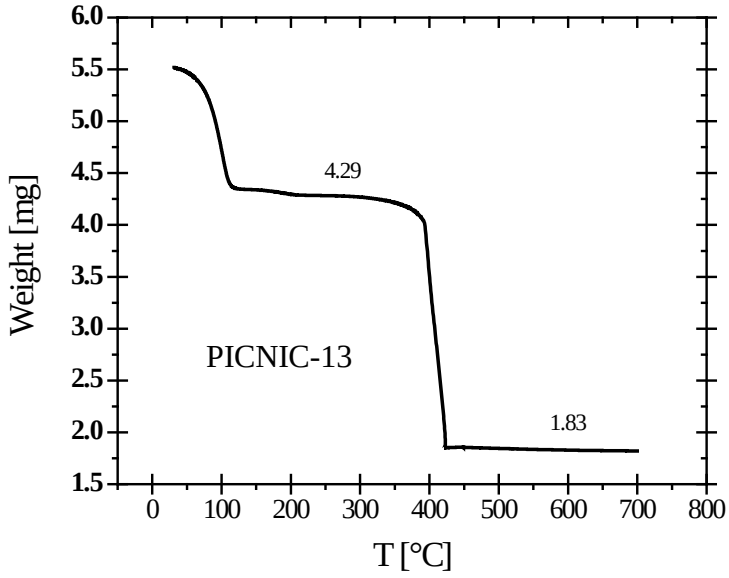

Figure S24. Ni(2,6-Naph)Ni(CN)$_4$ $CHCl_3$ extracted, ran in air 15 C/min.

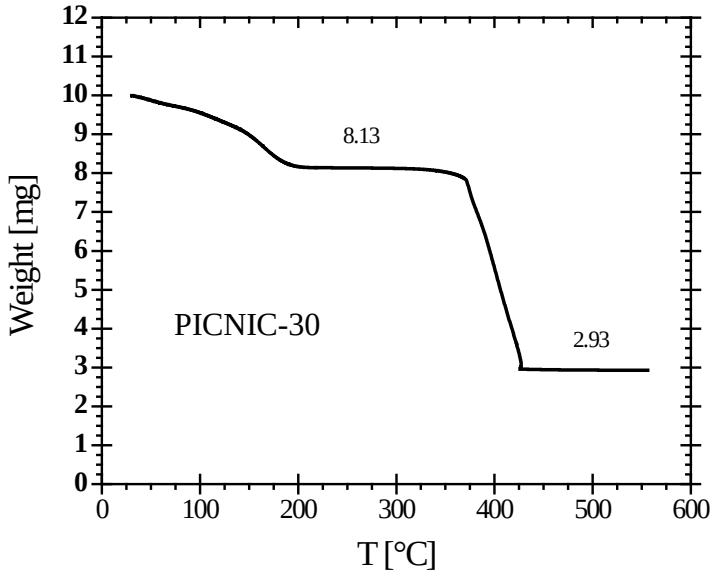

Figure S25. Ni(PINA)Ni(CN)$_4$ acetone extracted, ran in air 15 C/min.

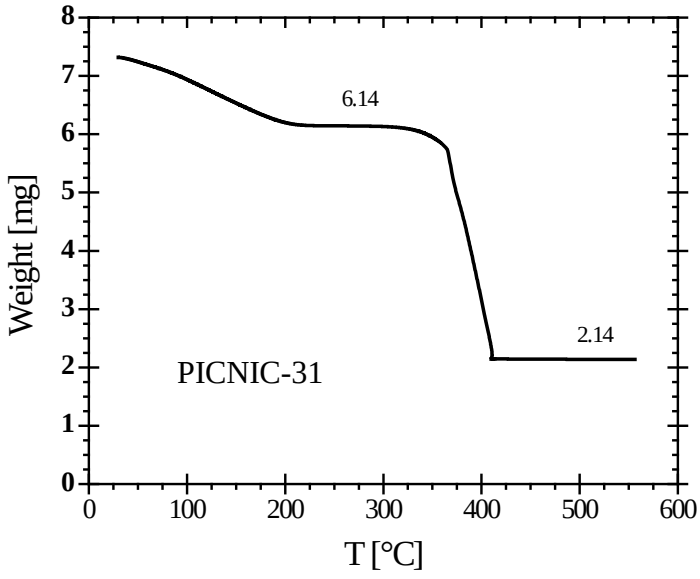

Figure S26. Ni(PINA-Me)Ni(CN)$_4$ acetone extracted, ran in air 15 C/min.

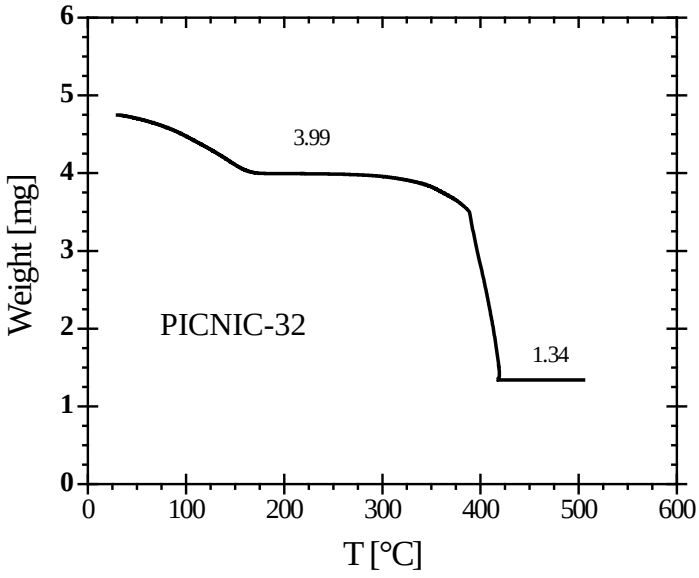

Figure S27. Ni(PINA-F)Ni(CN)$_4$ acetone extracted, ran in air 15 C/min.

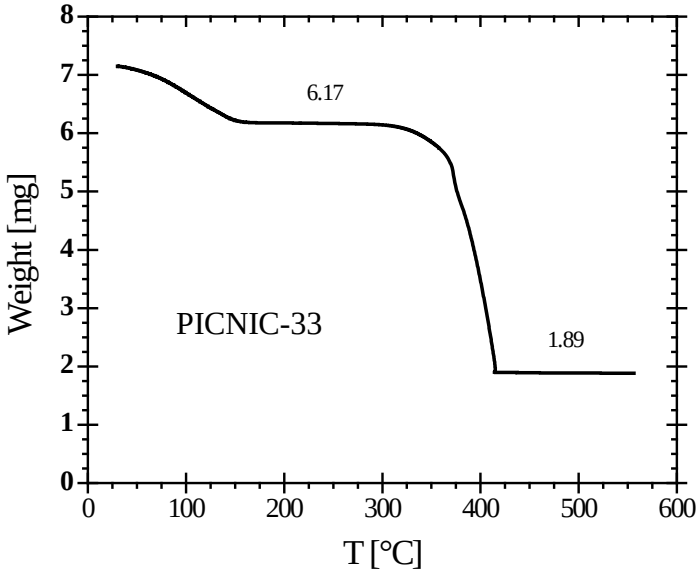

Figure S28. Ni(PINA-NO2)Ni(CN)$_4$ acetone extracted, ran in air 15 C/min.

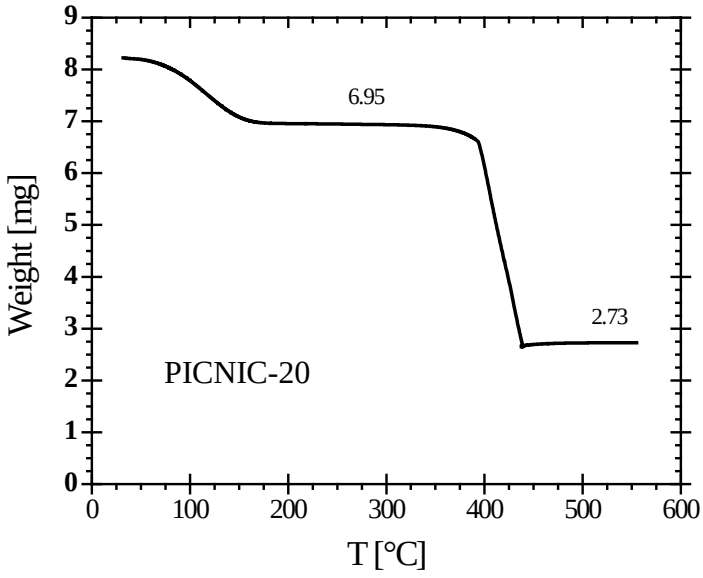

Figure S29. Ni(Bpy)Ni(CN)$_4$ $CHCl_3$ extracted, ran in air 15 C/min.

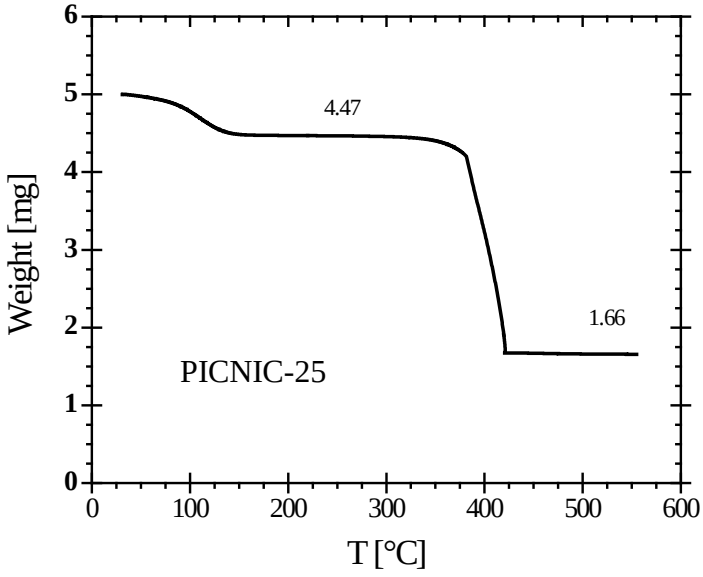

Figure S30. Ni(Bpy-Ald)Ni(CN)$_4$ acetone extracted, ran in air 15 C/min.

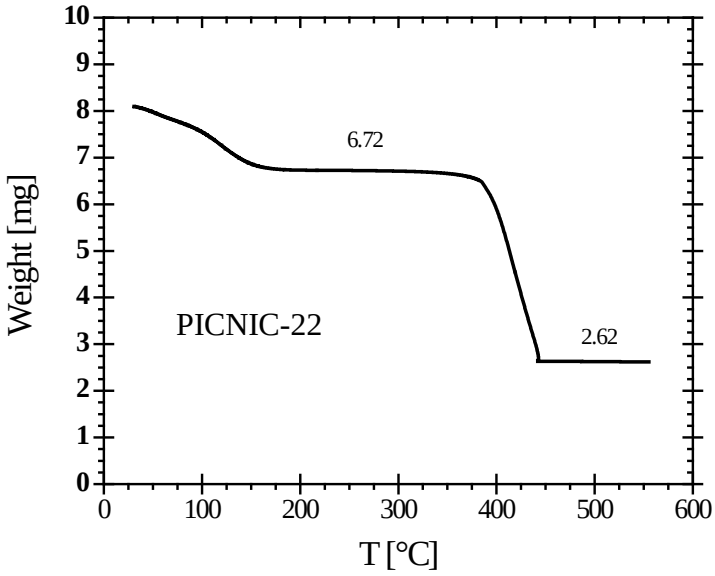

Figure S31. Ni(Bpy-NH2)Ni(CN)$_4$ $CHCl_3$ extracted, ran in air 15 C/min.

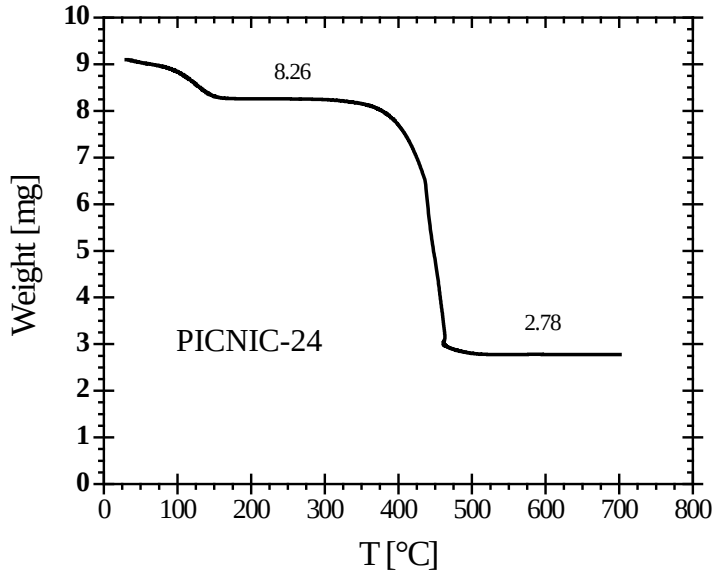

Figure S32. Ni(Bpy-CF3)Ni(CN)$_4$ acetone extracted, ran in air 15 C/min.

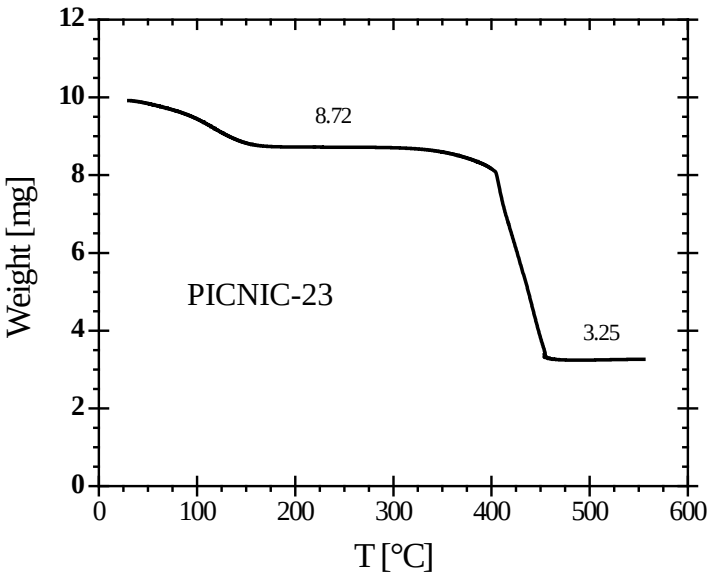

Figure S33. Ni(Bpy-F)Ni(CN)$_4$ acetone extracted, ran in air 15 C/min.

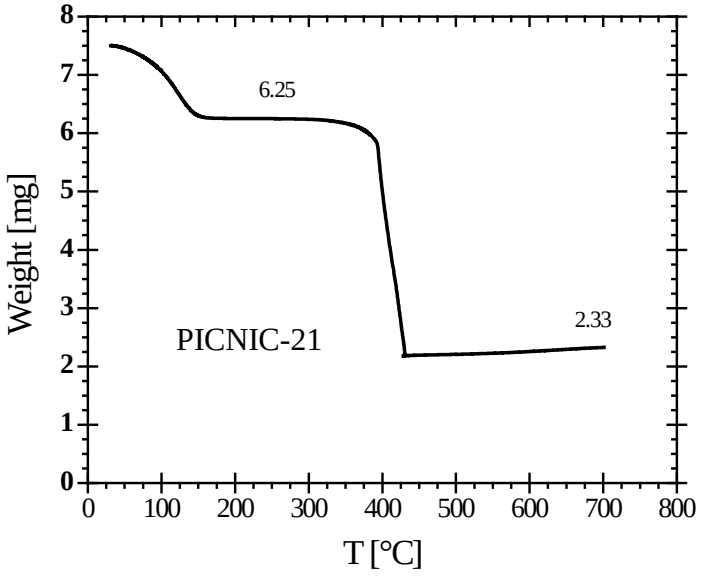

Figure S34. Ni(Bpy-Me)Ni(CN)$_4$ acetone extracted, ran in air 15 C/min.

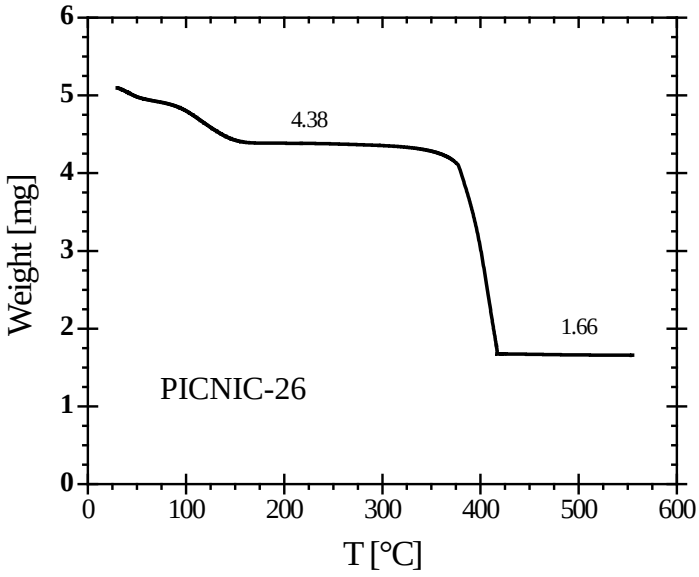

Figure S35. Ni(Bpy-OMe)Ni(CN)$_4$ acetone extracted, ran in air 15 C/min.

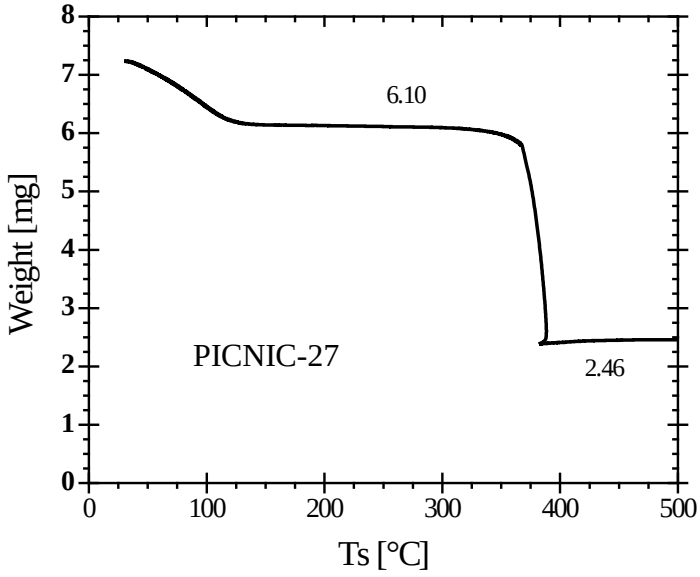

Figure S36. Ni(4,4'-Bpm)Ni(CN)$_4$ acetone extracted, ran in air 15 C/min.

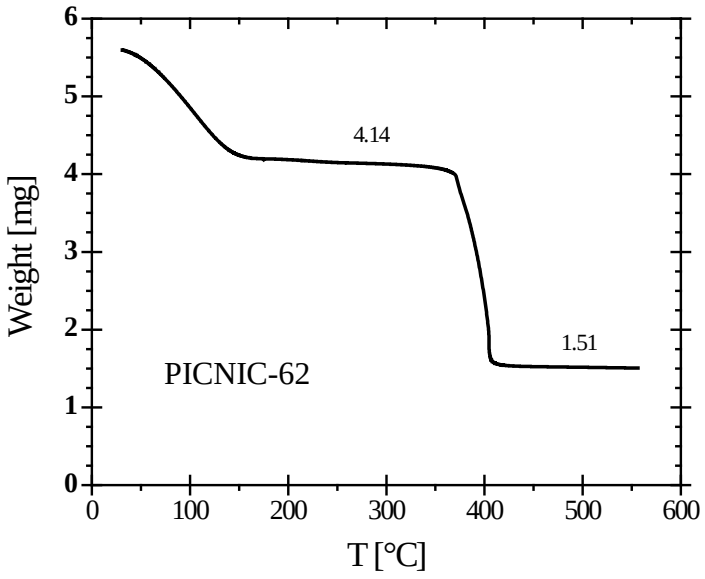

Figure S37. Ni(Azopyr)Ni(CN)$_4$ $CHCl_3$ extracted, ran in air 15 C/min.

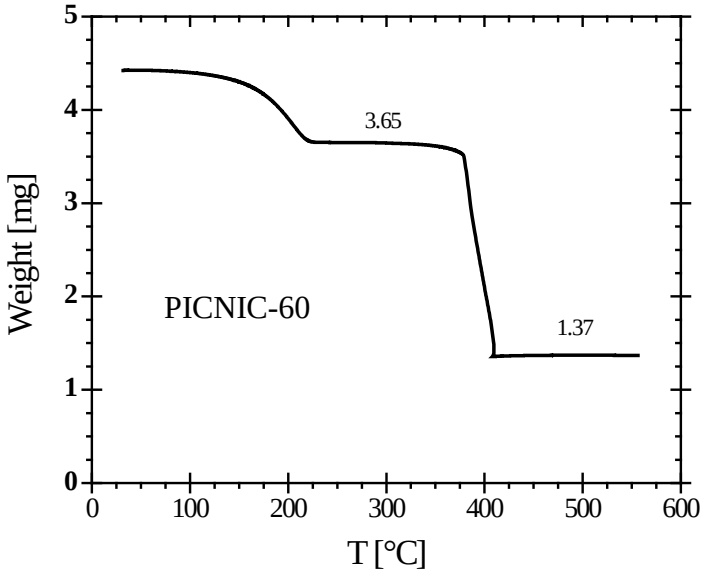

Figure S38. Ni(Bpene)Ni(CN)$_4$ in toluene, ran in air 15 C/min.

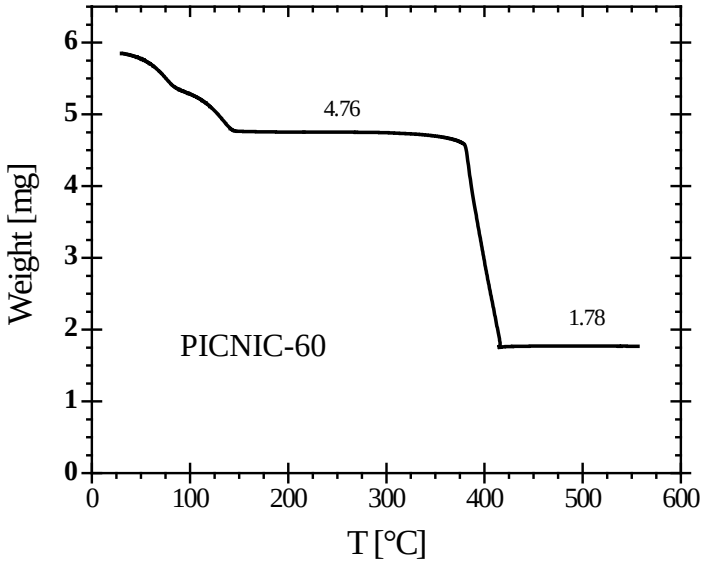

Figure S39. Ni(Bpene)Ni(CN)$_4$ toluene after acetone extraction, ran in air 15 C/min.

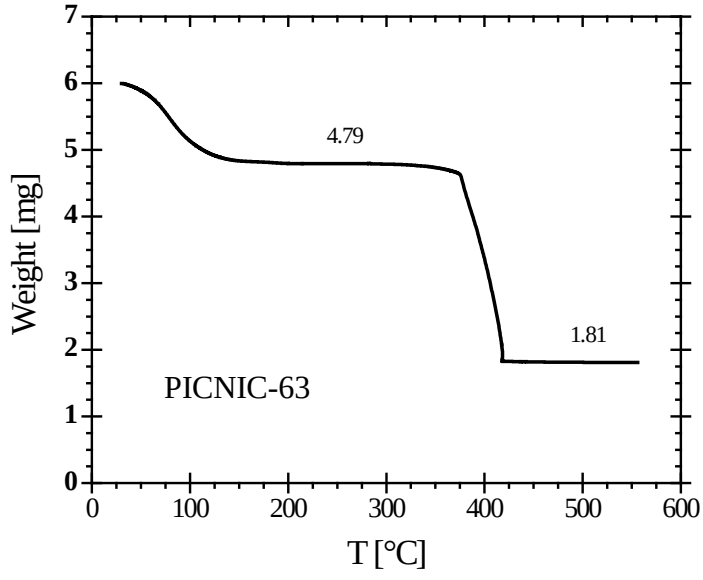

Figure S40. Ni(DPAC)Ni(CN)$_4$-acetonitrile, ran in air 15 C/min.

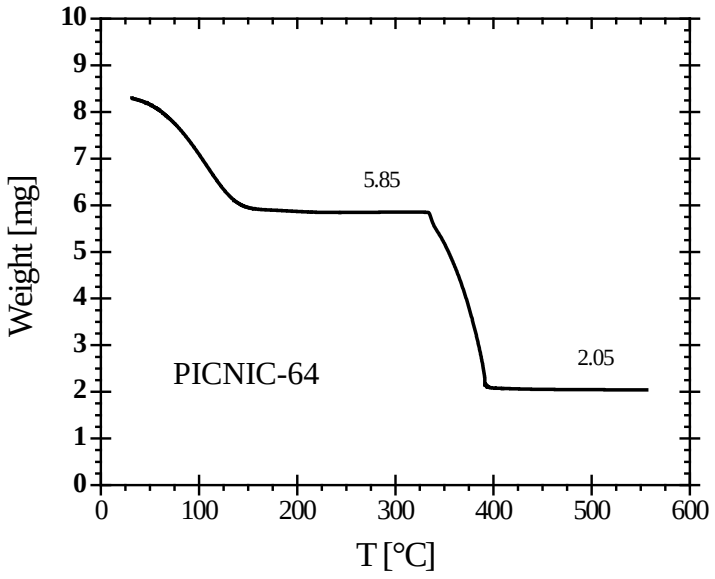

Figure S41. Ni(DPBD)Ni(CN)$_4$ $CHCl_3$ extracted, ran in air 15 C/min.

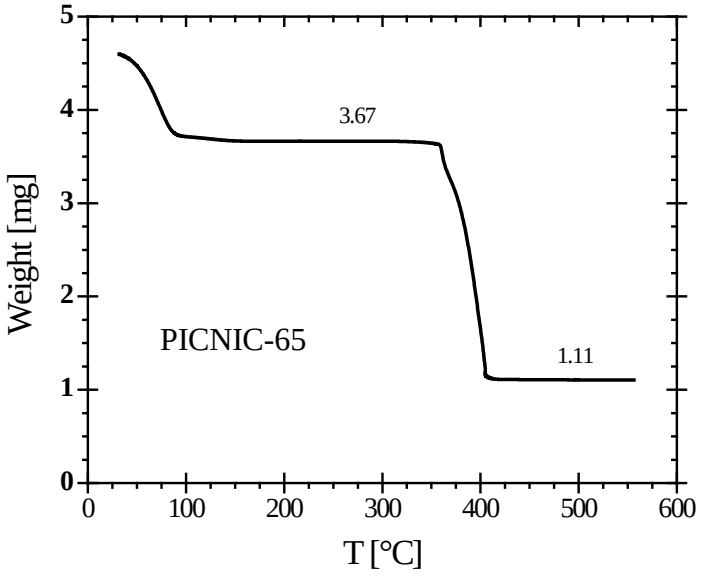

Figure S42. Ni(DPAC-Bz)Ni(CN)$_4$ $CHCl_3$ extracted, ran in air 15 C/min.

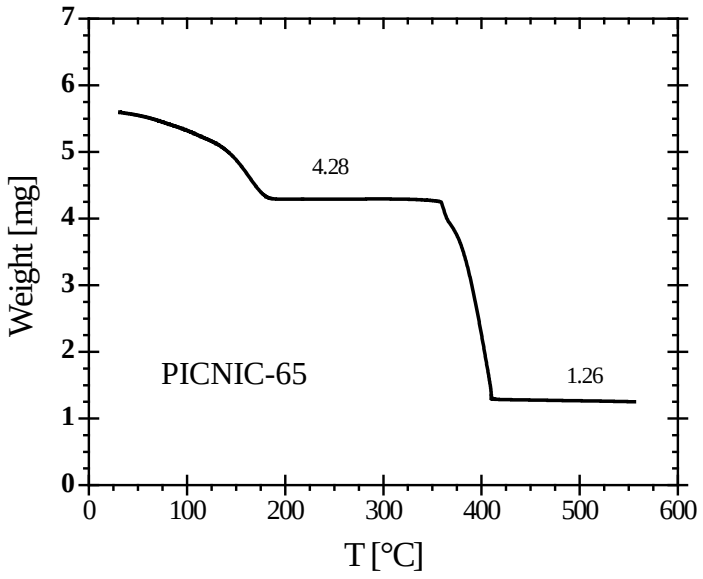

Figure S43. Ni(DPAC-Bz)Ni(CN)$_4$-p-xylene, ran in air 15 C/min.

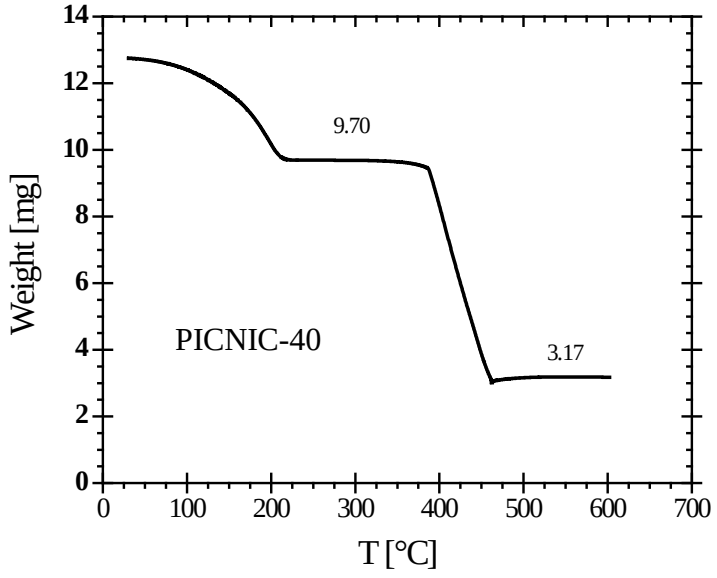

Figure S44. Ni(DPBz)Ni(CN)$_4$-toluene, ran in air 15 C/min.

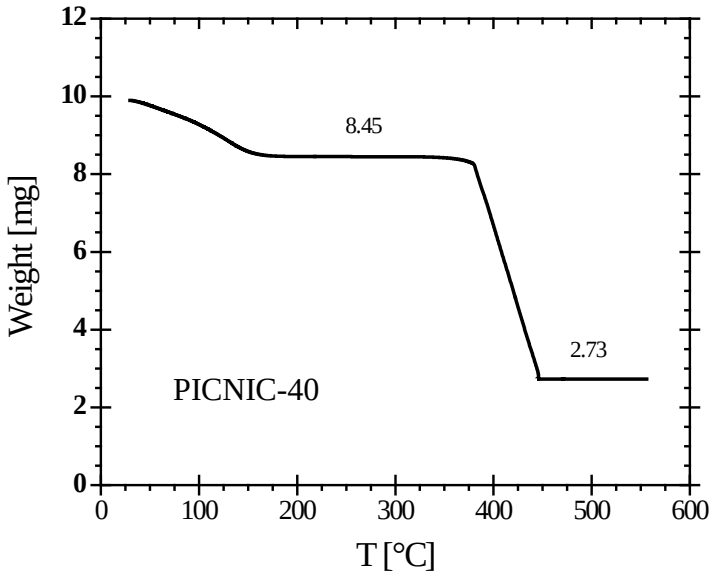

Figure S45. Ni(DPBz)Ni(CN)$_4$ after extraction with acetone, ran in air 15 C/min.

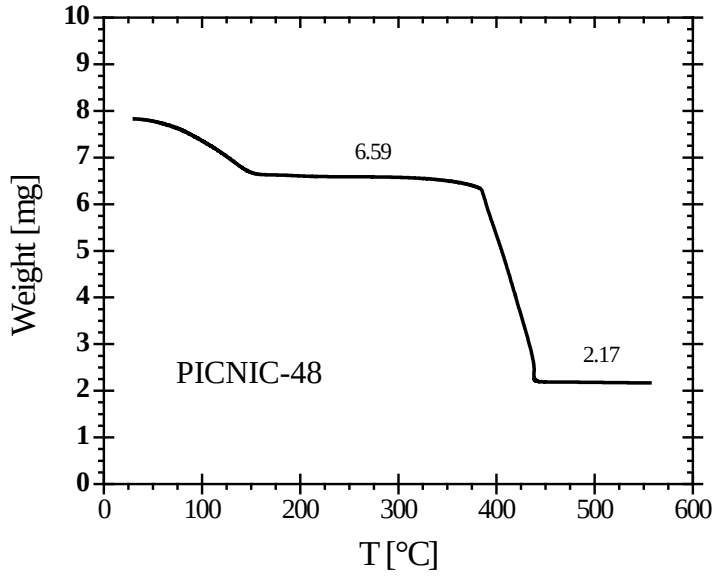

Figure S446 Ni(DPBz-Ald)Ni(CN)$_4$ $CHCl_3$ extracted, ran in air 15 C/min.

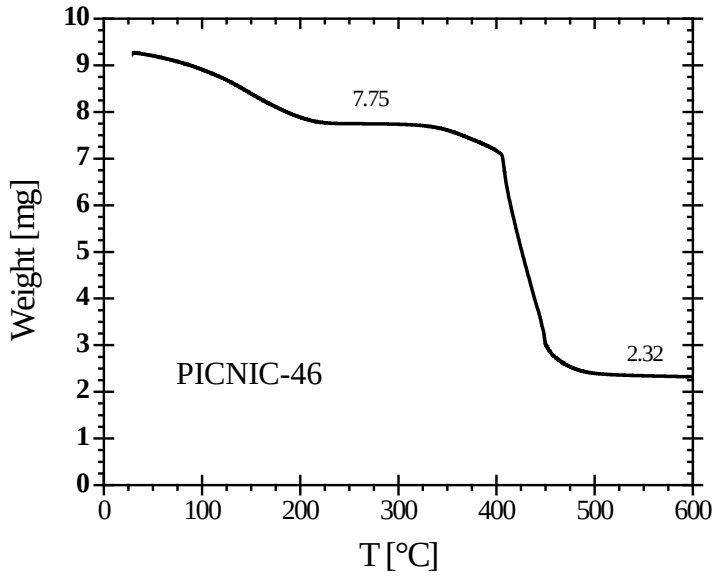

Figure S47. Ni(DPBz-CF3)Ni(CN)$_4$-toluene, ran in air 15 C/min.

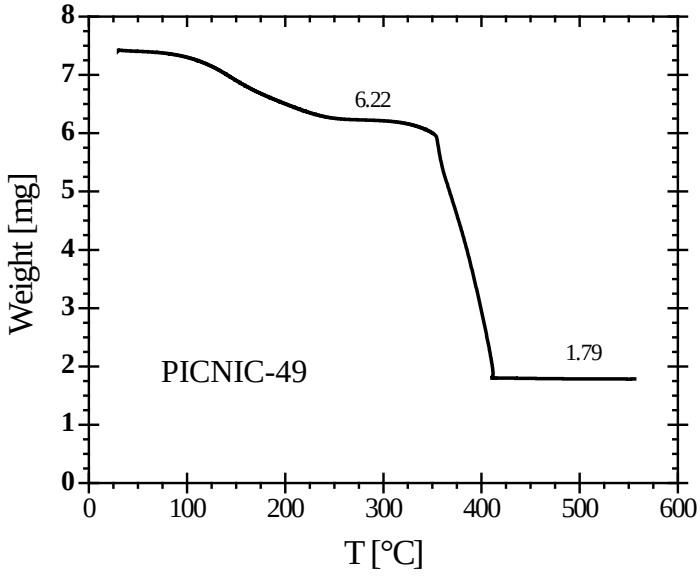

Figure S48. Ni(DPBz-Est)Ni(CN)$_4$-p-xylene, ran in air 15 C/min.

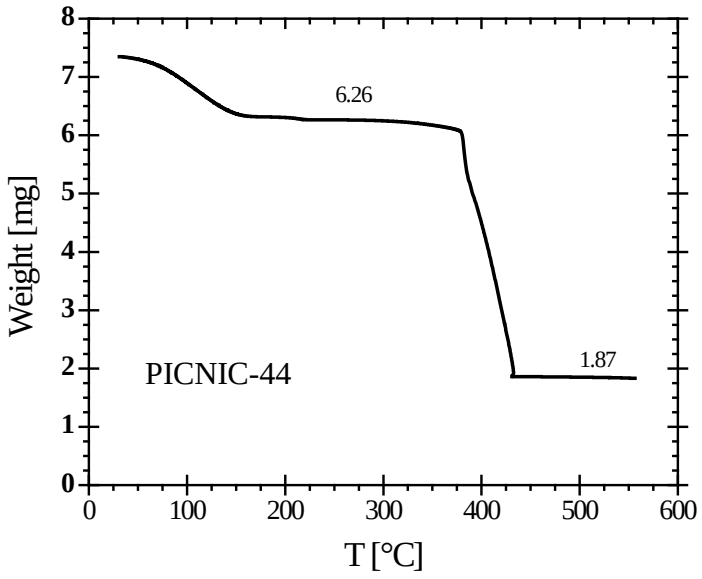

Figure S49. Ni(DPBz-NO2)Ni(CN)$_4$ $CHCl_3$ extracted, ran in air 15 C/min.

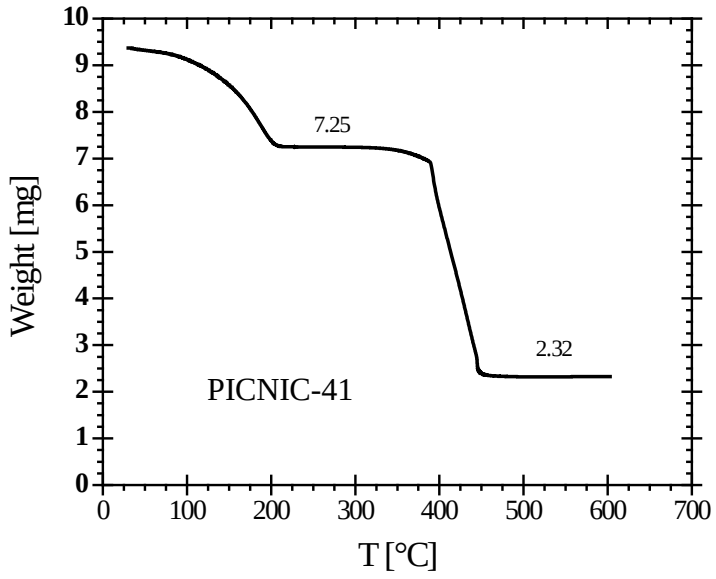

Figure S50. Ni(DPBz-F1)Ni(CN)$_4$-toluene, ran in air 15 C/min.

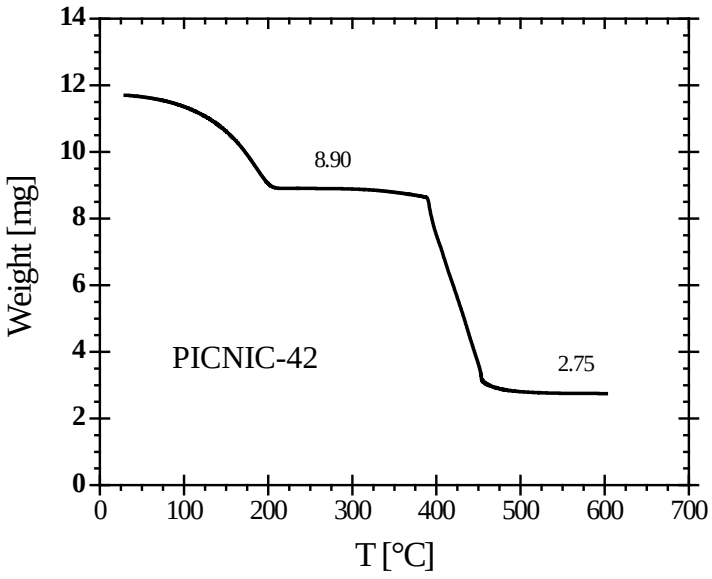

Figure S51. Ni(DPBz-F2)Ni(CN)$_4$-toluene, ran in air 15 C/min.

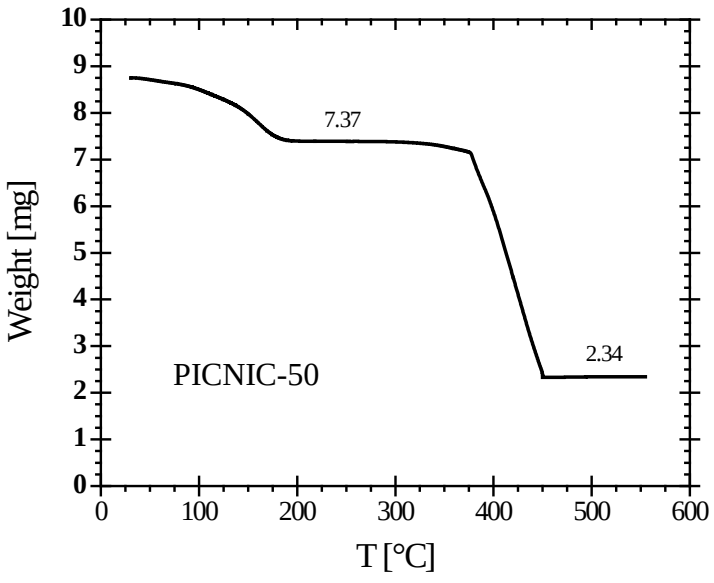

Figure S52. Ni(DPBz-NH2)Ni(CN)$_4$-toluene, ran in air 15 C/min.

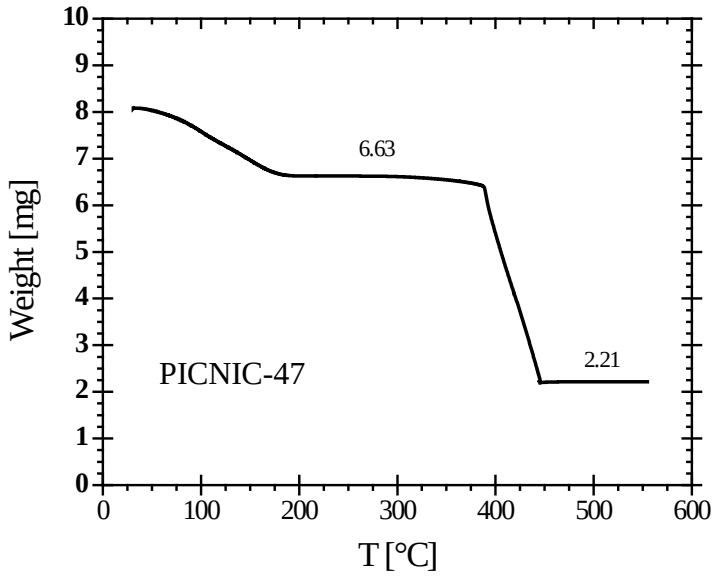

Figure S53. Ni(DPBz-Et)-toluene, ran in air 15 C/min.

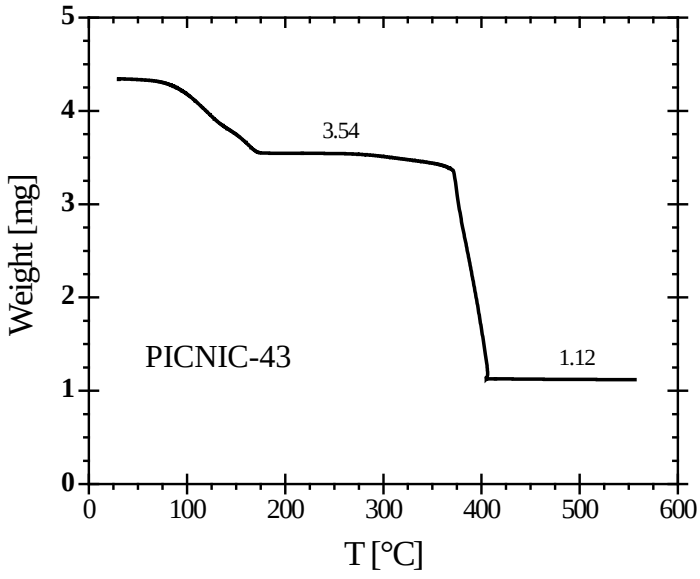

Figure S54. Ni(DPBz-OMe)$Ni(CN)_4$-p-xylene, ran in air 15 C/min.

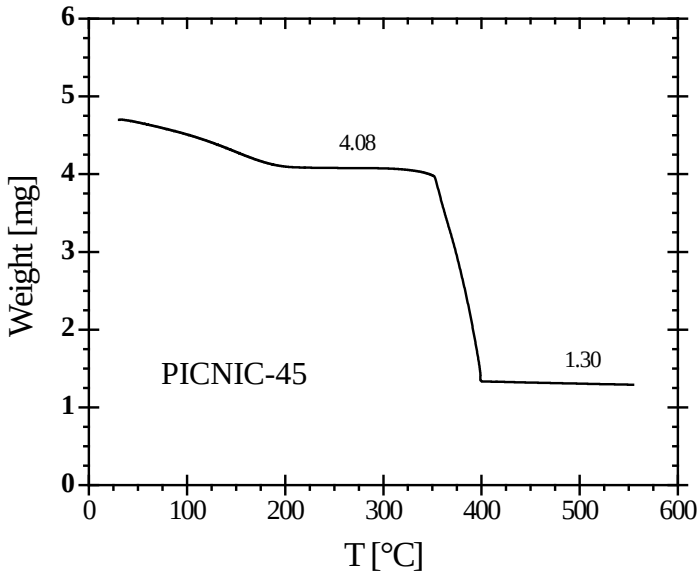

Figure S55. Ni(DPBz-AmMe)Ni(CN)$_4$-toluene, ran in air 15 C/min.

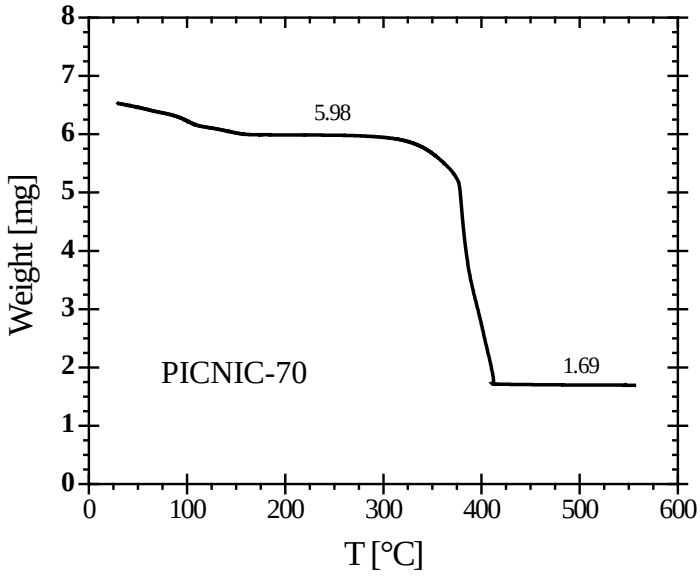

Figure S56. Ni(IsoNic-Bz)Ni(CN)$_4$-toluene, ran in air 15 C/min.

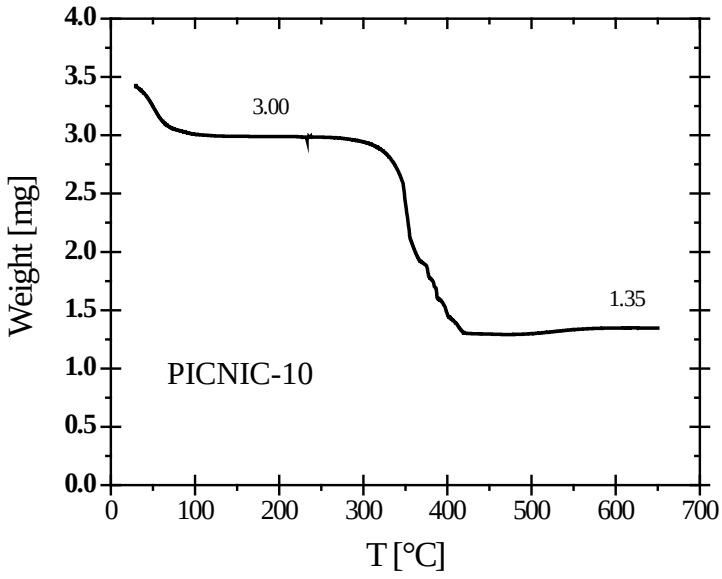

Figure S57. Ni(AmMe-Pyr)Ni(CN)$_4$ $CHCl_3$ extracted, ran in air 15 C/min.

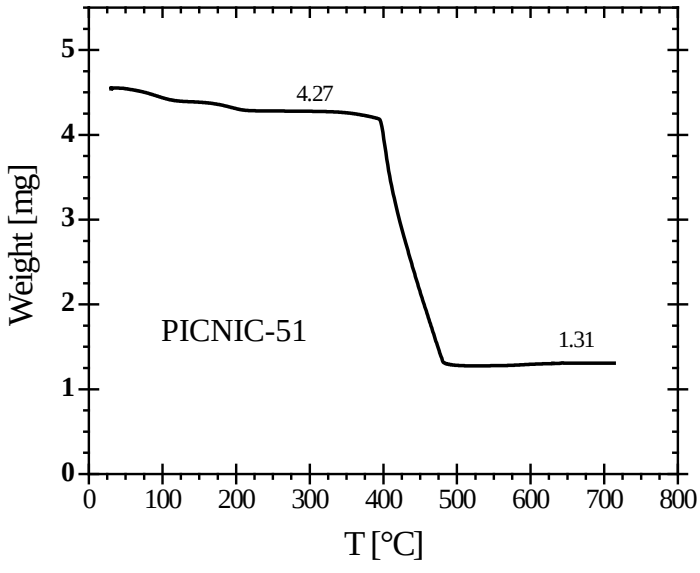

Figure S58. Ni(DP-Naph)Ni(CN)$_4$-p-xylene, ran in air 15 C/min.

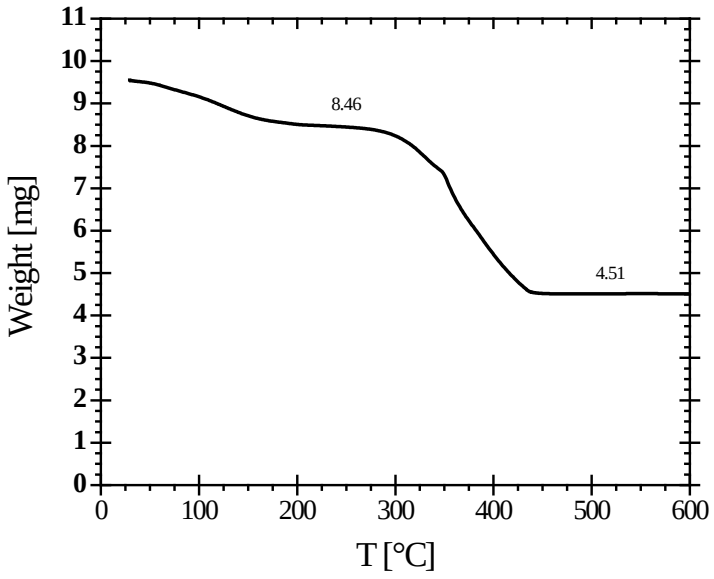

Figure S59. Fe(Pyz)Ni(CN)$_4$-acetonitrile, ran in air 15 C/min.

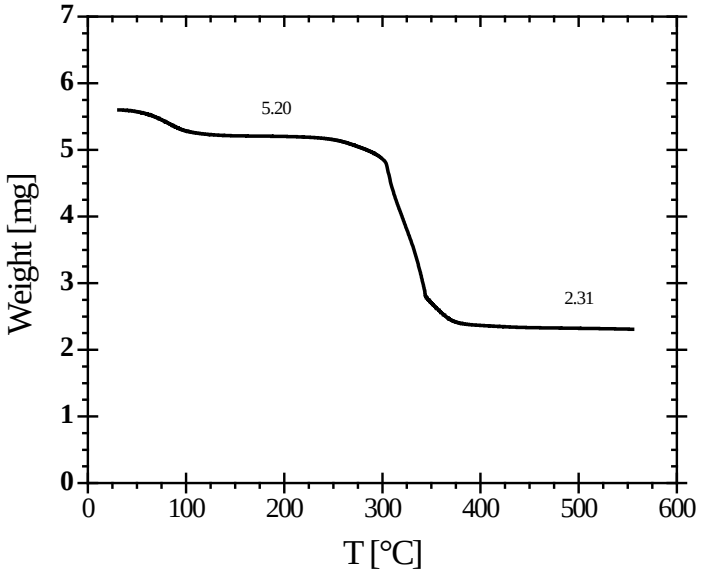

Figure S60. Fe(pXdAm)Ni(CN)$_4$ $CHCl_3$ extracted, ran in air 15 C/min.

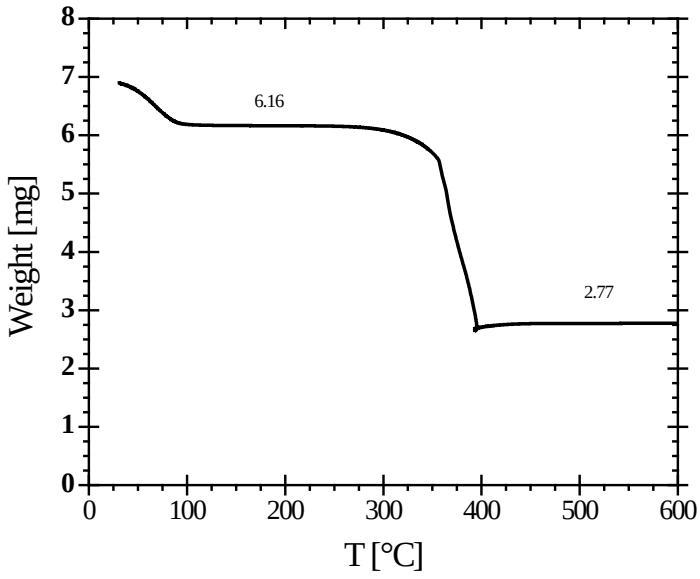

Figure S61. Fe(Bpene)Pd(CN)$_4$ $CHCl_3$ extracted, ran in air 15 C/min.

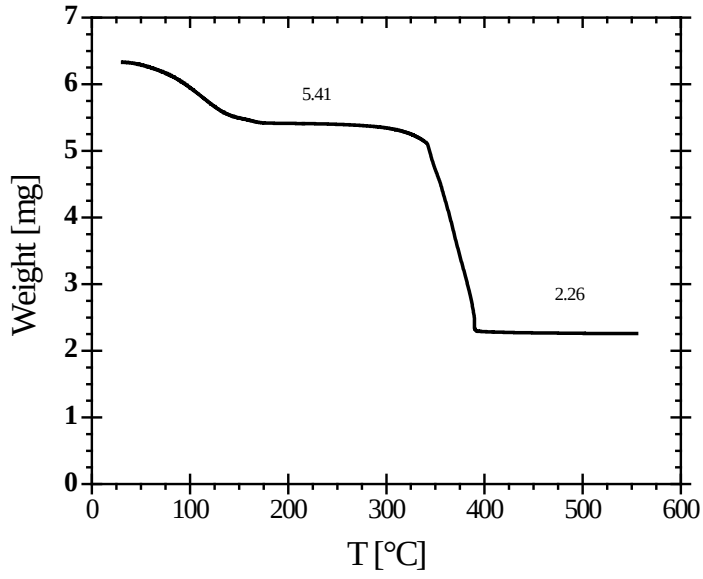

Figure S62. Fe(Bpy)Ni(CN)$_4$-acetonitrile, ran in air 15 C/min.

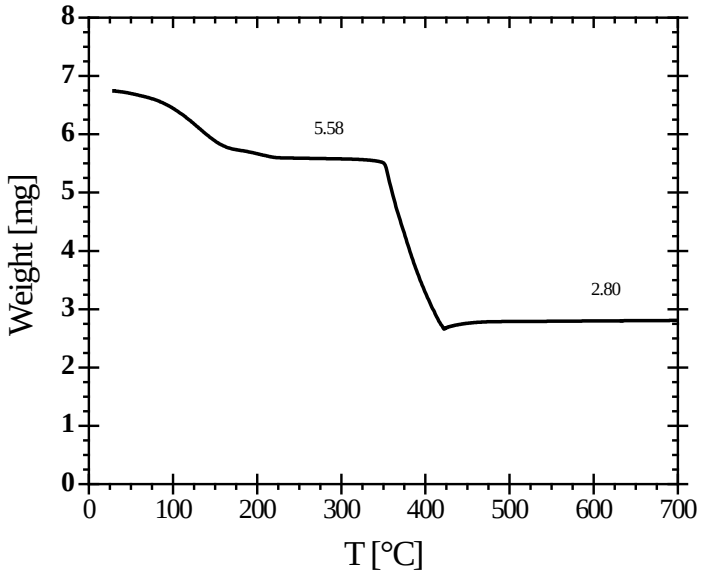

Figure S63. Fe(Bpy)Pd$(CN)_4$-acetonitrile, ran in air 15 C/min.

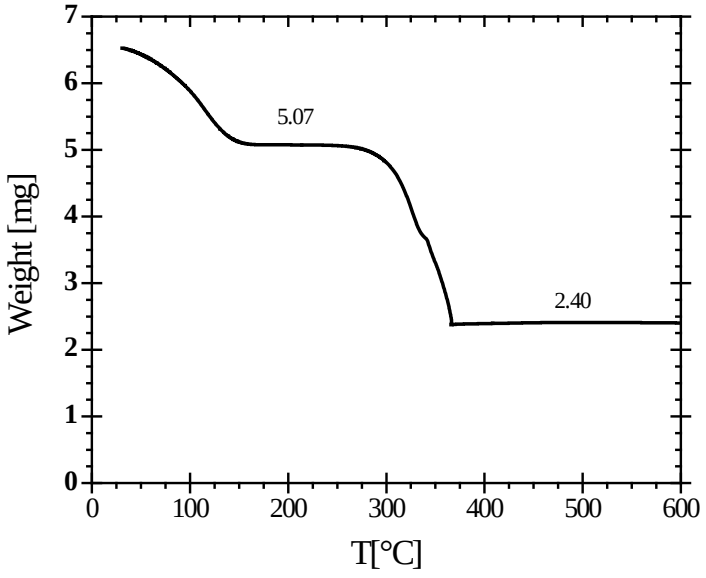

Figure S64. Co(AmMe-Pyr)Ni$(CN)_4$ $CHCl_3$ extracted, ran in air 15 C/min.

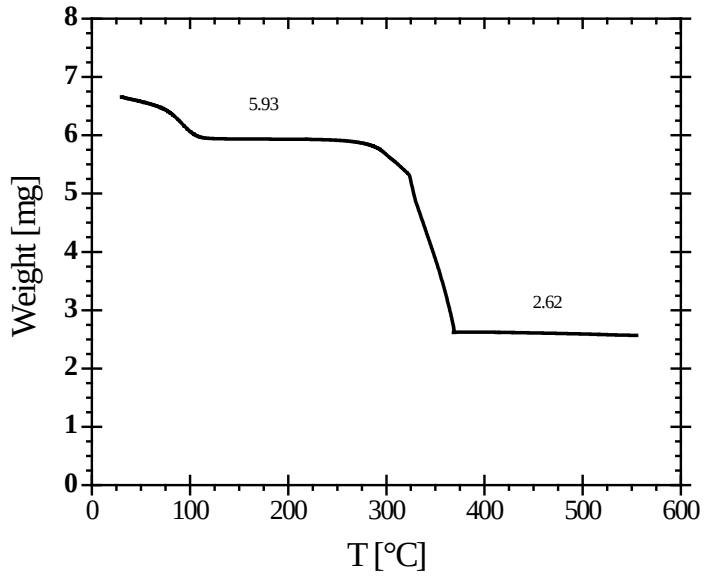

Figure S65. Co(pXdAm)Ni(CN)$_4$ CHCl$_3$ extracted, ran in air 15 C/min.

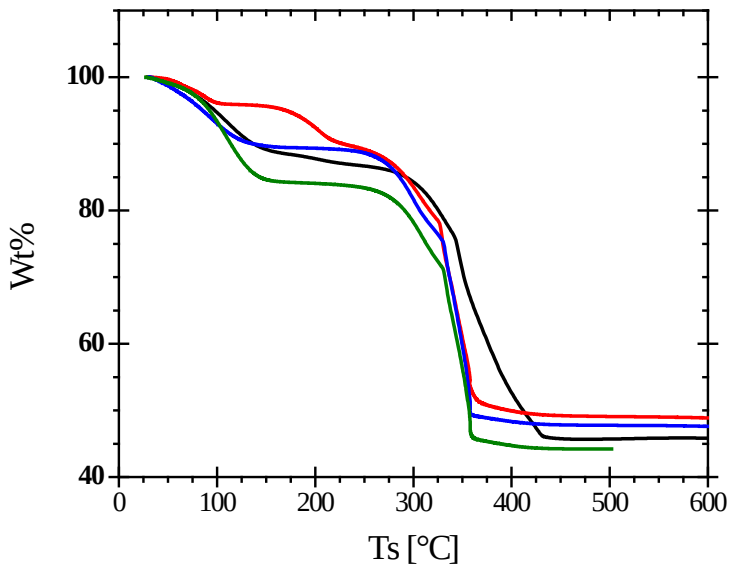

Figure S66. Co(pXdAm)Ni(CN)$_4$ CHCl$_3$ extracted, ran in air 15 C/min.

Figure S67. Powder diffraction of residual FeNi oxide after TGA of FeNi PICNICs in air with peak assignments indicated for best match to powder diffraction database (Si added as internal standard). The composition of $Ni_{1.25}Fe_{1.85}O_4$ is equivalent to $NiFeO_{2.5}$ with Ni in a 2^+ oxidation state and Fe in a 3^+ oxidation state and this composition was used in TGA calculations as described in the main article.

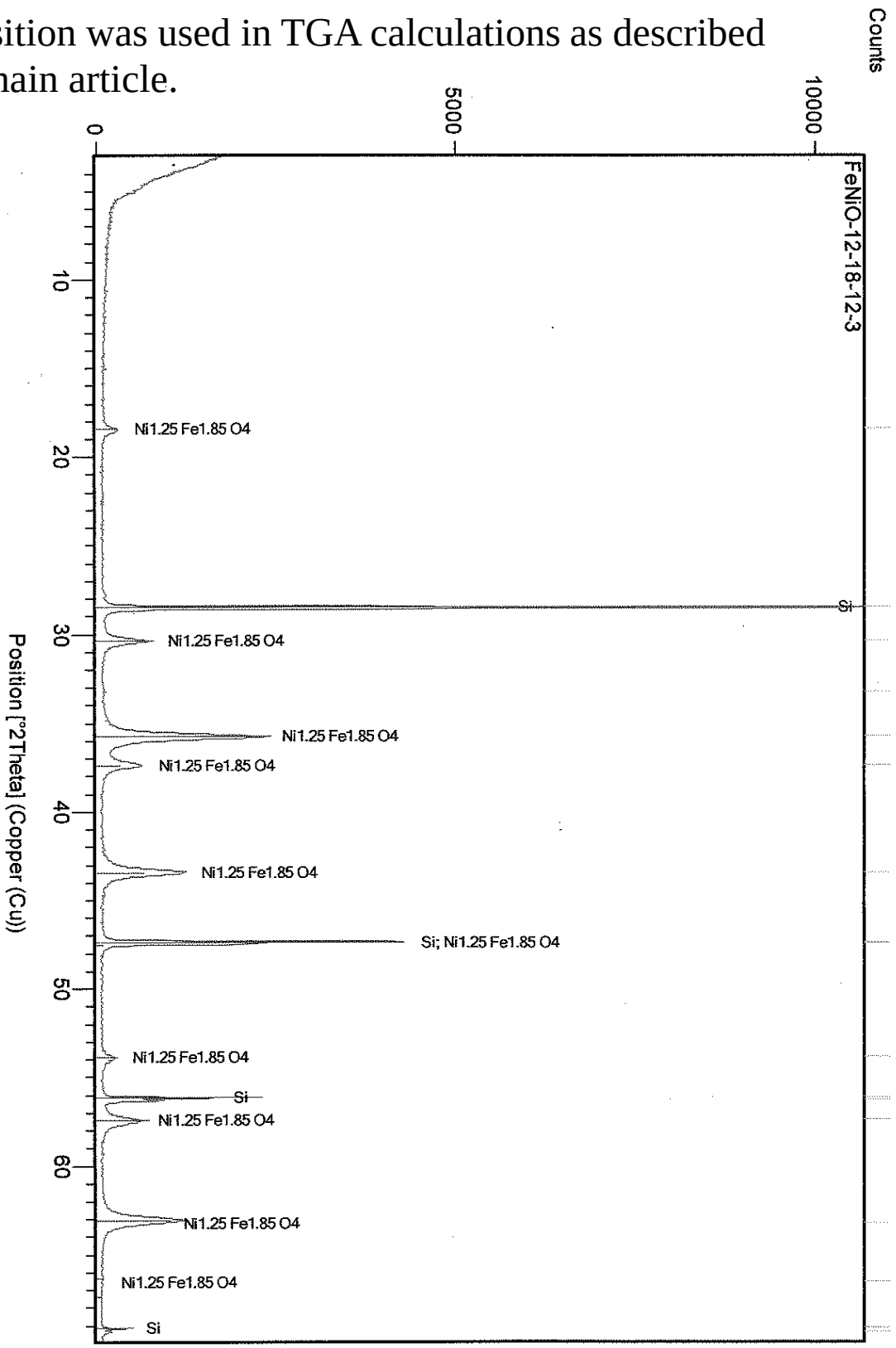

Figure S68. Powder diffraction of residual CoNi oxide after TGA of CoNi PICNICs in air. Best matches from library are labeled. Sample is a mixture of Co3O4 and NiO. For TGA calculations, the oxide was approximated the same as Ni-Fe Oxide from Figure S67, with a formula of $Ni(II)Co(III)O_{2.5}$